

Coastal Climate

-3 Lectures-

Hans von Storch

GKSS Research Centre,

Institute of Hydrophysics,

Geesthacht, Germany

I The Global and Regional Climate Systems

- Historical note
- The formation of the global climate
- The formation of regional climates
- The role of local processes for the global climate

II Climate Variability and Change

- Climate variability and change
- Dynamics of climate variability
- Modelling climate change
- The detection problem

III Storms, Waves and Storm Surges

- The WASA project: Waves and storms in the Nord Atlantic
Empirical evidence
TheWASA hindcast
- Excursion: The downscaling problem
Example: statistical downscaling-the Baltic Sea
Example: dynamical downscaling-the North Sea
- Changing statistics of storm surges....the case Cuxhaven
Statistical and dynamical downscaling

The Global and Regional Climate Systems

- ⇒ the formation of the global climate

- ⇒ the formation of the regional climates

- ⇒ the rôle of local processes for the formation of the global climate

The Formation of the Global Climate

Energy Balance Models

Emergence of Planetary Scale
Atmospheric State from a State of Rest

Historical note

Köppen's (and others) applied view
of mapping the climate of the earth

Hadley's (and others) theoretical view of
understanding major features of global climate

Question:

$$\text{global climate} \stackrel{?}{=} \sum_{\text{regions}} \text{regional climates}$$

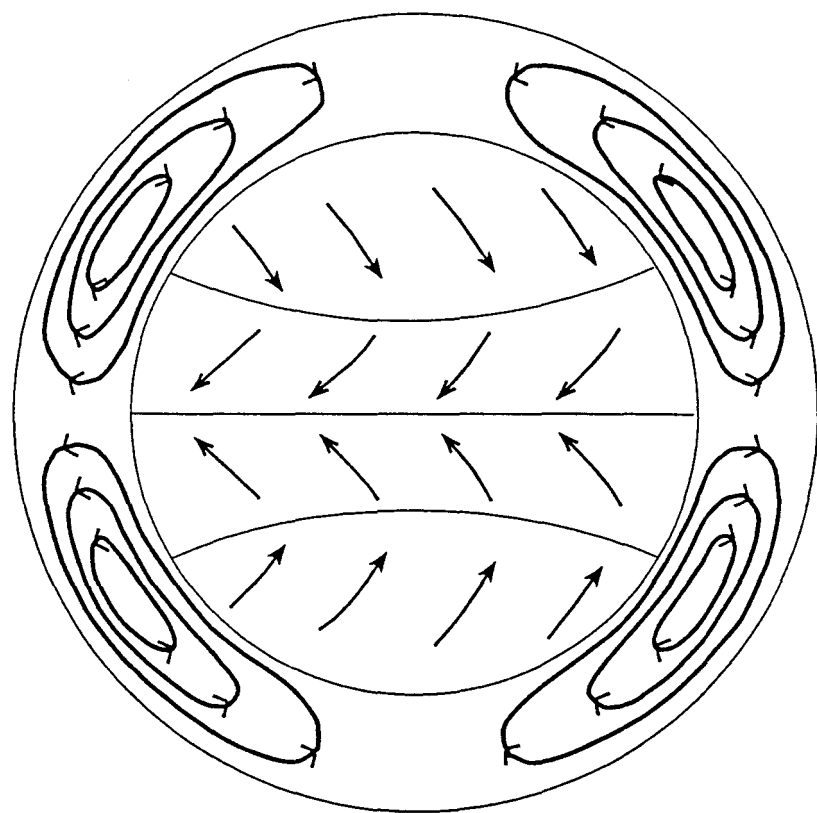
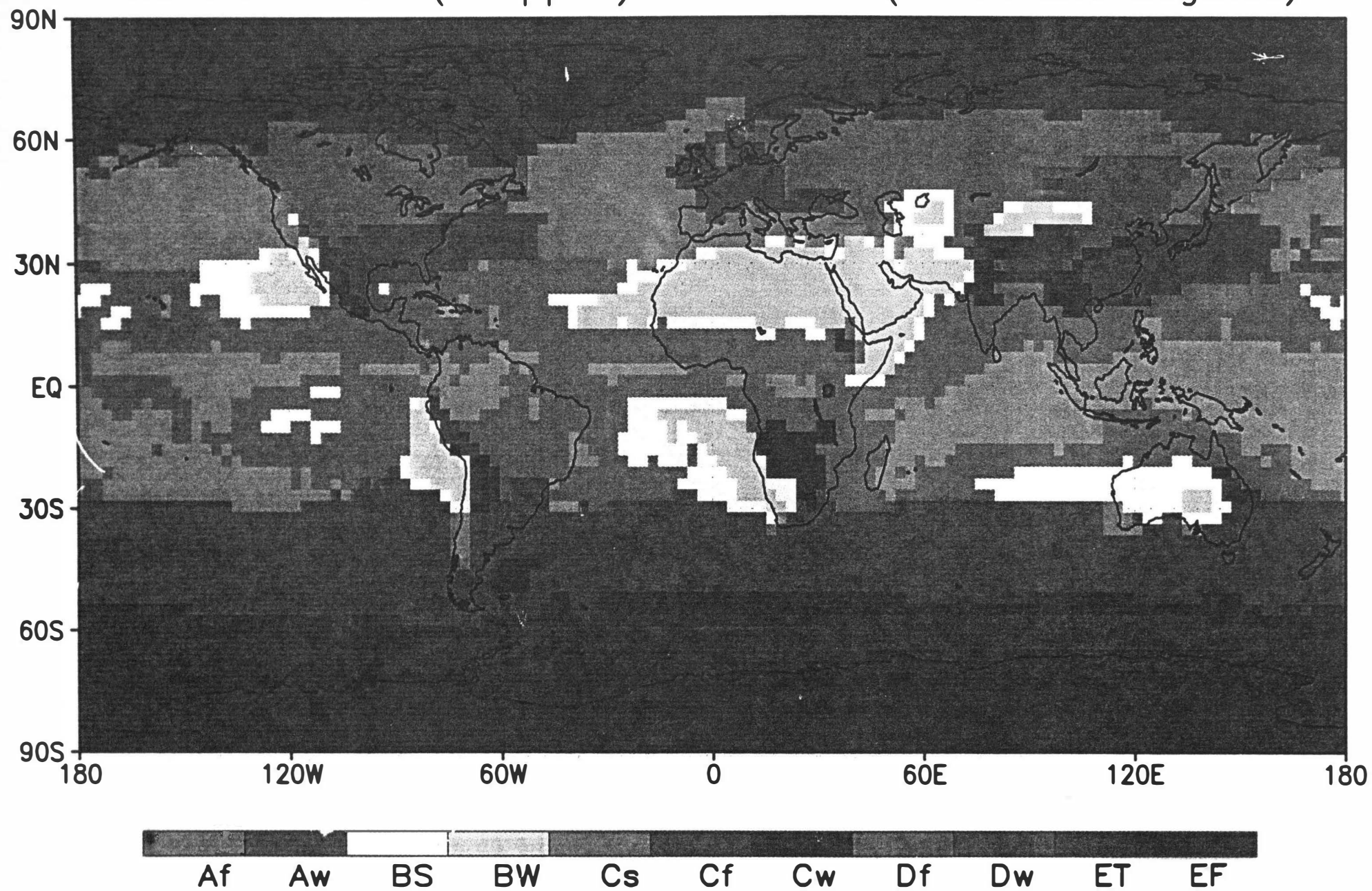


Figure : A schematic representation of the general circulation of the atmosphere as envisioned by Hadley (1735).

Lohmann, 1993

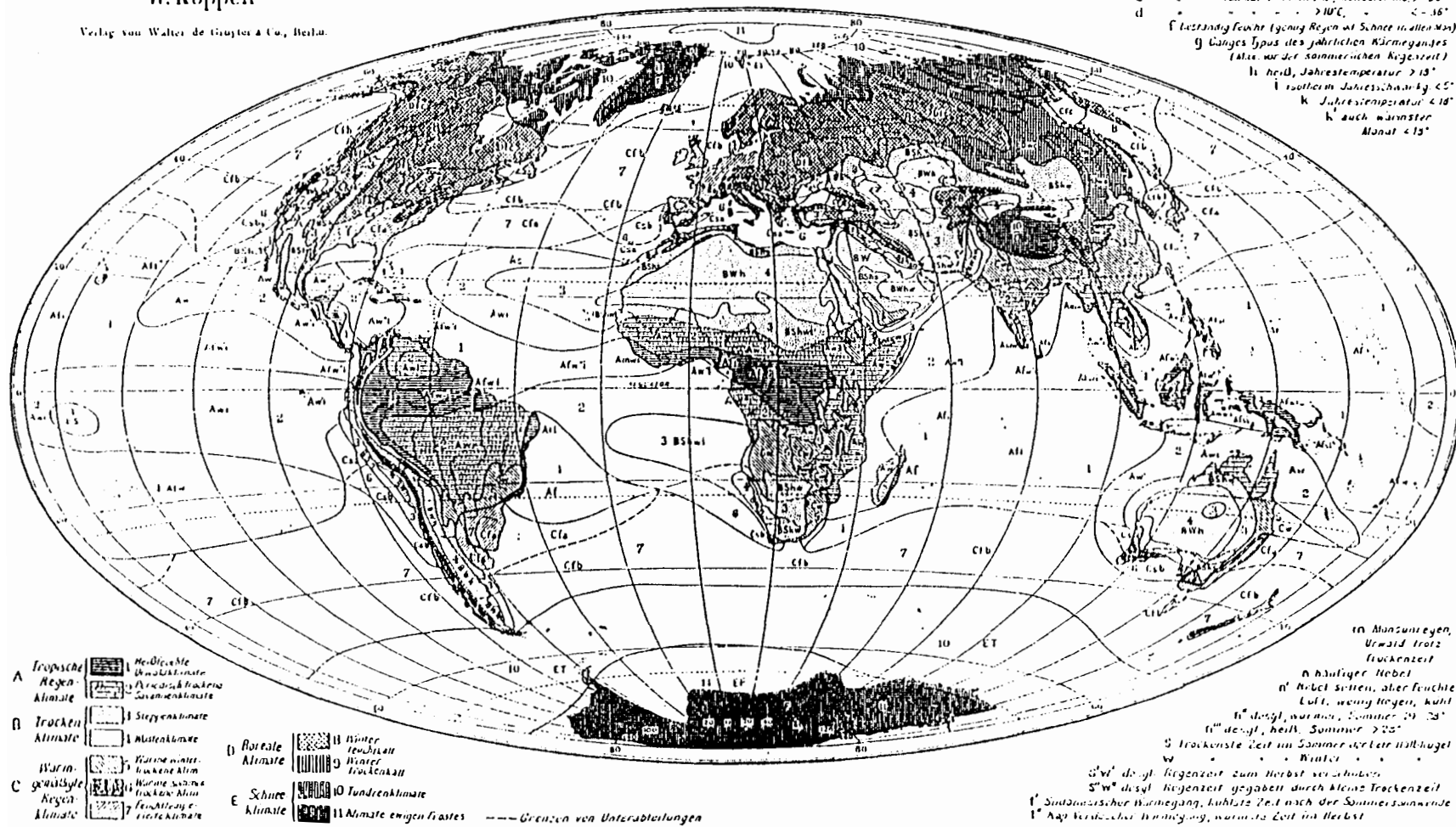
Climate Zones (Koeppen) from Obs. (Jones and Legates)



KLIMATE DER ERDE

von
W. Köppen

Verlag von Walter de Gruyter & Co., Berlin.



Conclusion

Physicists' view

global climate = $f(\text{global forcing, planetary scale features})$

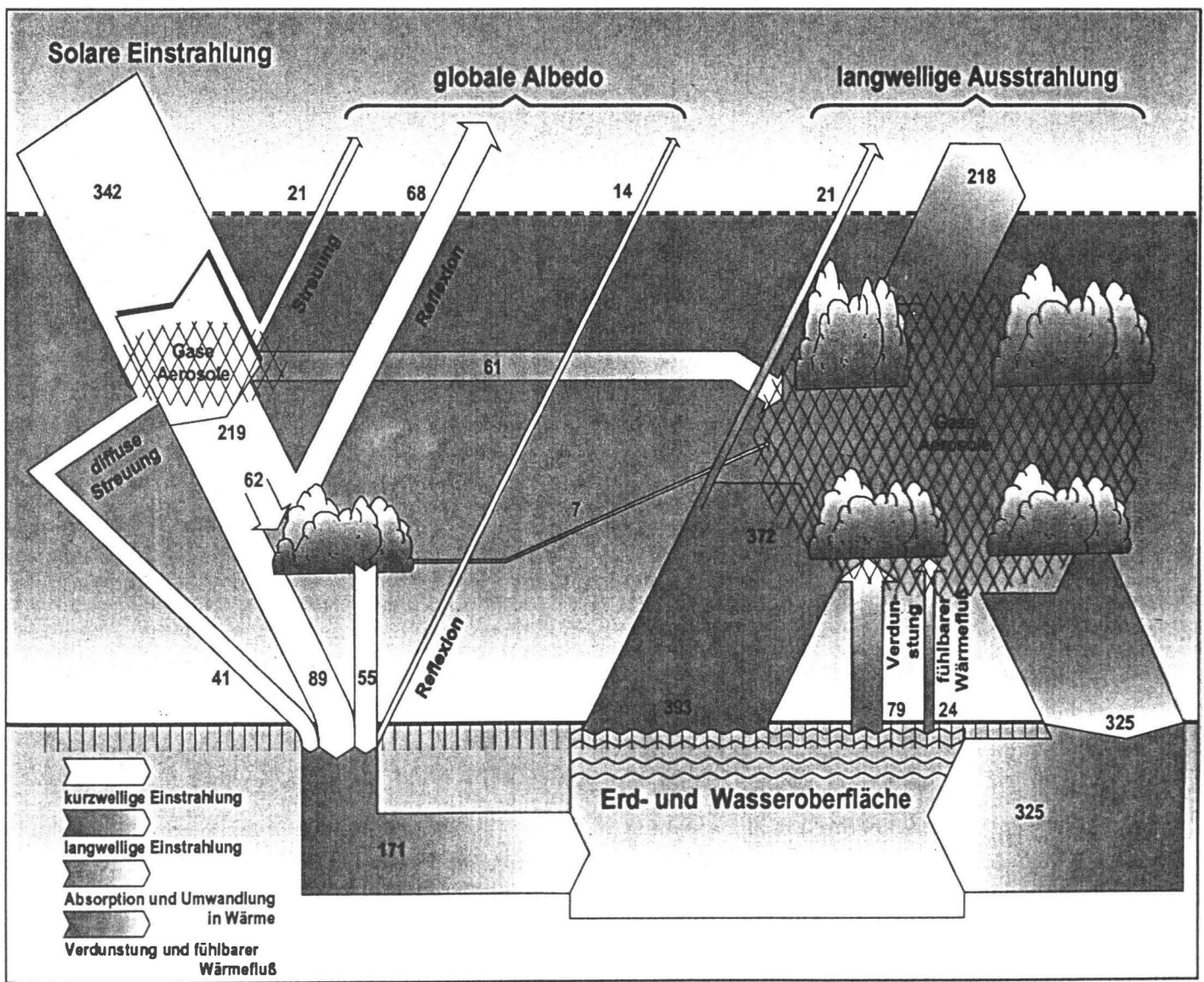
is right and

global climate = \sum_{regions} regional climate

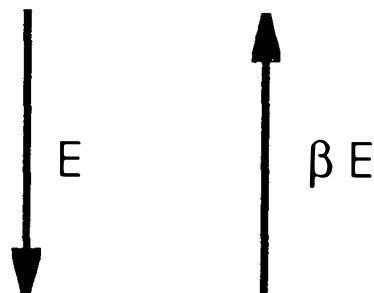
is inadequate.

- ⇒ Therefore General Circulation Models (GCMS) with limited spatial resolution (e.g. $6^\circ \times 6^\circ$ longitude x latitude) can simulate the global climate.
- ⇒ The success of GCMS on the planetary scale does not imply their success on the regional scale.

Die globale Bilanz der Strahlungsenergie, die Zahlenwerte in Watt beziehen sich auf einen m^2 Erdoberfläche. Links die kurzweligen Strahlungsflüsse, rechts rechts die langwelligen und die Wärme flüsse (fühlbar und latent)

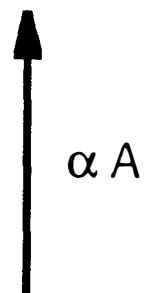


Kurzwellige Einstrahlung

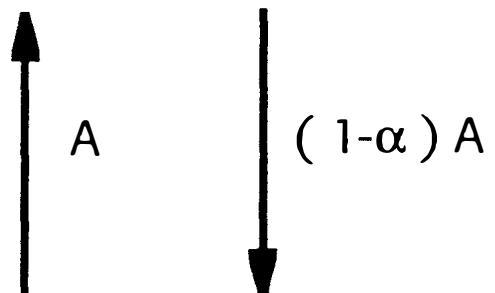
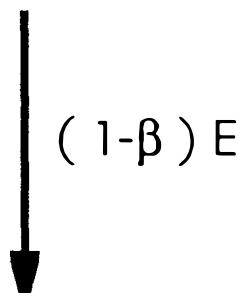


Substanzen

Langwellige Ausstrahlung



Substanzen



**Erdoberfläche
Ausstrahlung $A = \kappa\sigma T^4$**

Balance erfordert

$$(1-\beta)E = \alpha A$$

Daher, bei reduzierter „Durchlässigkeit“ α

$$\alpha \downarrow \Rightarrow A \uparrow \Rightarrow T \uparrow$$

Figure 1.4: Assumed nonlinear dependency of albedo ϕ upon the global mean temperature. From von Storch et al. (1998)

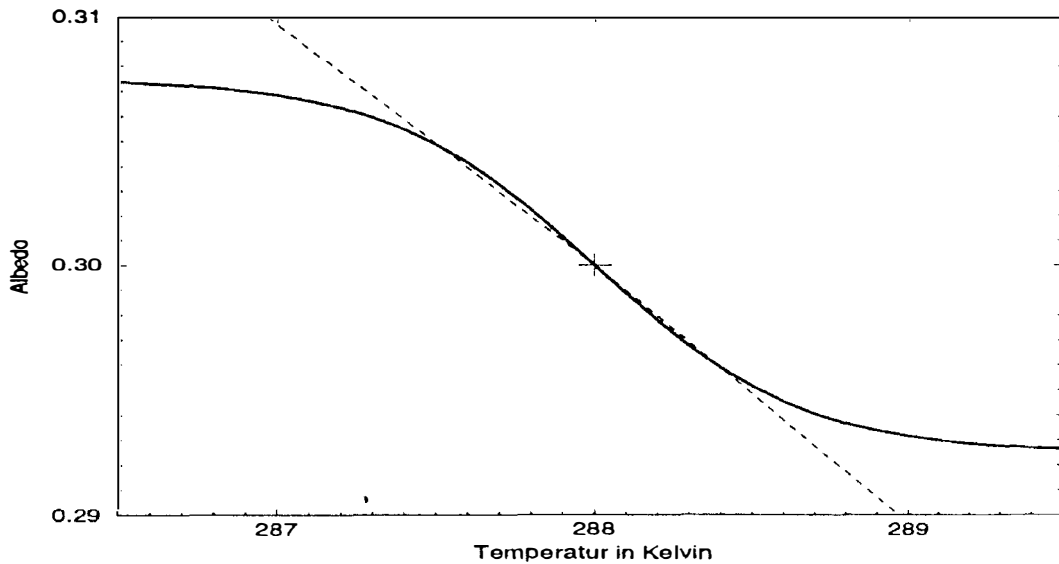
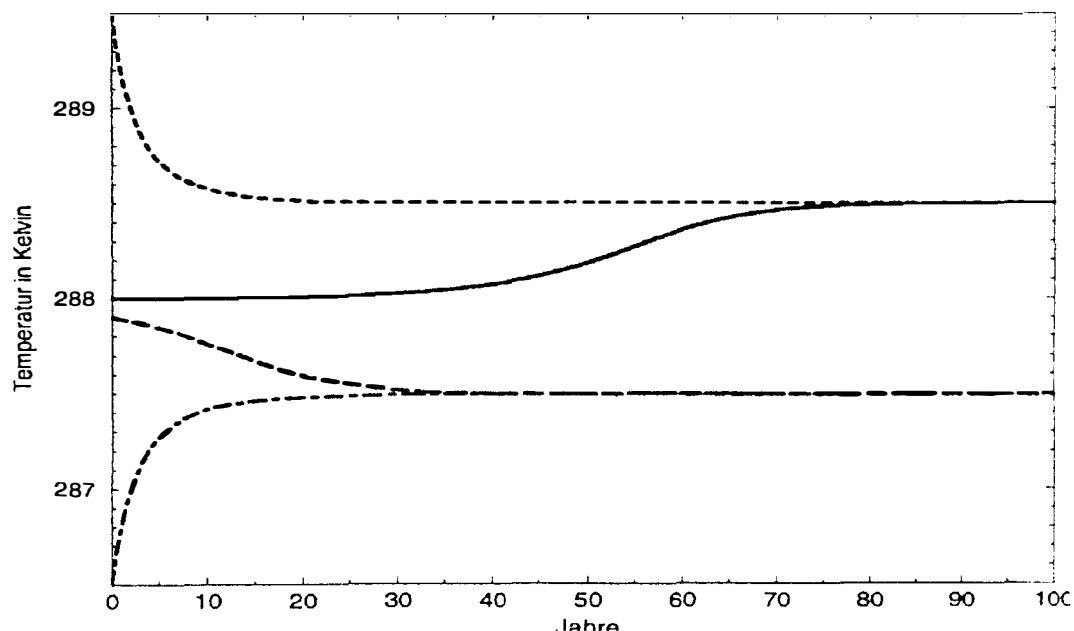


Figure 1.5: Convergence towards stable equilibrium solution of the Energy Balance Model (1.4) with temperature dependent albedo. From von Storch et al. (1998)



EBMs

$$R_{\text{incoming}} = R_{\text{outgoing}}$$

$$R_{\text{sw}} = \alpha R_{\text{sw}} + R_{\text{lw}}$$

$$R_{\text{lw}} = k \sigma T^4$$

σ : constant

$$\Rightarrow T_{\text{eq}} = \left[\frac{(1-\alpha) R_{\text{sw}}}{k \sigma} \right]^{1/4}$$

k = transmissivity
of the atmosphere

$$k = 1 \quad (\text{no atmosphere}) : \quad T_{\text{eq}} \approx -4^\circ\text{C}$$

$$k = 0.64, \alpha = 30\% \quad T_{\text{eq}} \sim 15^\circ\text{C}.$$

⇒ We can determine the global mean temperature without knowing the (details of) regional temperatures.

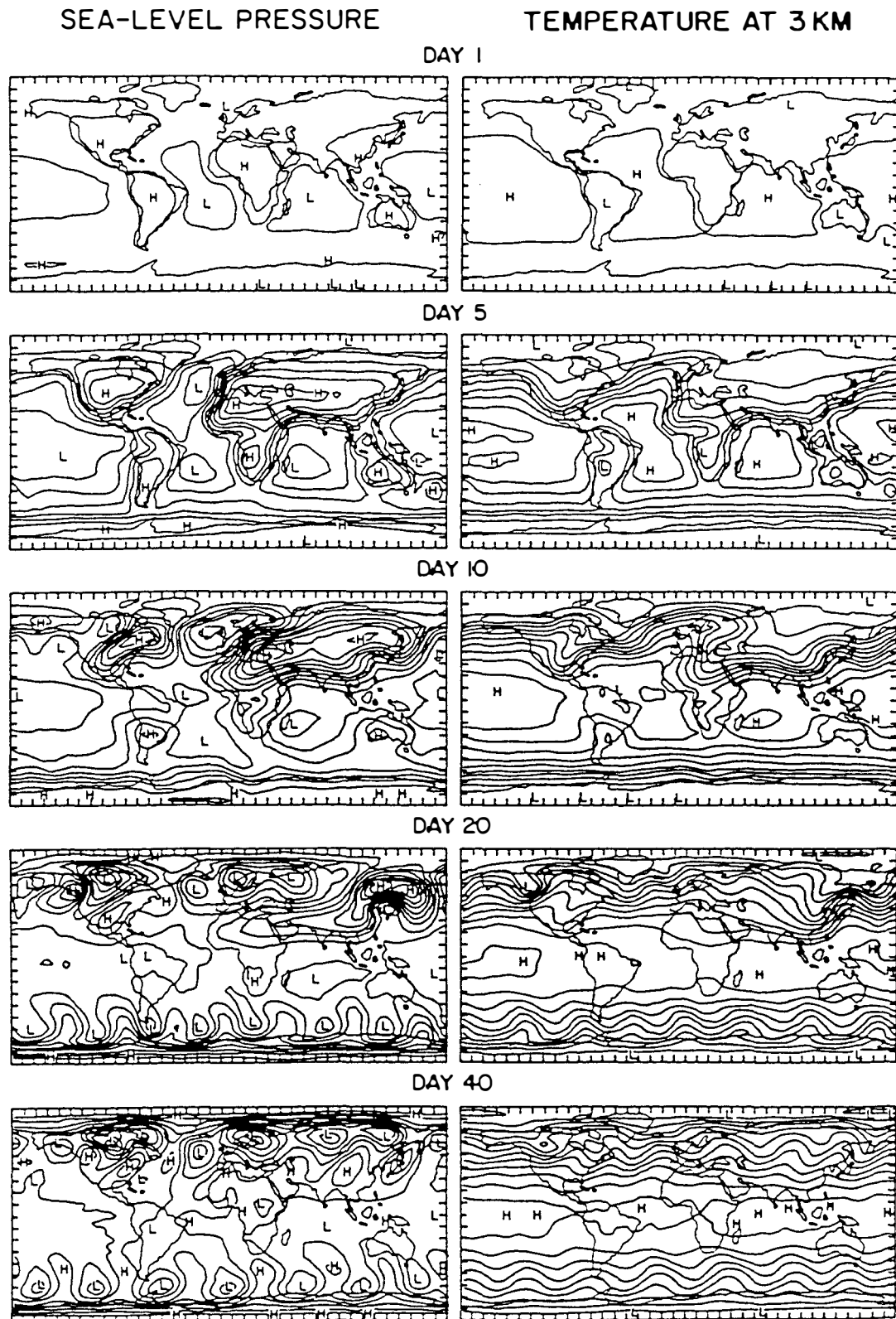


Fig. 5.1 Time sequences of sea level pressures and 3 km temperatures from a perpetual January simulation of a two-layer atmospheric GCM starting at rest with a 240 K isothermal atmosphere. The pressure contours are drawn at intervals of 4 mb and the temperature contours at intervals of 5 K. The contour lines on day 1 are at 1000 mb and 245 K. [From Washington (1968).]

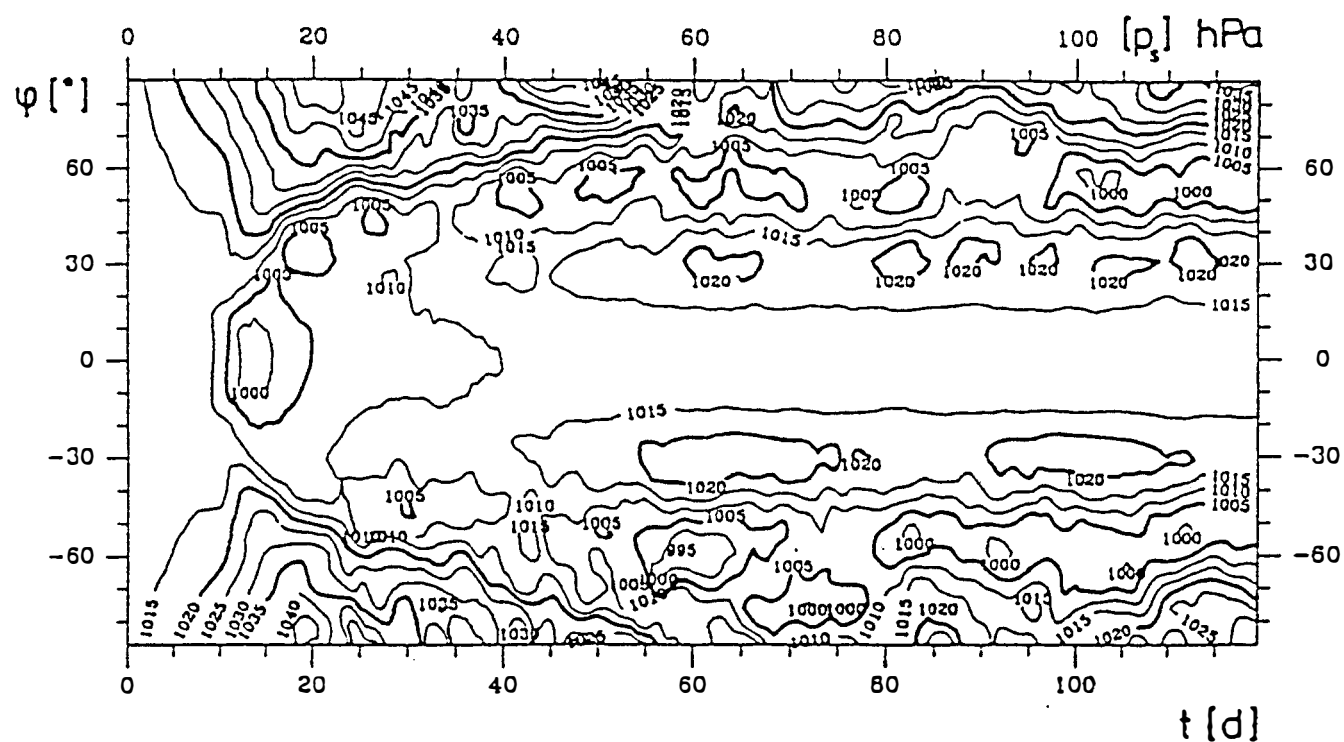
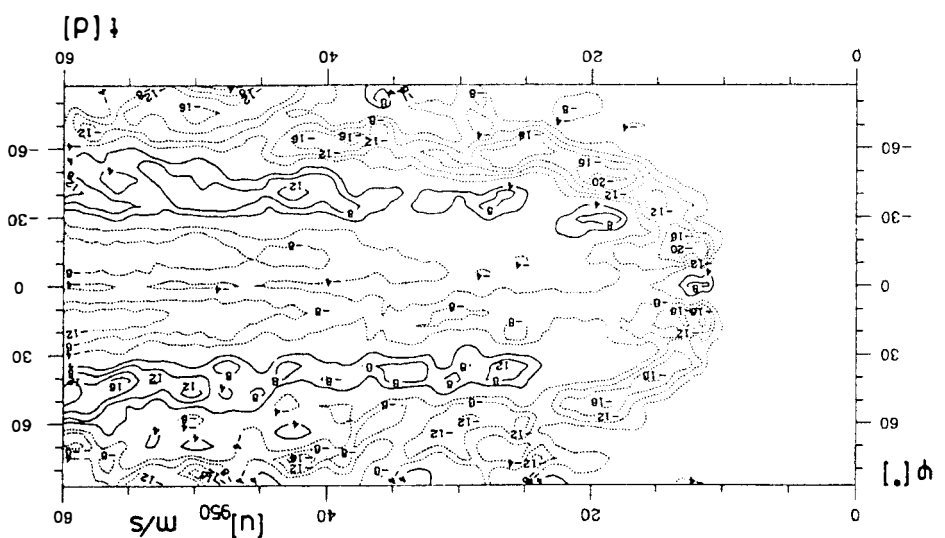
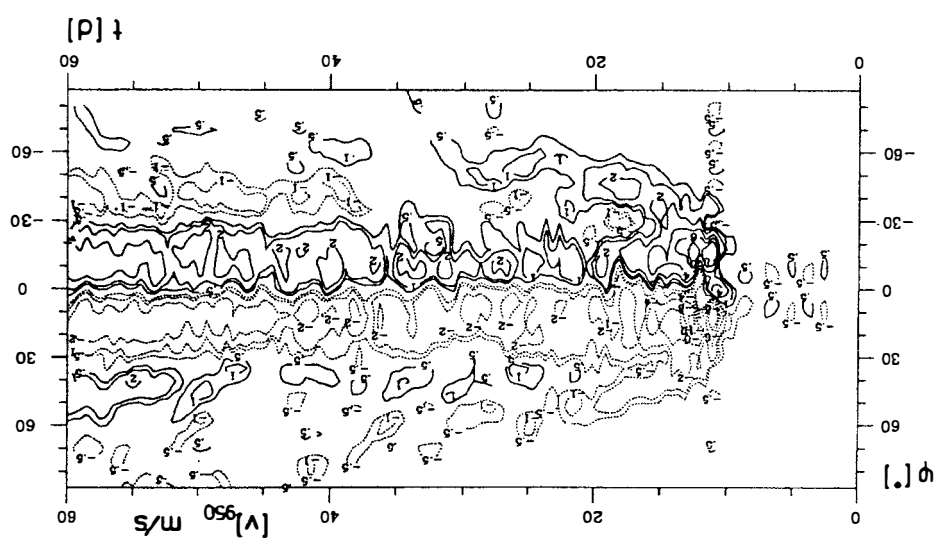
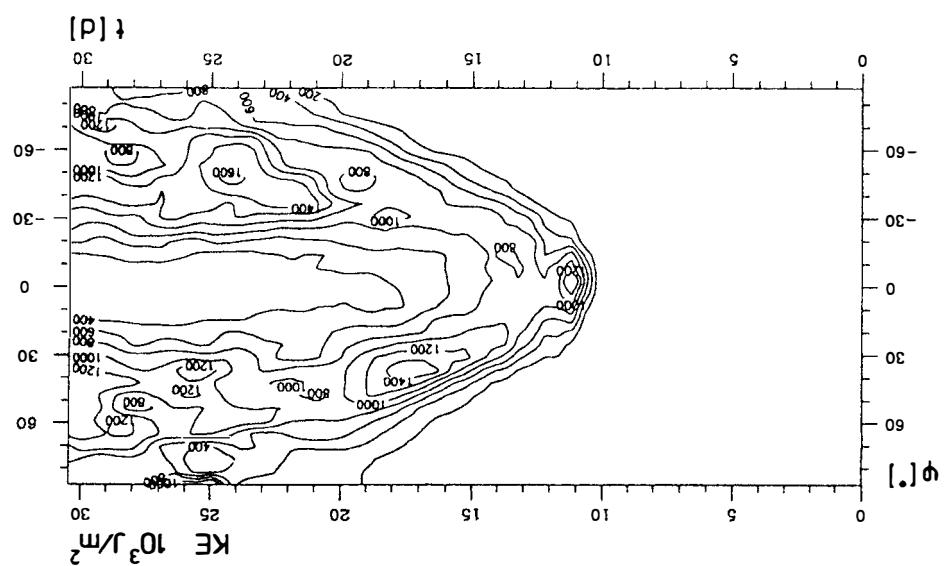


Abb. 2. Zeitliche Entwicklung des zonal gemittelten Bodendrucks als Funktion der geographischen Breite. Isolinienabstand 5 hPa.

Fig. 2. Latitude-time diagramme of the zonally averaged surface pressure; spacing 5 hPa.



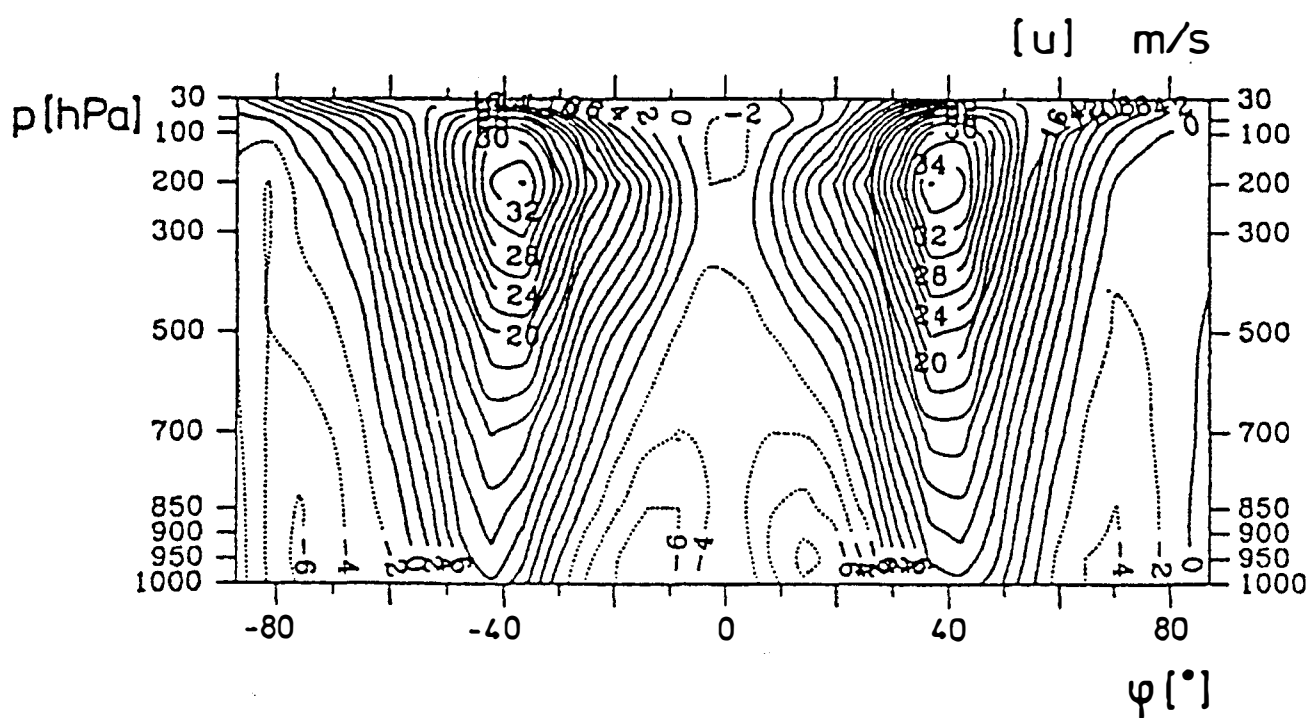


Abb. 5. Meridionalschnitt der Zonalwindverteilung im Mittel des 4. Monats. Ostwindgebiete sind gestrichelt, Isolinienabstand 2 m/s.

Fig. 5. Latitude-height cross section of the zonal wind averaged over month 4. Areas with easterly winds are stippled, spacing of isolines 2 m/s.

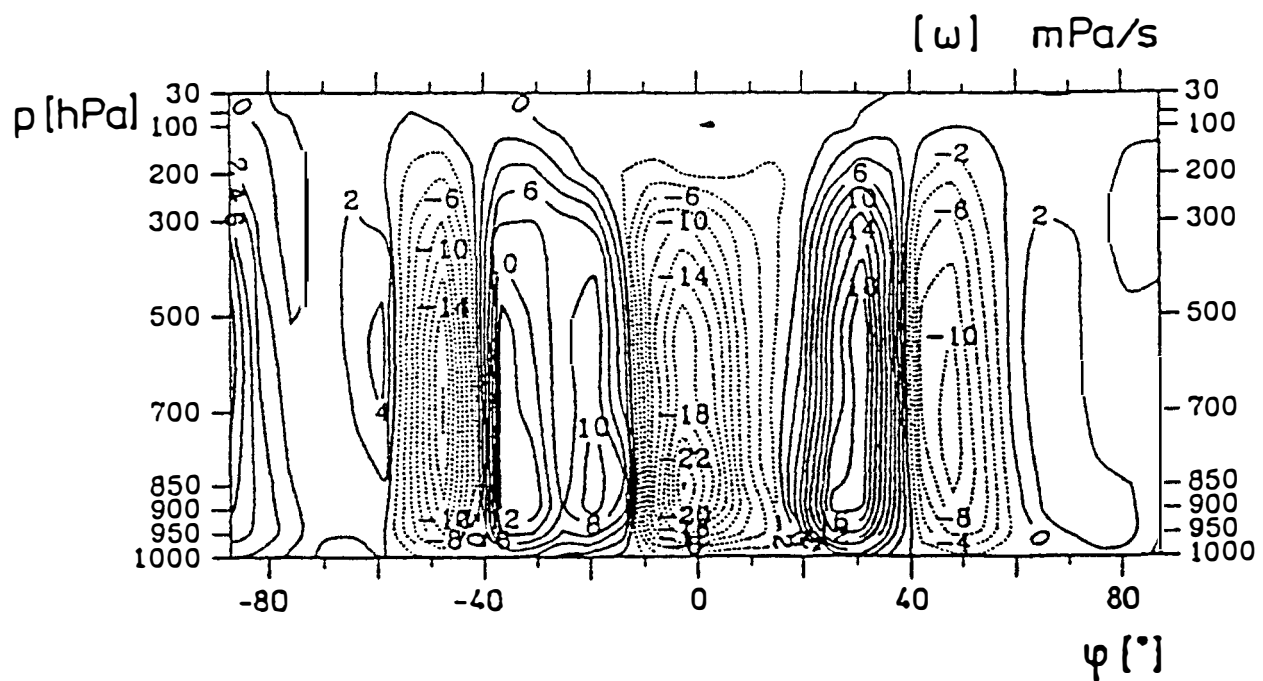
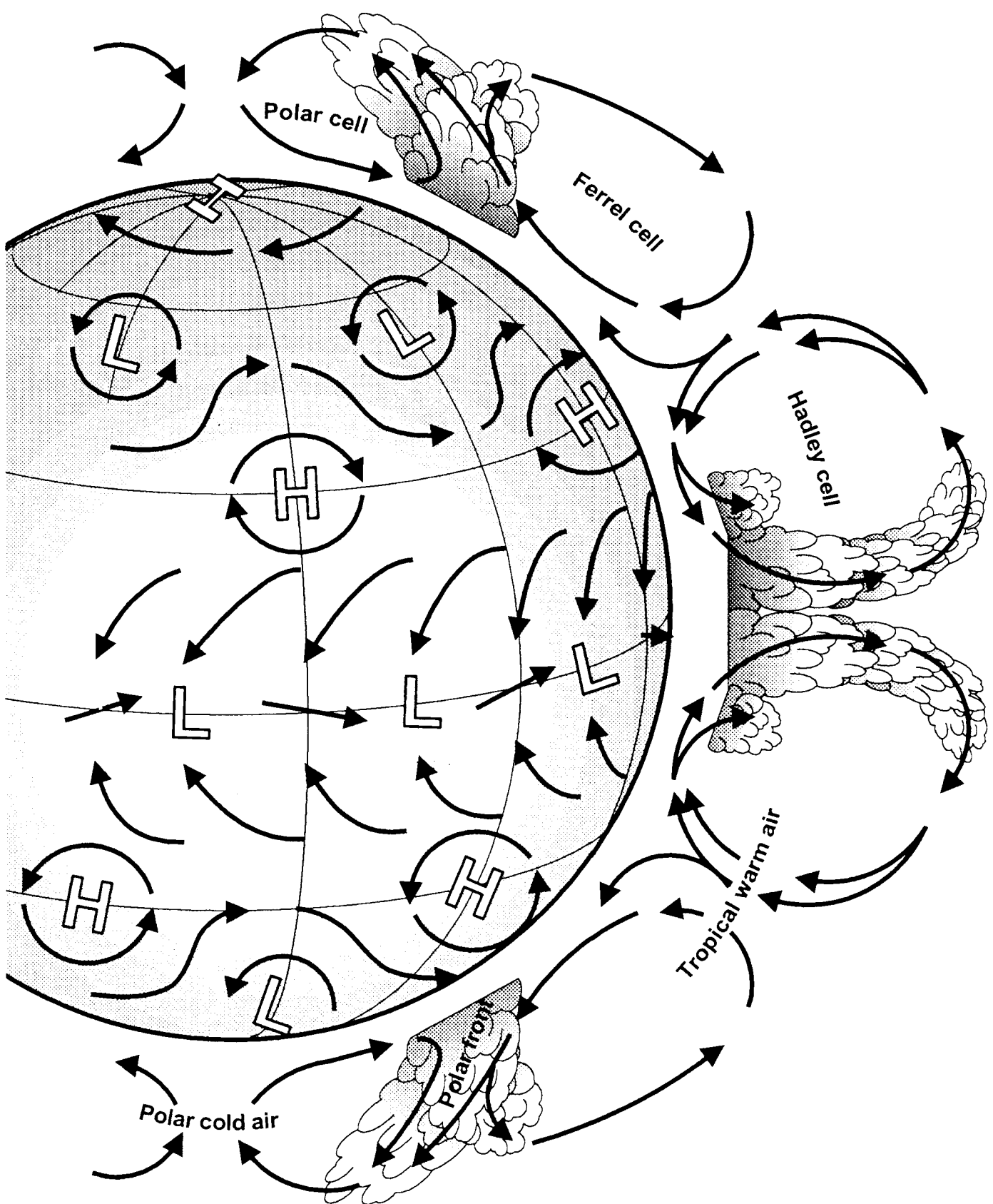


Abb. 6. Meridionalschnitt des Vertikalwindes im Mittel des 4. Monats. Gebiete mit aufsteigender Bewegung sind gestrichelt. Isolinienabstand $2 \cdot 10^{-1}$ mPa/s.

Fig. 6. Latitude-height cross section of the vertical p-velocity averaged over month 4. Areas with ascending motions are stippled, spacing $2 \cdot 10^{-1}$ mPa/s.



obs win (dly) mean 500mb geopotential-1980s (m)

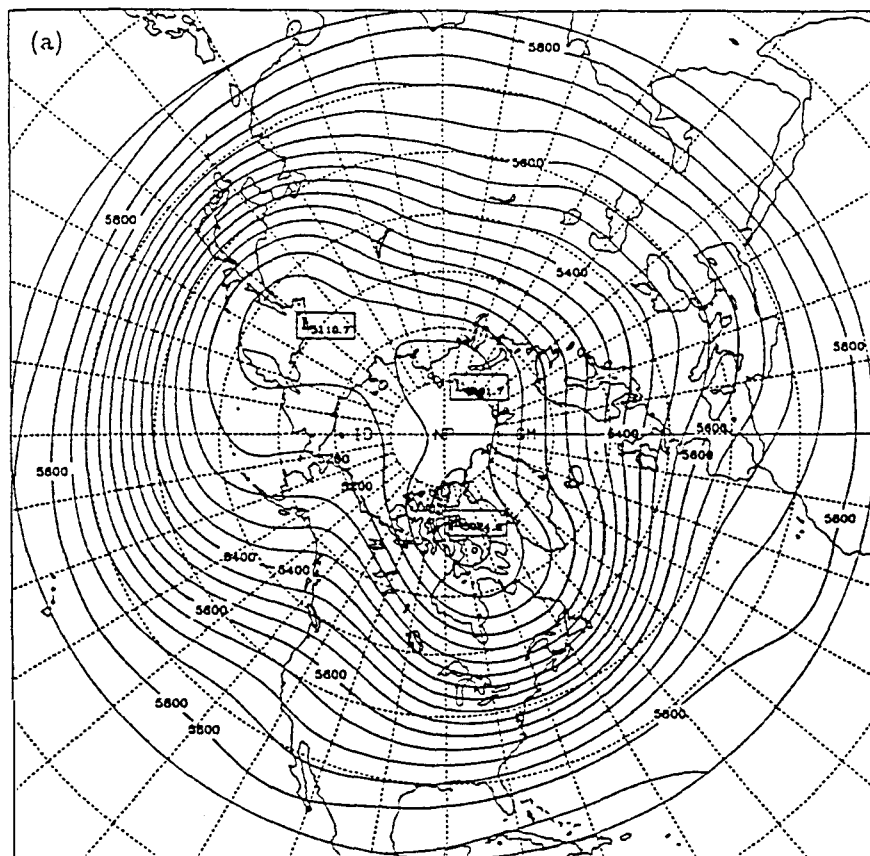


FIG. 8. Winter mean geopotential height at 500-hPa for (a) NMC observations, (b) CCM1, and (c) CCM2. The winter mean is an average over December, January, and February (for the 1980s for observations and over ten years of model simulation for models).

Risbey & Stone, 1996

obs winter mean 200mb zonal wind - 1980s (m/s)

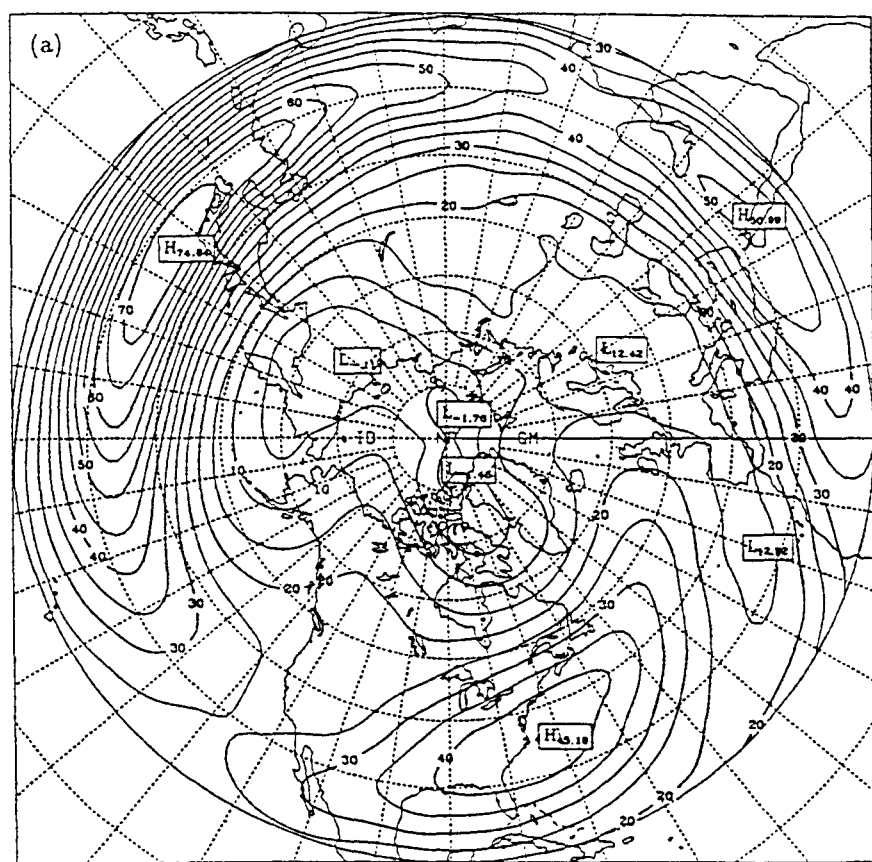


FIG. 6. Winter mean zonal wind at 200 hPa for (a) NMC observations, (b) CCM1, and (c) CCM2. The winter mean is an average for December, January, and February over the 1980s for observations and over ten years of model simulation for models.

Risbey & Stone, 1996

obs win bandpass rms 500mb geoptl-1980s (m)

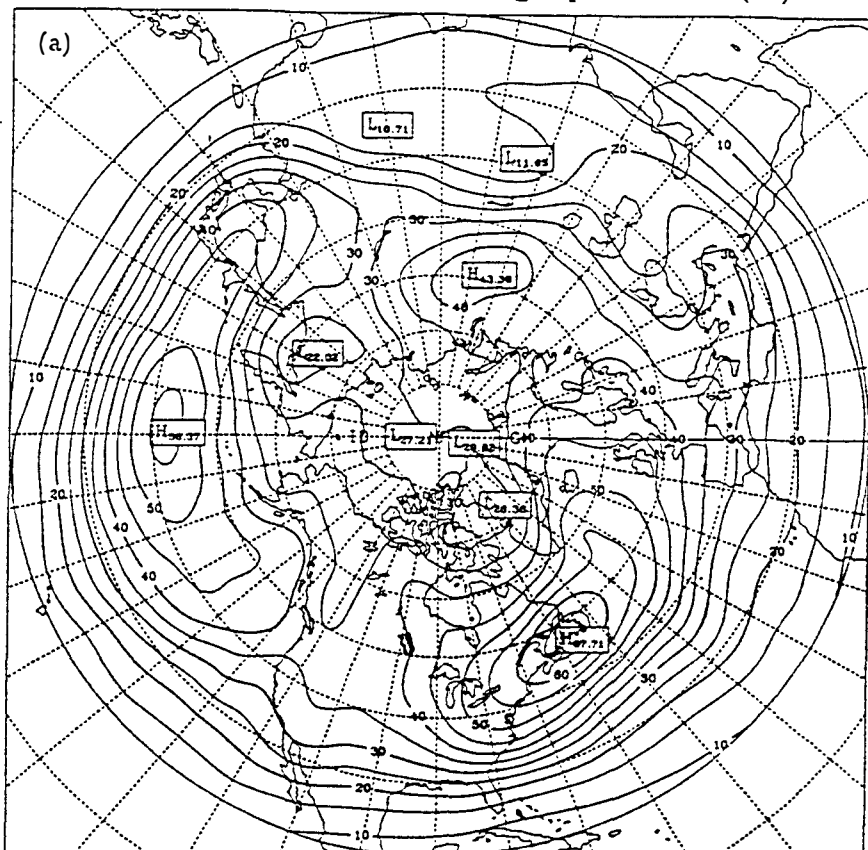
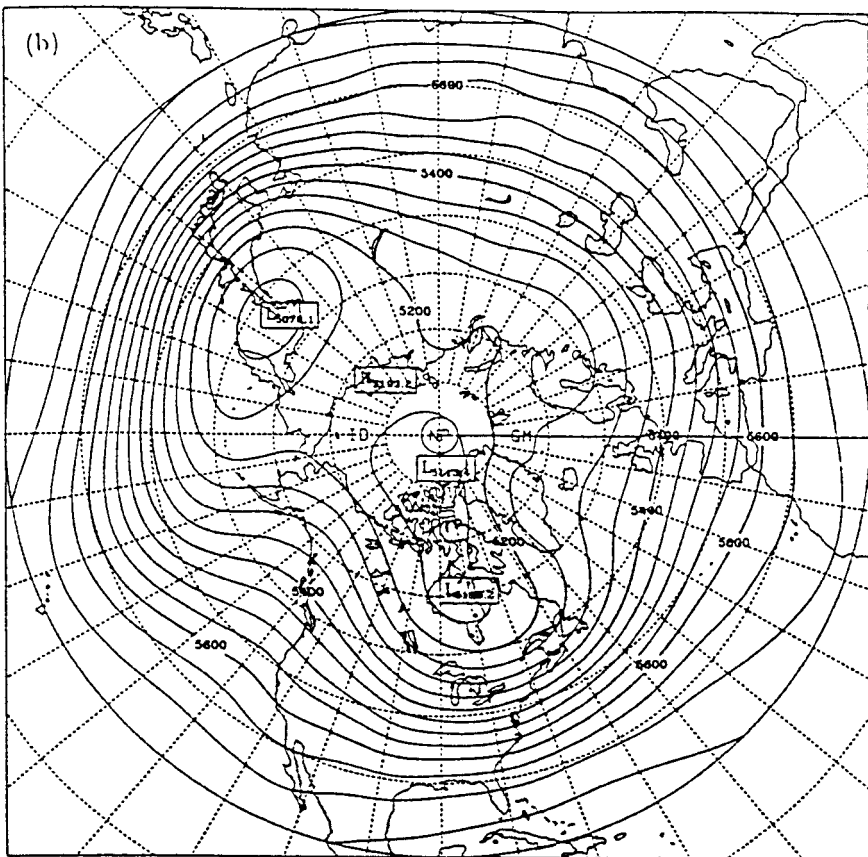


FIG. 9. Winter-mean bandpass filtered rms geopotential height at 500-hPa for (a) NMC observations, (b) CCM1, and (c) CCM2. The winter mean is an average for December, January, and February over the 1980s for observations and over ten years of model simulation for models. The filtering retains periods in the range between 2.5 and 6 days.

Risbey and Stone, 1996

ccm1 win (dly) mean 500mb geopotential-1980s (m)



ccm2 win (dly) mean 500mb geopotential-1980s (m)

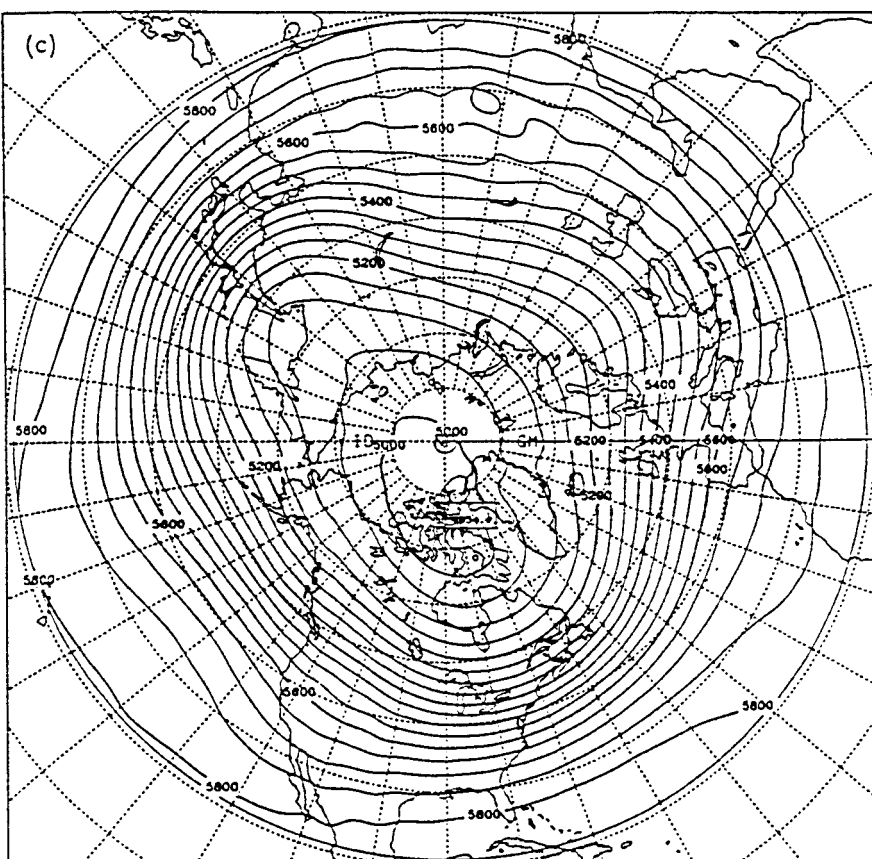
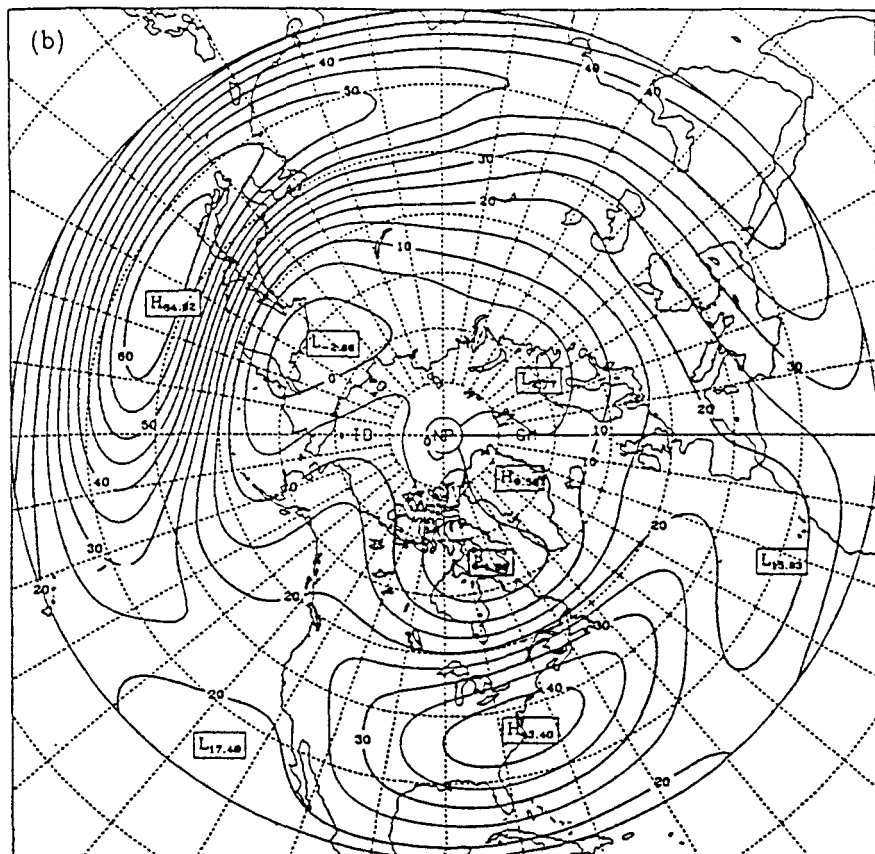


FIG. 8. (Continued)

ccm1 winter mean 200mb zonal wind - 1980s (m/s)



ccm2 winter mean 200mb zonal wind - 1980s (m/s)

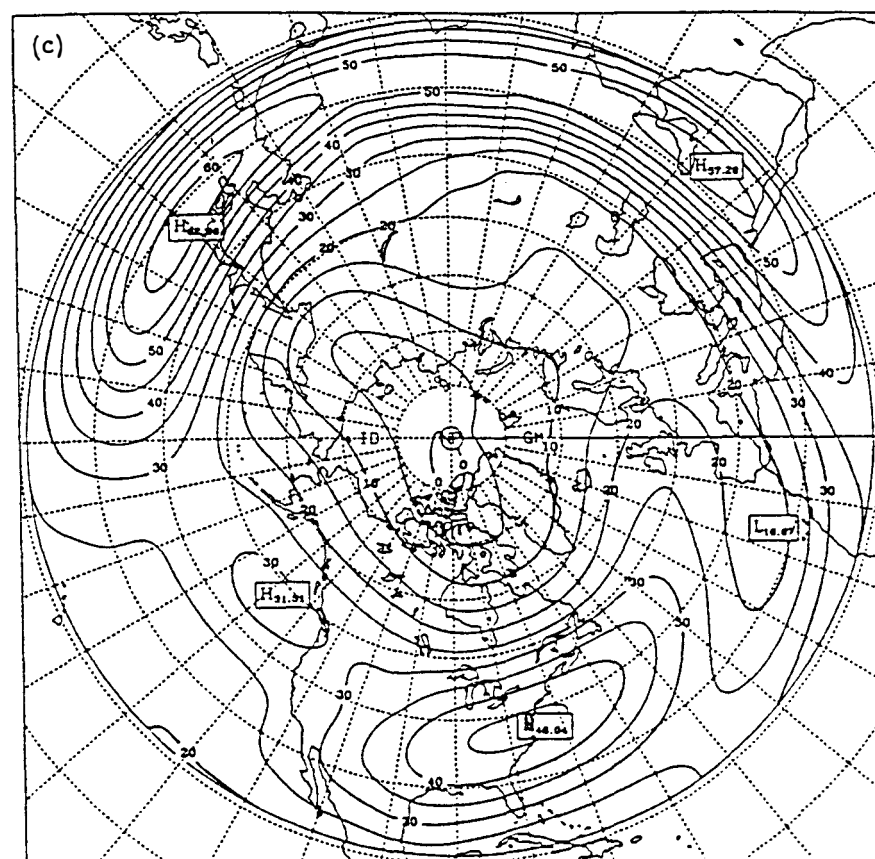
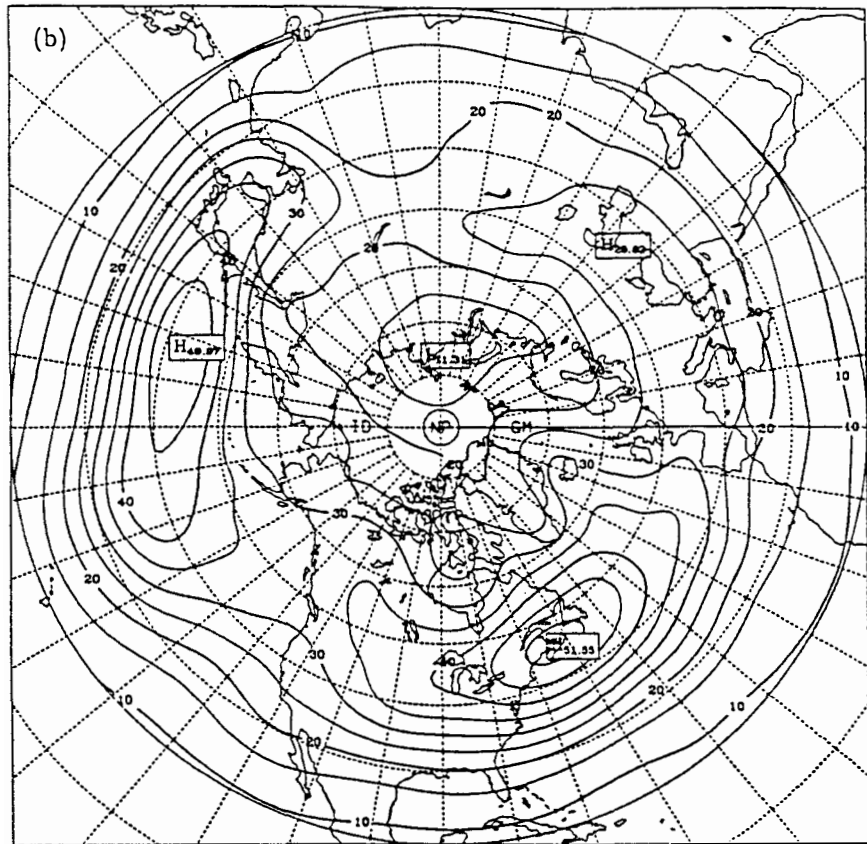


FIG. 6. (Continued)

ccm1 win bandpass rms 500mb geoptl-1980s (m)



ccm2 win bandpass rms 500mb geoptl-1980s (m)

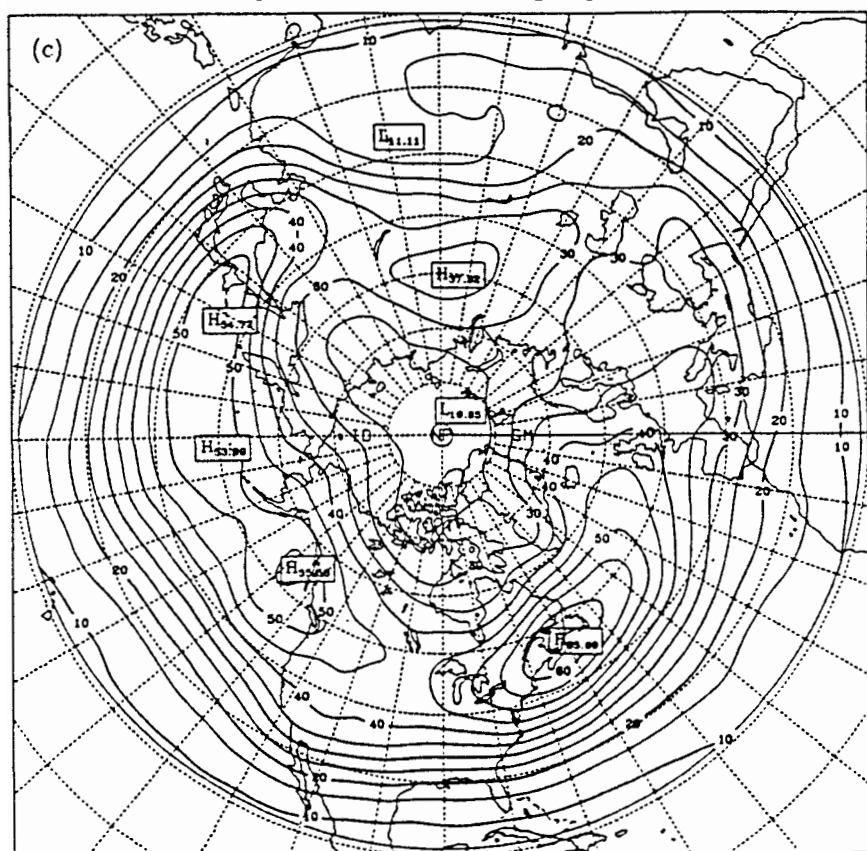


FIG. 9. (Continued)

The Formation of Regional Climates

- ⇒ Case : Sacramento Valley
a synoptic analysis

- ⇒ Conditional Statistical Models
Canonical Correlation Analysis
and Redundancy Analysis as a tool
for specifying conditional means

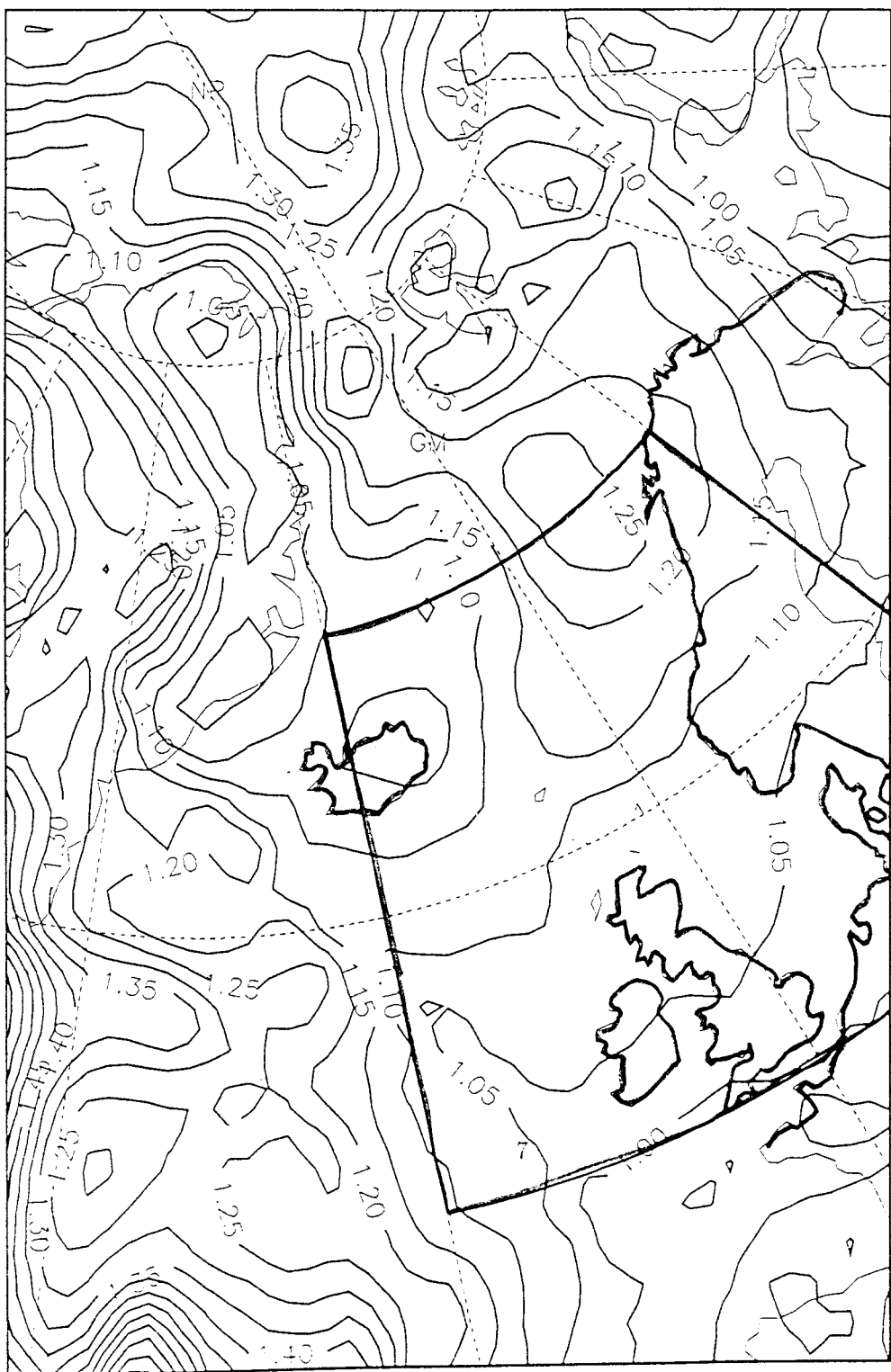
- ⇒ Cases : Romanian precipitation and
North Atlantic wave height statistics

1. The General Nature of Weather Forecasting. The general problem of forecasting weather conditions may be subdivided conveniently into two parts. In the first place, it is necessary to predict the state of motion of the atmosphere in the future; and, secondly, it is necessary to interpret this expected state of motion in terms of the actual weather which it will produce at various localities. The first of these problems is essentially of a dynamic nature, inasmuch as it concerns itself with the mechanics of the motion of a fluid. The second problem involves a large number of details because, under exactly similar conditions of motion, different weather types may occur, depending upon the temperature of the air involved, the moisture content of the air, and a host of local influences.

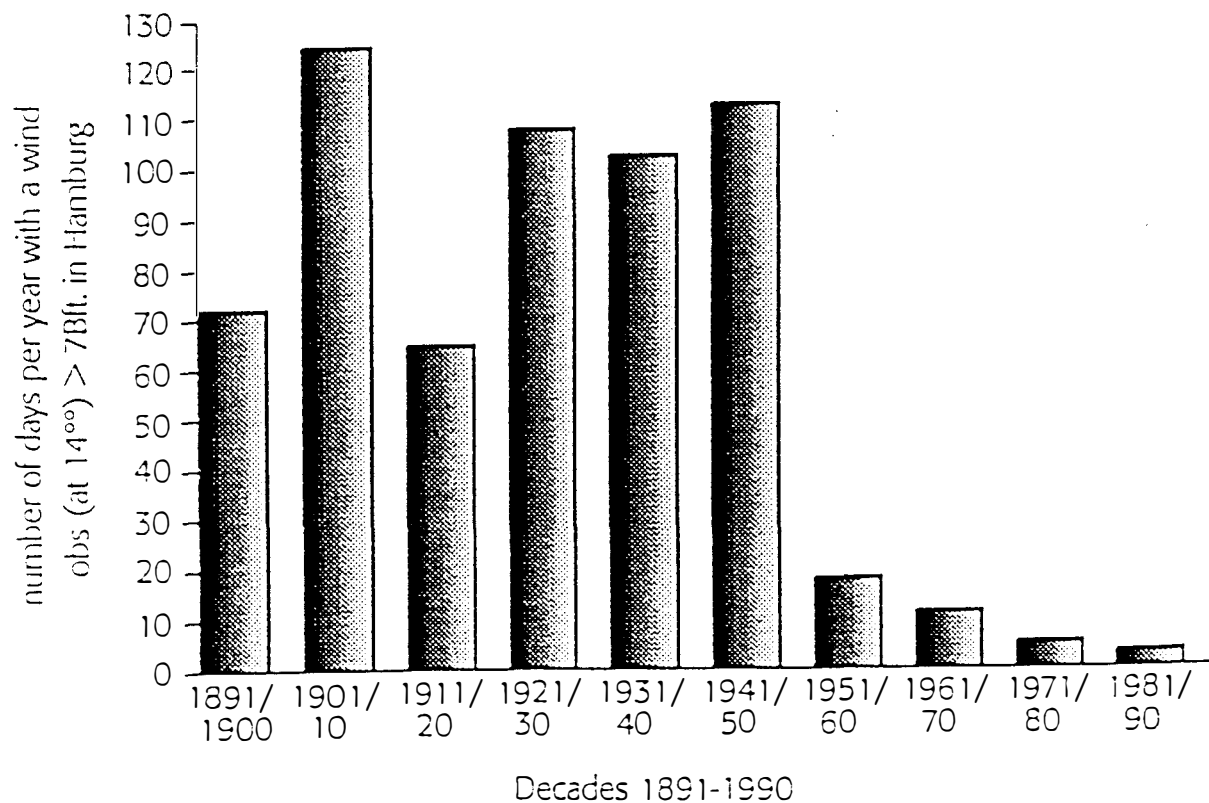
Victor Starr, 1942

Figure 7: Ratio of synoptic scale standard deviation of air pressure variations in winter (DJF) as derived from DNMI analysis in the decade 1984-93 and in the decade 1964-73. The area "A" south of 70° N and east of 20° W is marked.

SLP STD ratio (band-pass filtered)



Data: DNMI 1984-93 vs. 1964-73, DJF



WASA aims:

- Reconstruction of the storm and wave climate in the Northeast Atlantic and adjacent seas in the 20th century.
- Construction of the future perspectives of the storm and wave climate in the 21st century

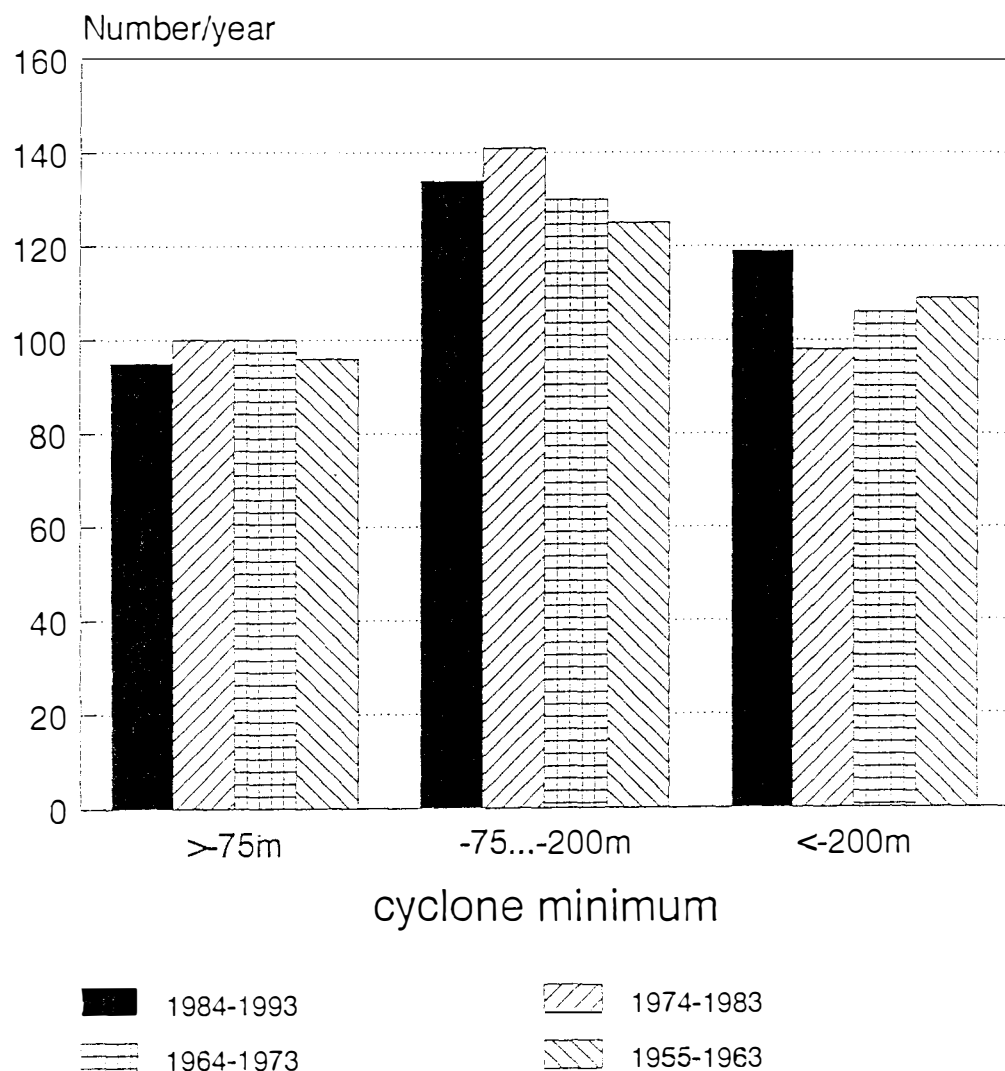
Two central questions:

- Is the storm climate in the past 100 years consistent with the notion of intensifying or more frequently forming storms in the Northeast Atlantic and adjacent seas?
- How was / might be the response of the wave field and the storm surge statistics to the past / possible future changes in the storm climate and other atmospheric features?

Strategy:

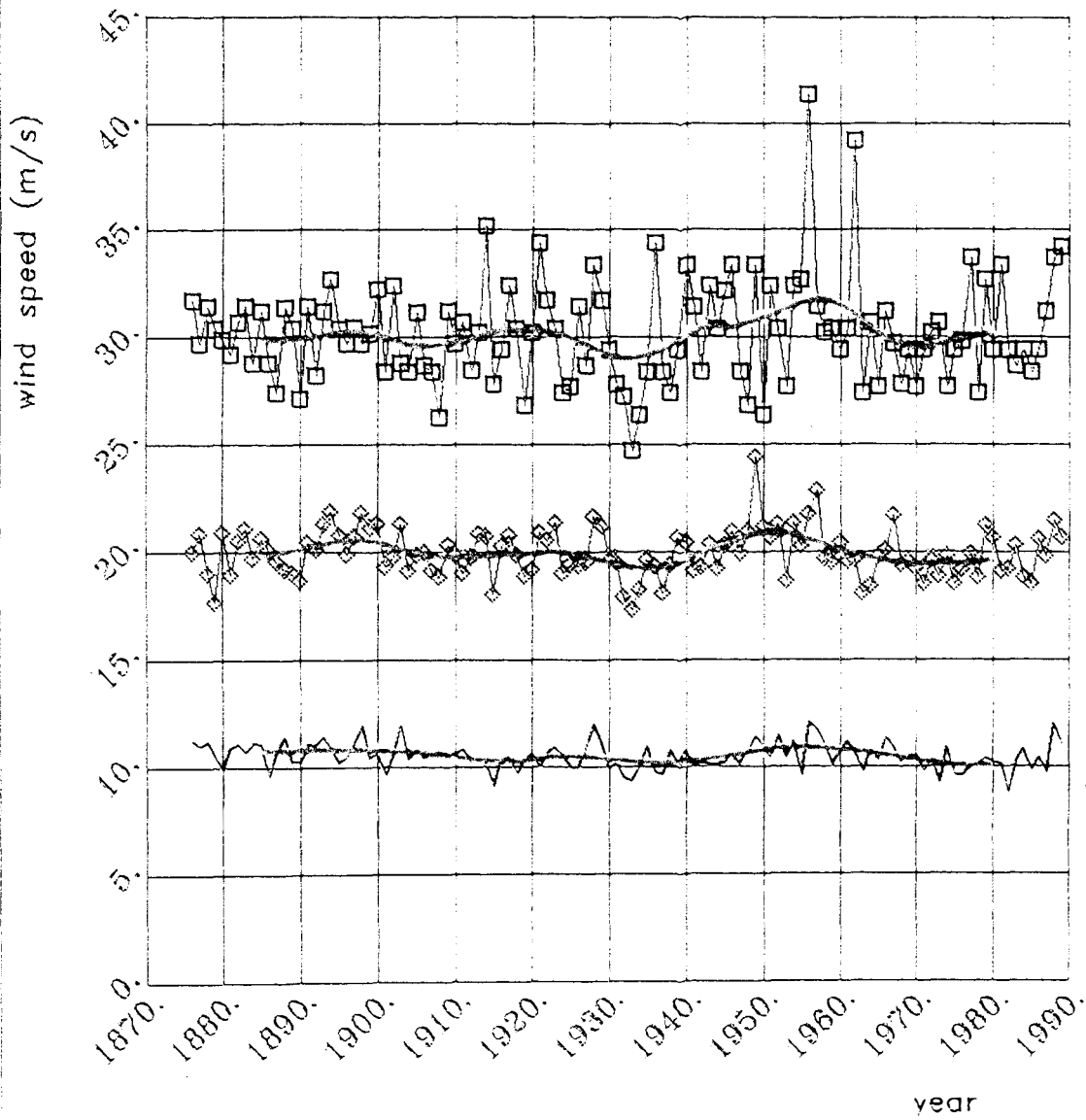
- examine long, homogeneous observational data series
- analyse extended hindcast experiments with wave models
- use the output of climate change scenario experiments to prepare scenarios for possible future wave climates.

Figure 11: *Storm count in the area between 70°N to 50° N and east of 20° W (see Figure 7) in the DNMI data in DJF for different multi-year intervals. The storms are sorted after the core value z of the 1000 hPa level in meters. The pressure in mb is approximately $z/8 + 1000$.*



DEUTSCHER WETTERDIENST
—Seewetteramt Hamburg—

◆ 10 percent
— 50 percent □ 1 percent



GEOSTROPHIC WIND
from pressure triangle Borkum-Hamburg-Fanøe.
Annual wind speeds for different levels
of probability of exceedance.

Schmidt, 1991, unpublished
Seewetteramt Hamburg

Figure 1: Time series of percentiles of geostrophic wind speed over Denmark. Units: m/s.

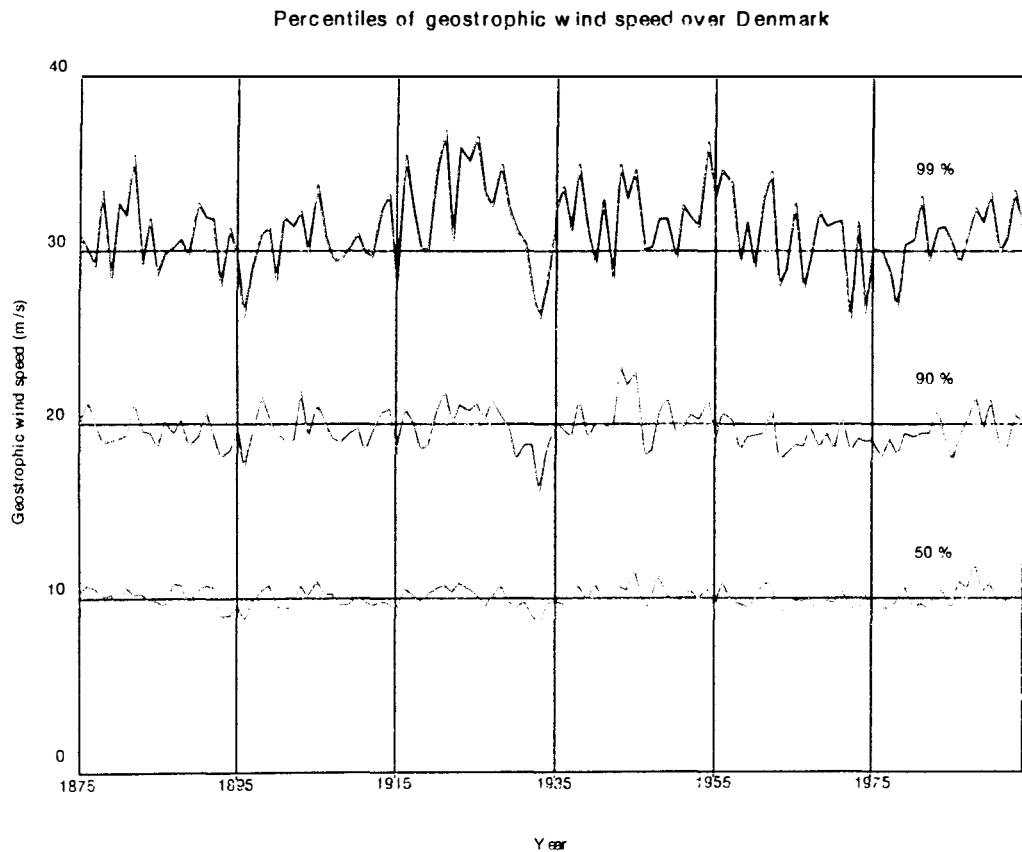


Figure 9: Percentile-percentile plot of station mean wind speed and geostrophic wind speed for the Danish triangle, derived from 5 years of daily data.

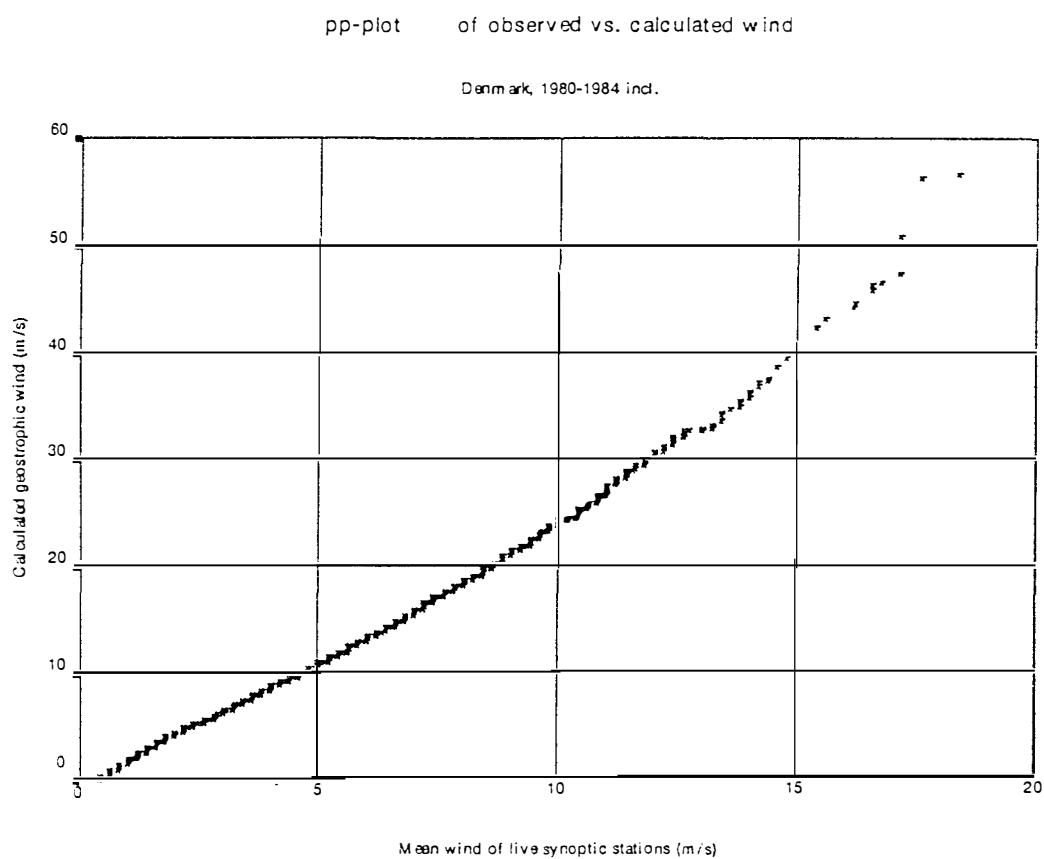


Figure 8: Scatterdiagram of station-mean wind speed and geostrophic wind speed over Denmark.

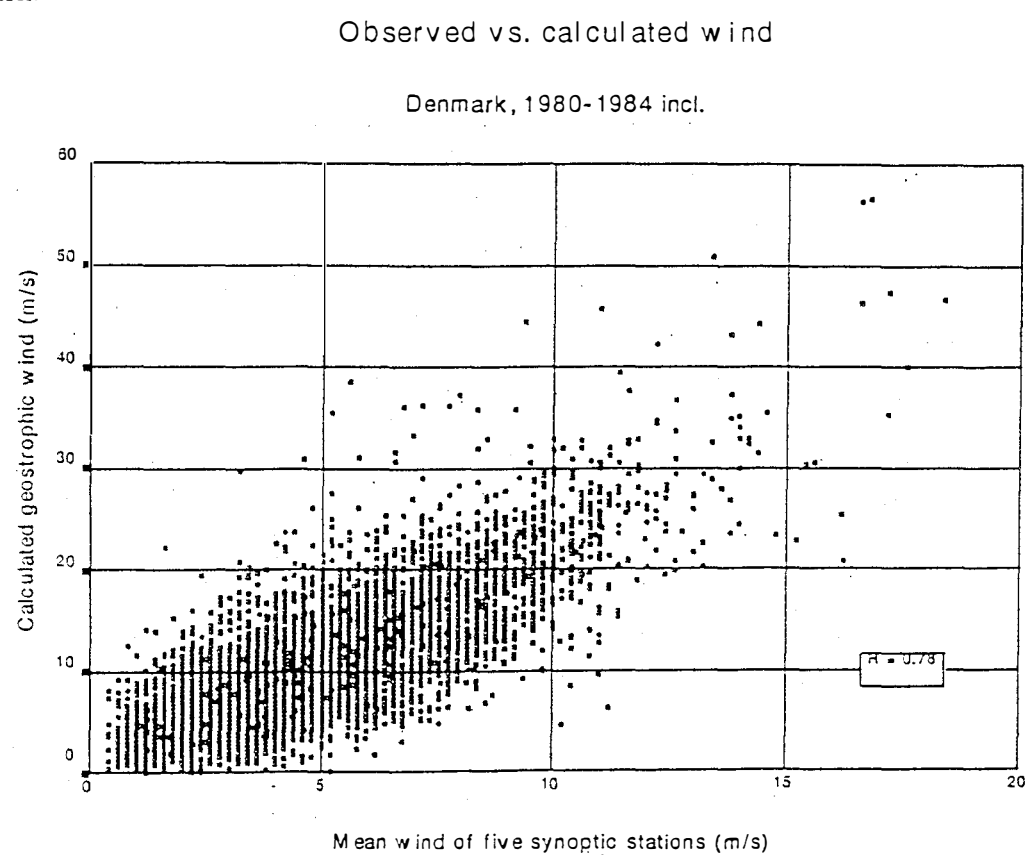


Figure 2: Time series of number of daily geostrophic wind speeds exceeding 25 m/s, derived from the triangle Göteborg-Visby-Lund in Southern Sweden. The solid line represents a low-pass filter.

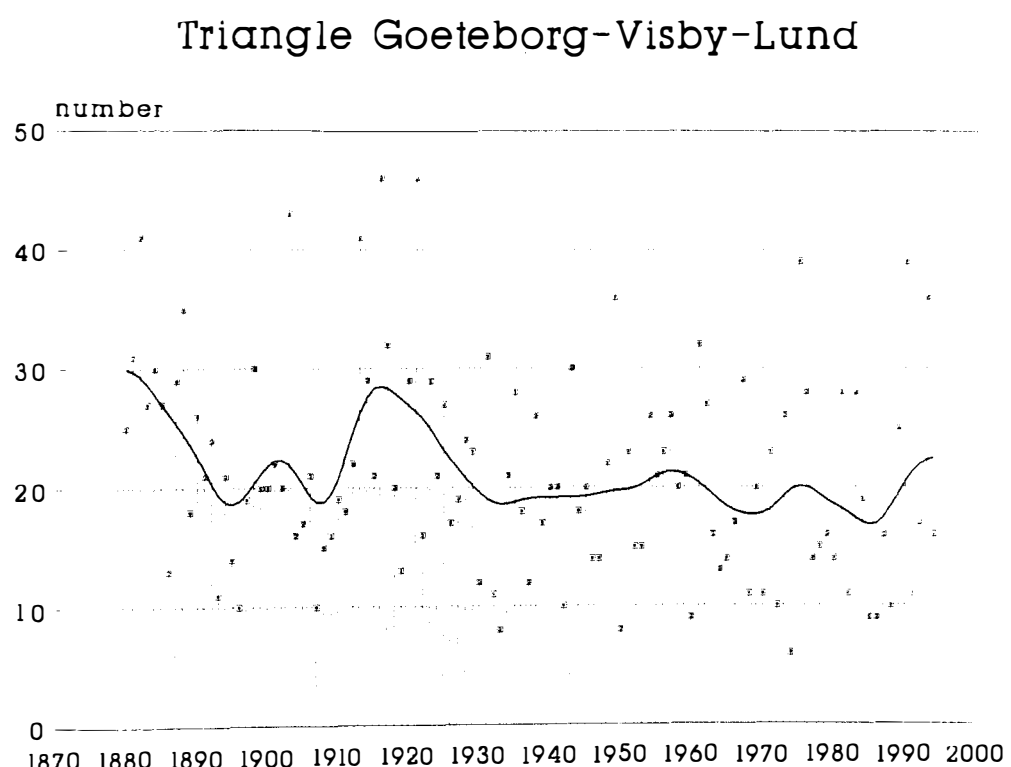
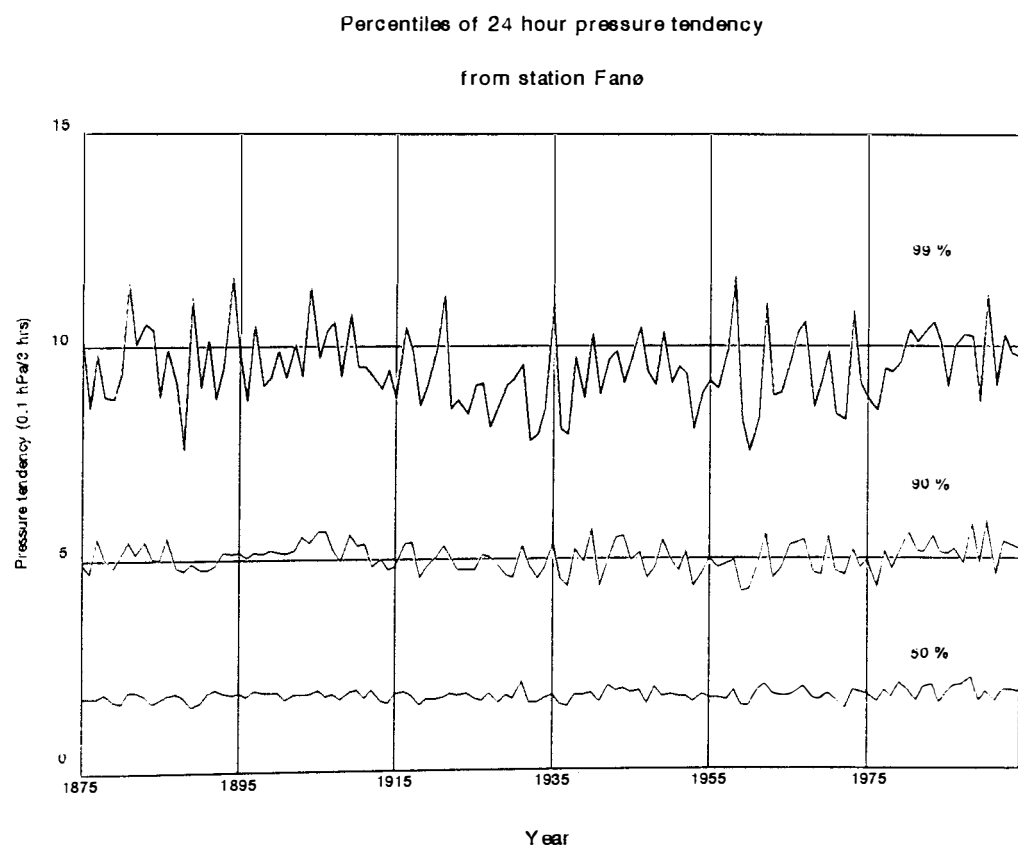


Figure 3: Time series of percentiles of 24-hour pressure tendencies over Denmark Units: 0.1 hPa/3 hrs.



Ocean Weather Station M Significant Wave Height [m]

Figure 5: Time series of ~~1%~~, ~~5%~~, ~~10%~~, ~~25%~~ and 50% percentiles of the annual wave height distribution at Ocean Weather Station M. Units: m.
Updated from WASA (1994).

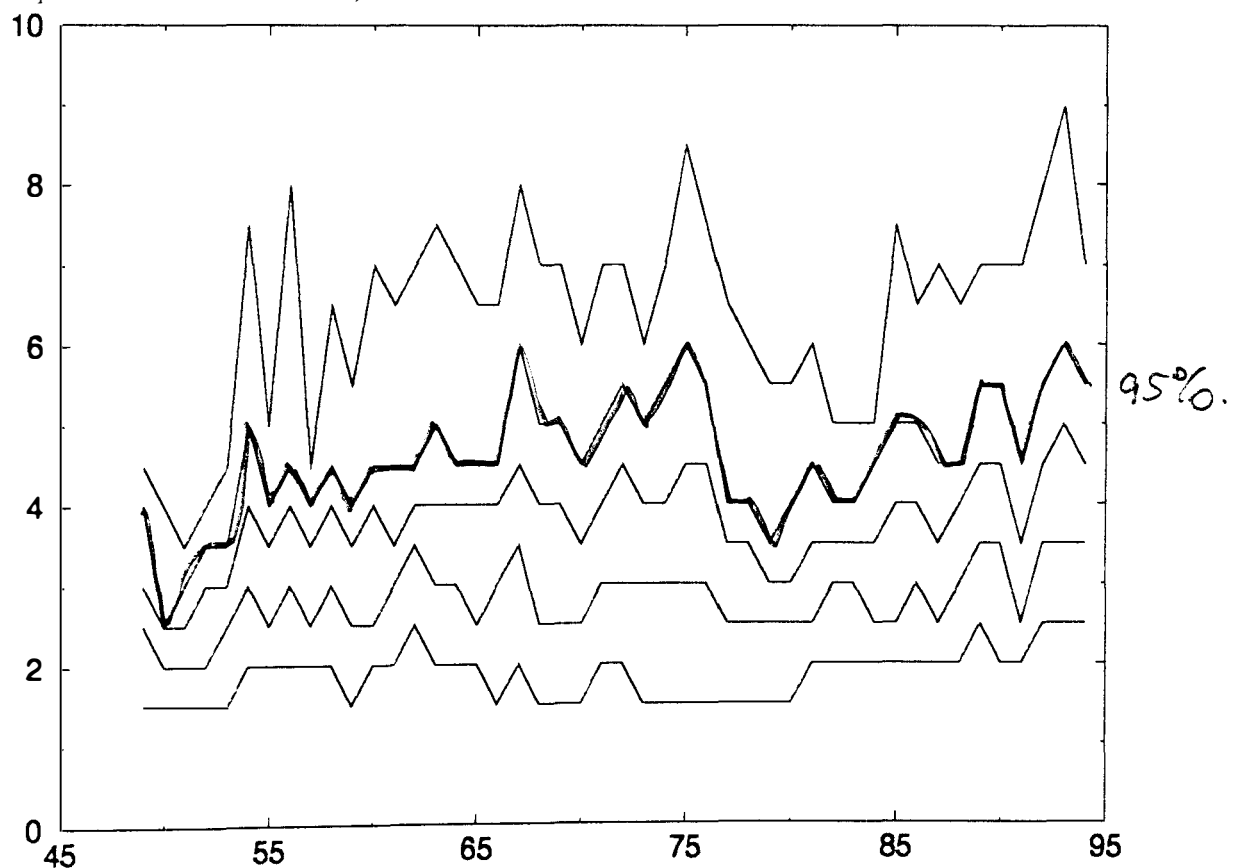


Figure 10: Example of a KNMI analysis of the wave height field prepared for shiprouting purposes.

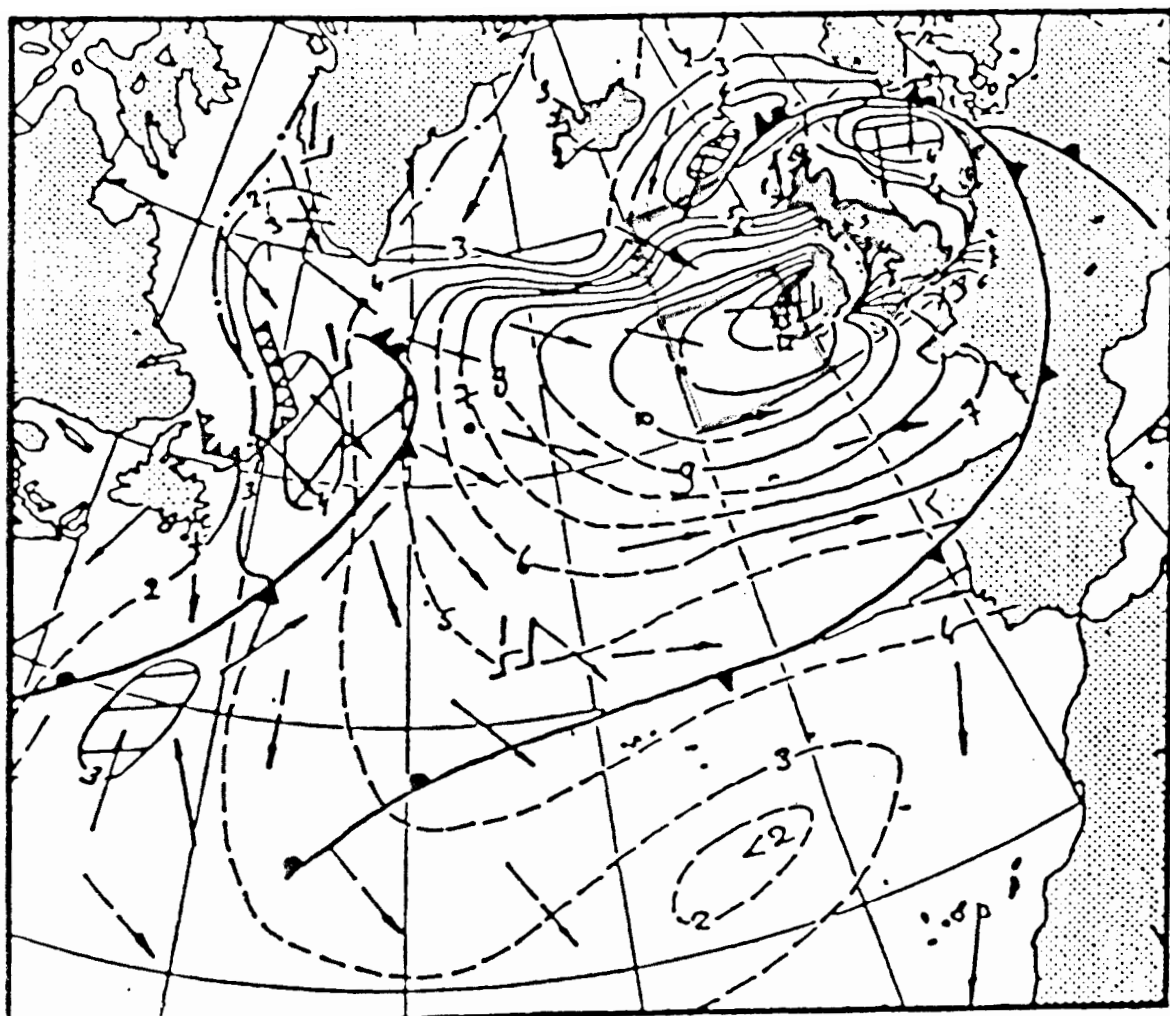
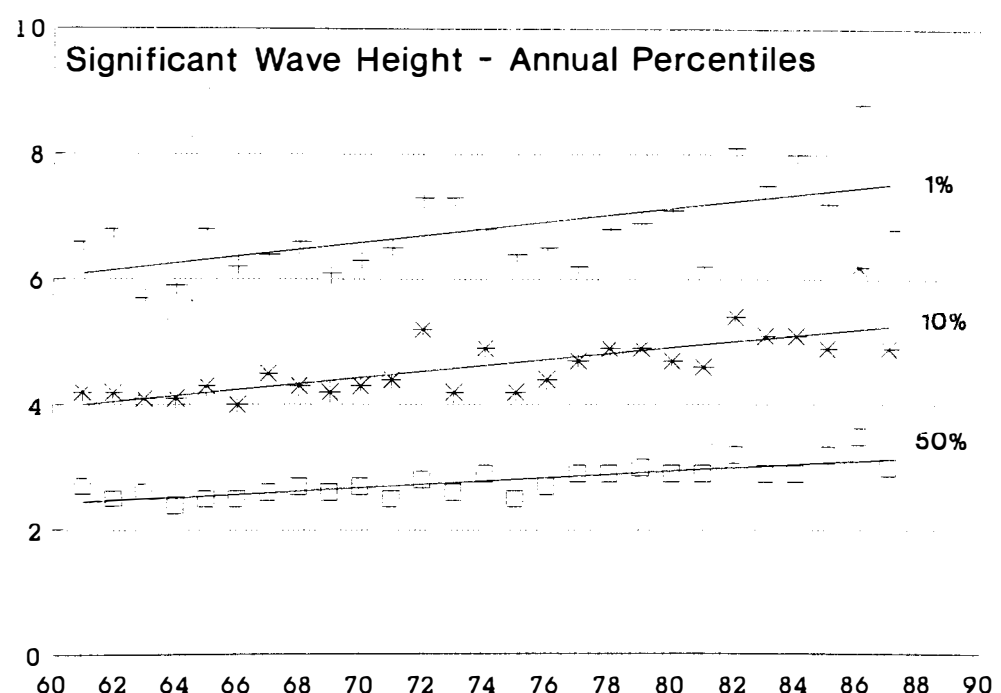


Figure 6: Time series of 1%, 10% and 50% percentiles of the annual wave height distribution in an area west of Ireland (10° - 20° W, 50° - 55° N) derived from operational shiprouting maps prepared by KNMI. Units: m.



WAM wave model set-up:



- coarse North Atlantic grid

78.0° W - 48.0° E, $\Delta = 1.50^\circ$

9.5° N - 80.0° N, $\Delta = 1.50^\circ$

deep water model with 2094 active grid points

- nested fine grid in the Northeast Atlantic

30.0° W - 45.0° E, $\Delta = 0.75^\circ$

38.0° N - 77.0° N, $\Delta = 0.50^\circ$

shallow water model with 4105 active grid points

- spectral resolution

15.0° for directions

25 frequencies from 0.042 - 0.411 Hz

- input wind fields

**coarse grid: operational wind analysis prepared
by FNOC, 6-hourly**

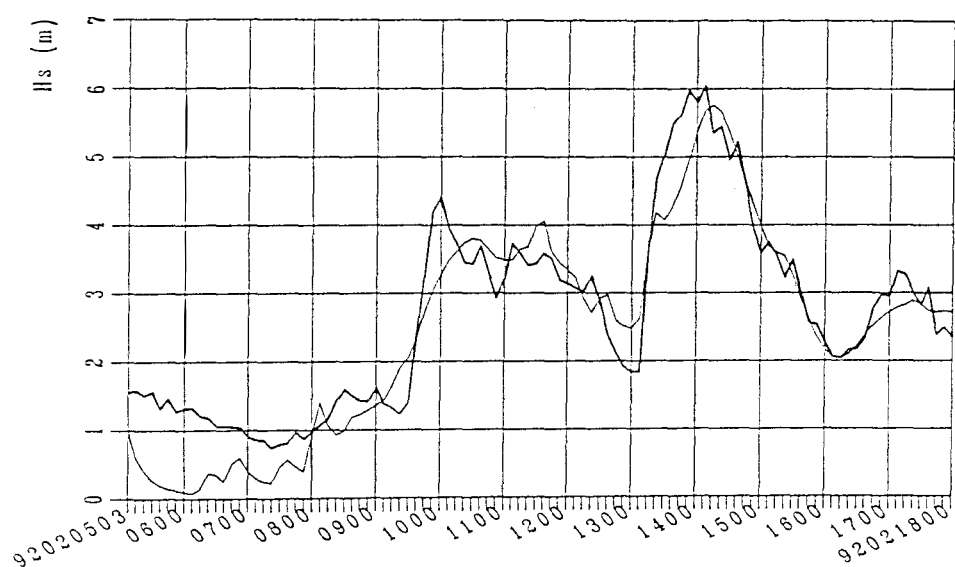
**fine grid: wind estimates from air-pressure analyses
prepared by DNMI, 6-hourly**

- monthly update of sea ice cover

- output every 3 hours at all grid points

**wave spectra,
integrated parameter**

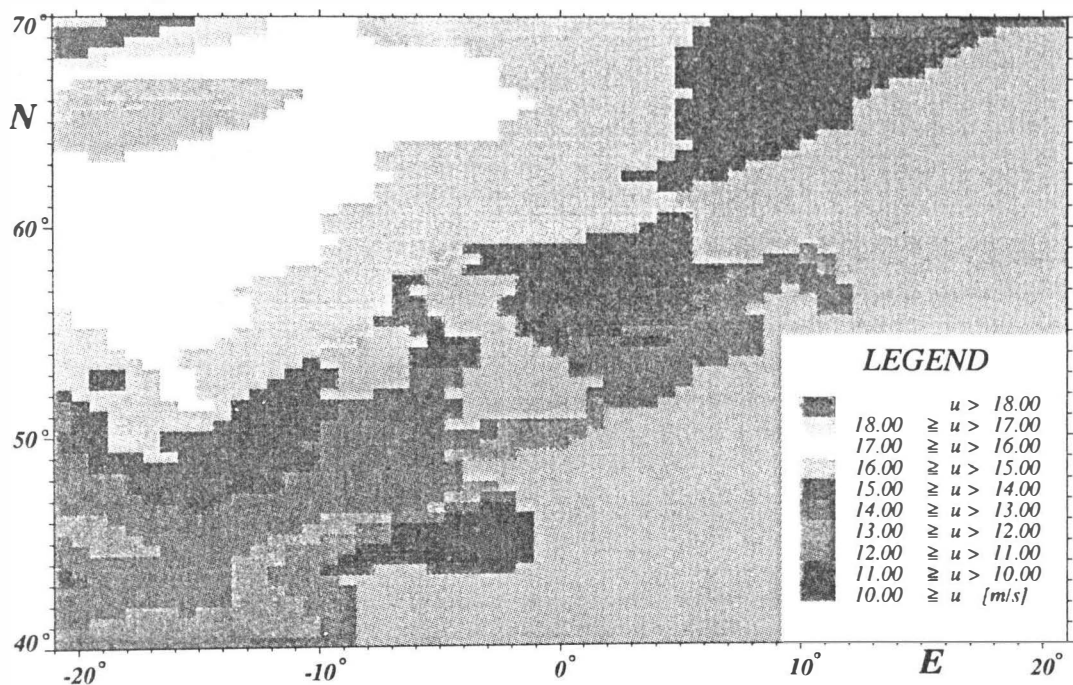
WAM/FNOC PBLM winds: BILBAO, Hs(m)
THIN LINE: MODEL / GROSS LINE: BUOY



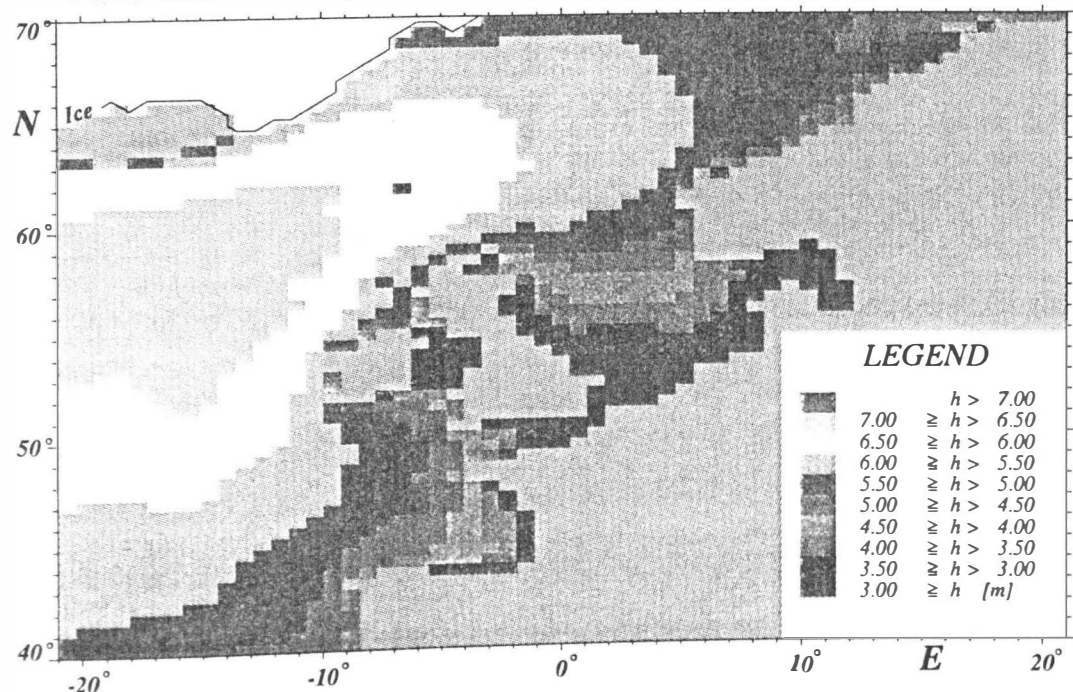
About WAM model:

- model runs for any given regional or global grid with a prescribed topographic data set
- the grid resolution can be arbitrary in space in time
- the propagation can be done on a ϕ, λ - or on a cartesian grid
- the model runs for deep and shallow water and includes depth and current refraction
- the integration can be interrupted and restarted at arbitrary times
- the source term integration is done with an implicit integration scheme
- the propagation scheme is a first order upwind flux scheme
- the model can be run in a nested mode

Wind speed : mean 90% 1955-1994

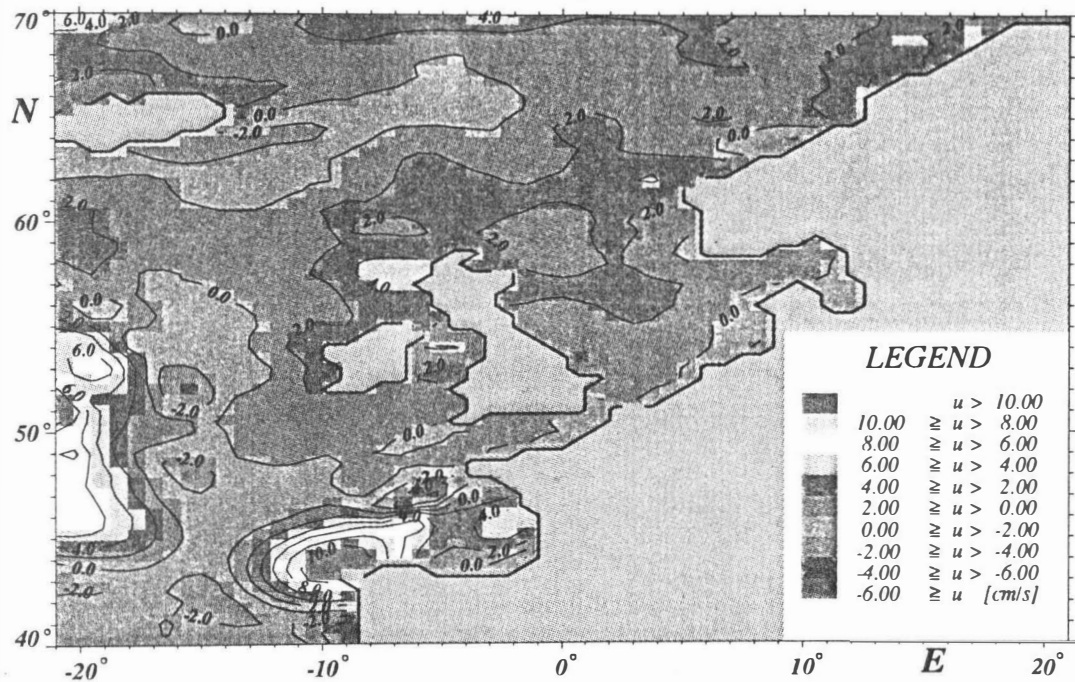


Significant wave height : mean 90% 1955-1994

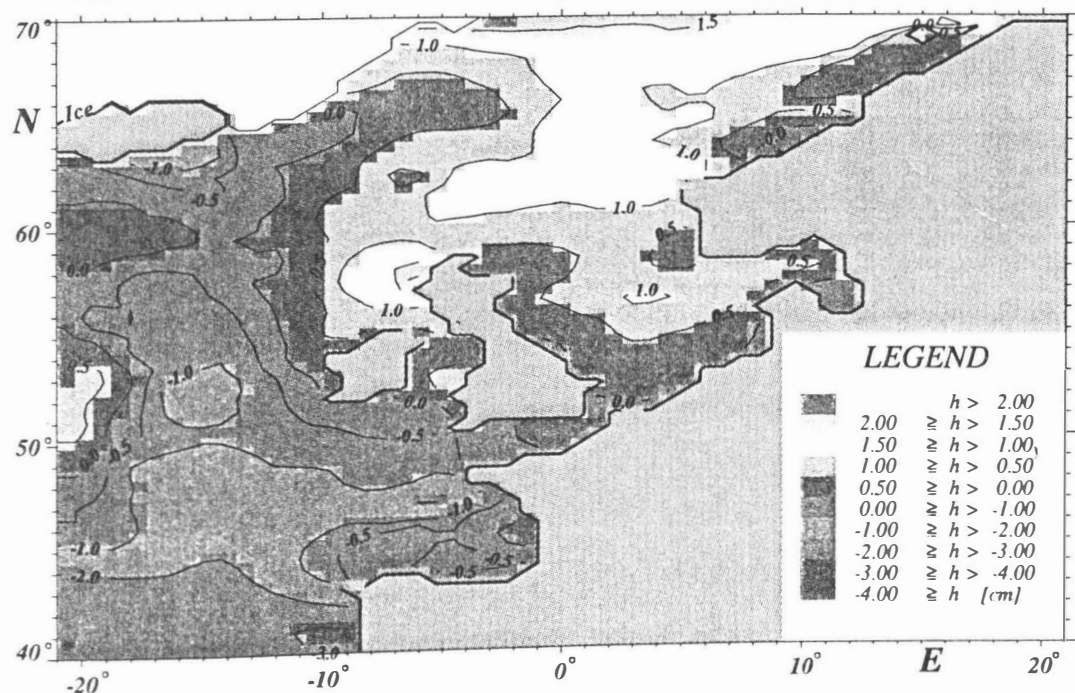


Distribution of mean 90 percentile of the wind speed (above) and SWH (below) based on analysis of 40 years wave model (1955-94) over the North Atlantic with forcing provided by DNMI.

Wind speed 90% : change/year [cm/s] 1955-1994

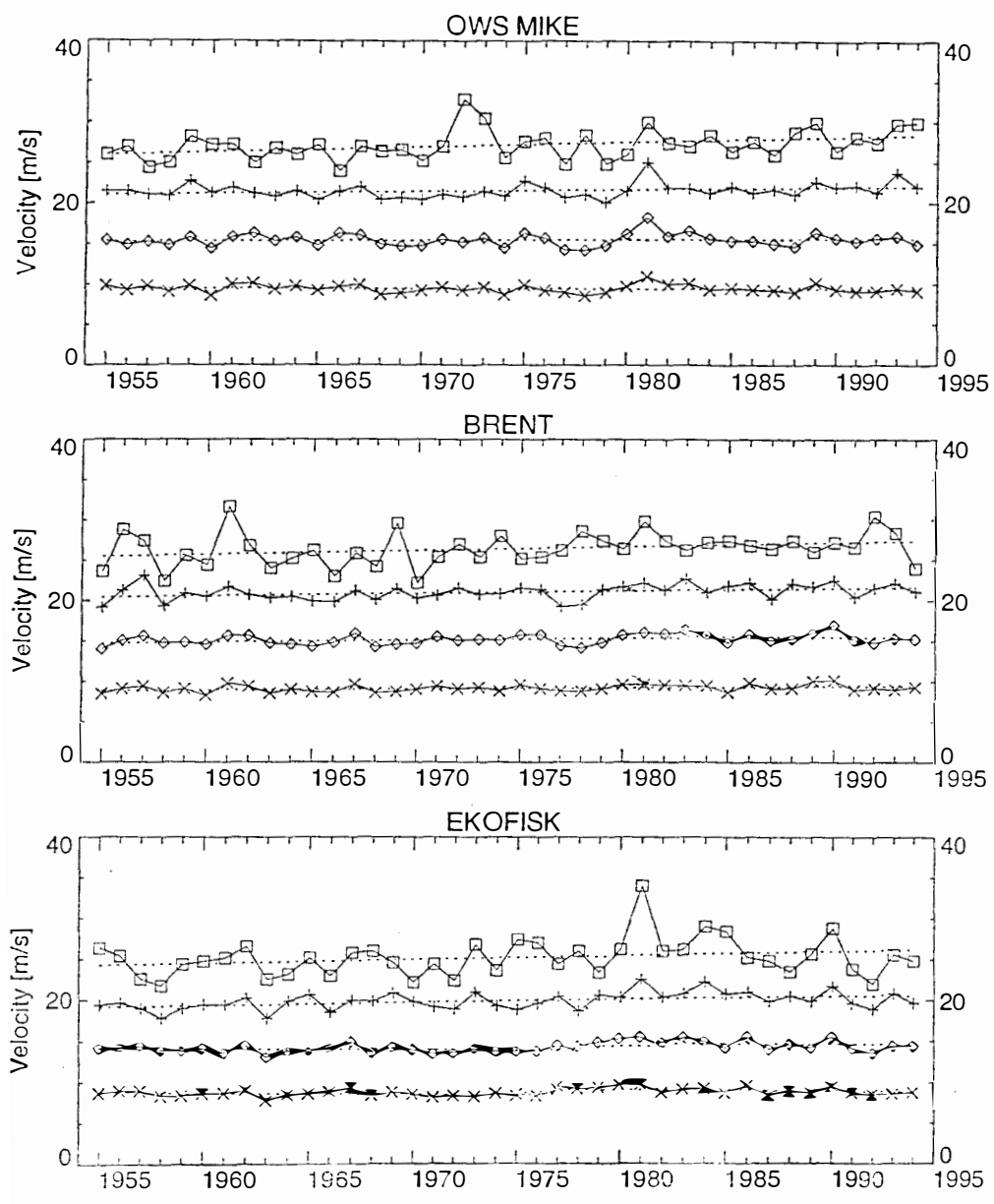


Significant wave height 90% : change/year [cm] 1955-1994

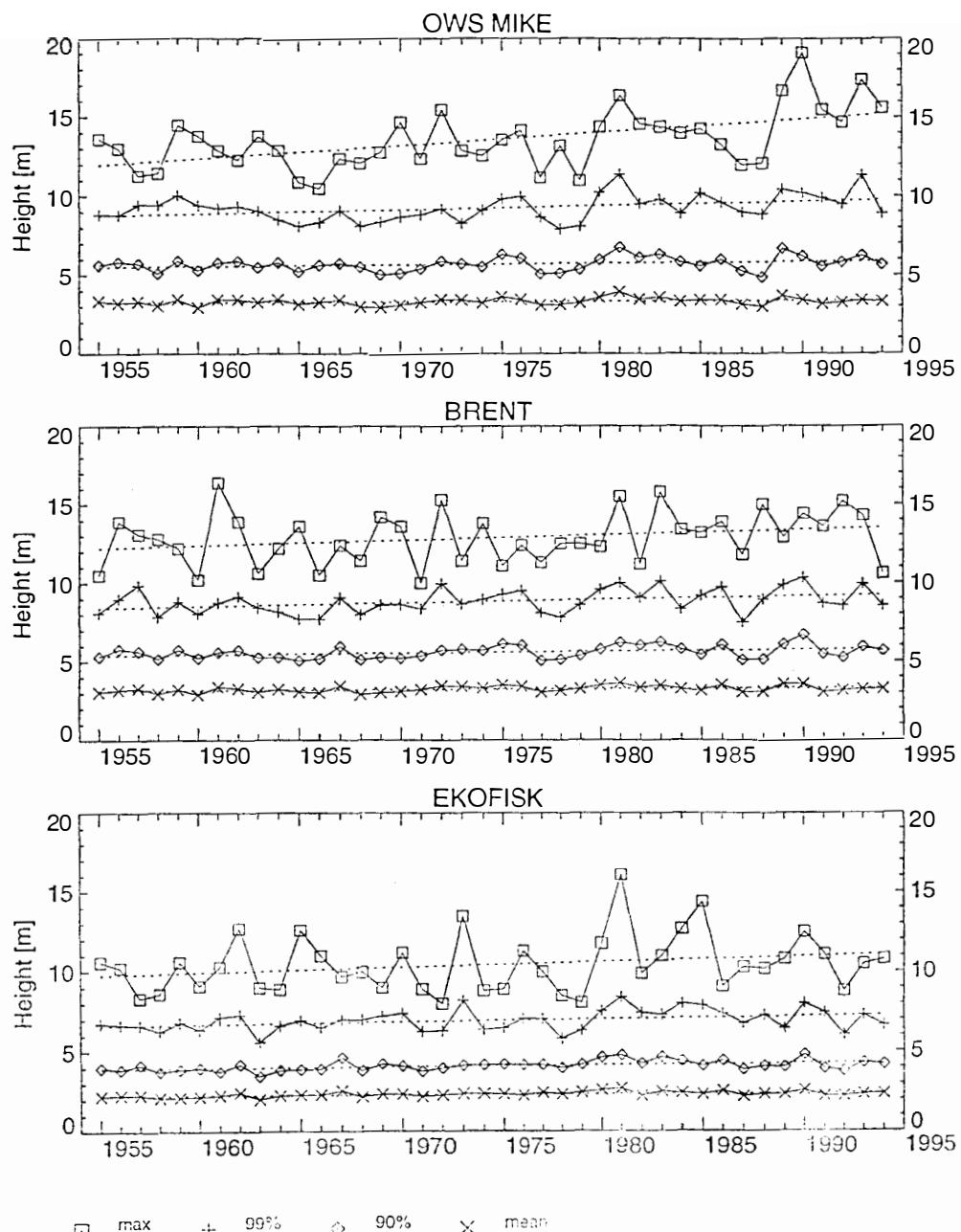


Distribution of changes per year of the 90% of the wind speed (above) and SWH (below) based on analysis of 40 years wave model (1955-94) over the North Atlantic with forcing provided by FNOC and DNMI.

Wind speed
 WASA fine grid run

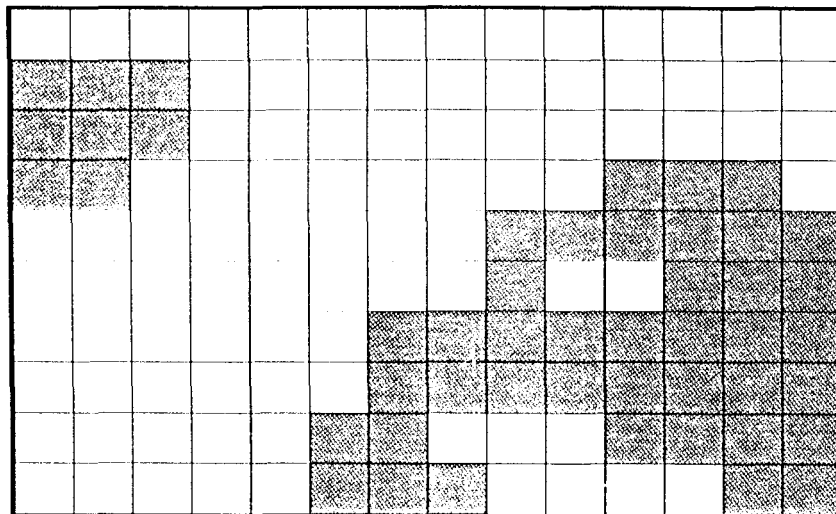


Total significant wave height
 WASA fine grid run

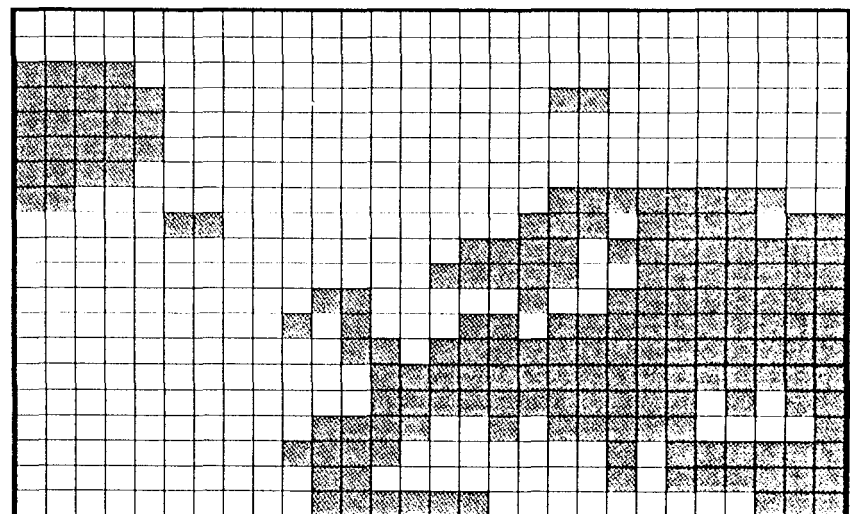


European part of the land-sea mask for different T-model resolutions

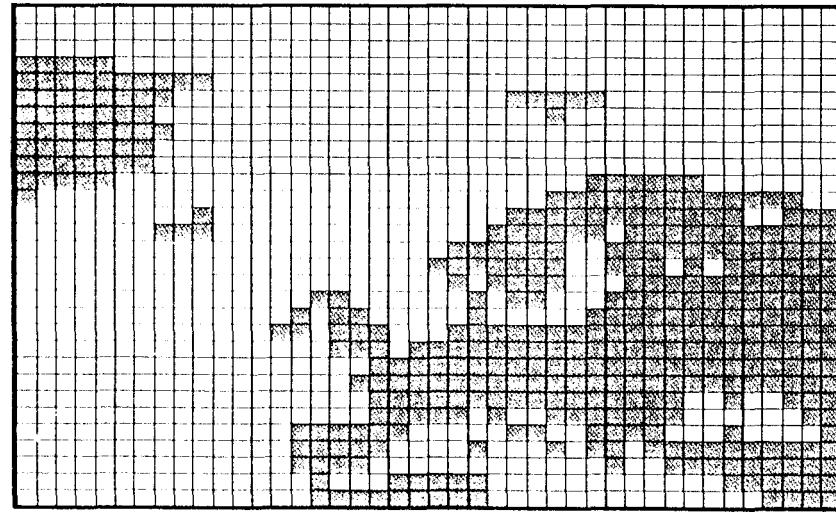
a) T21



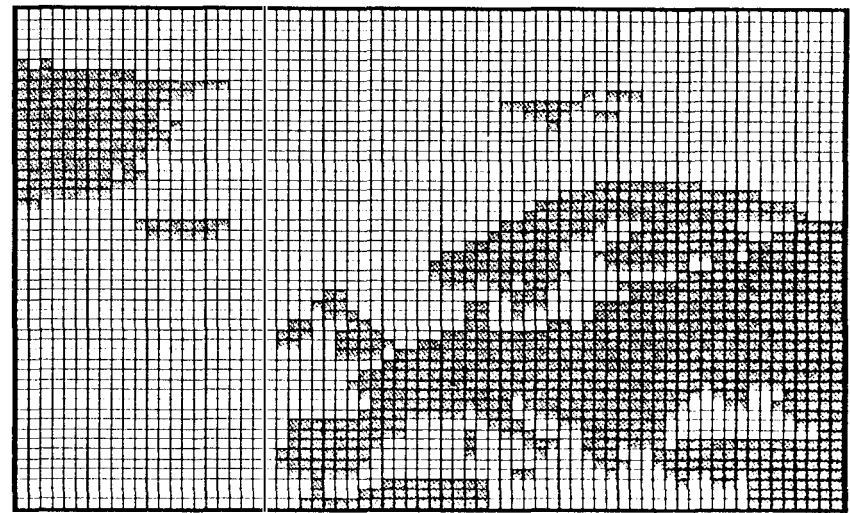
b) T42



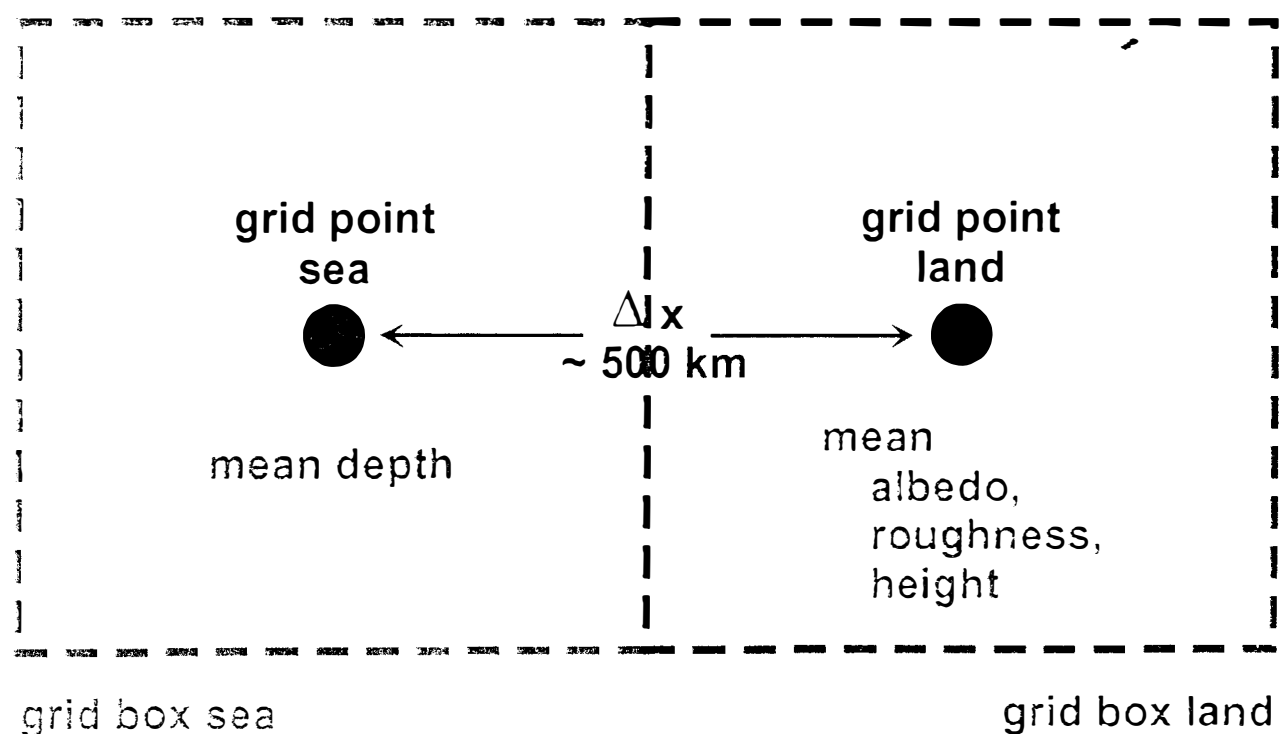
c) T63



d) T106

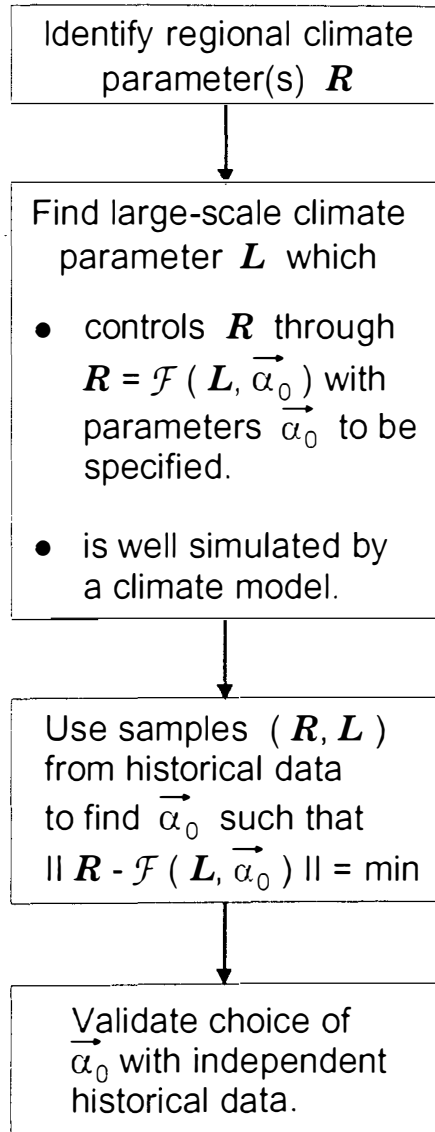


What does a climate model know about the coast ?

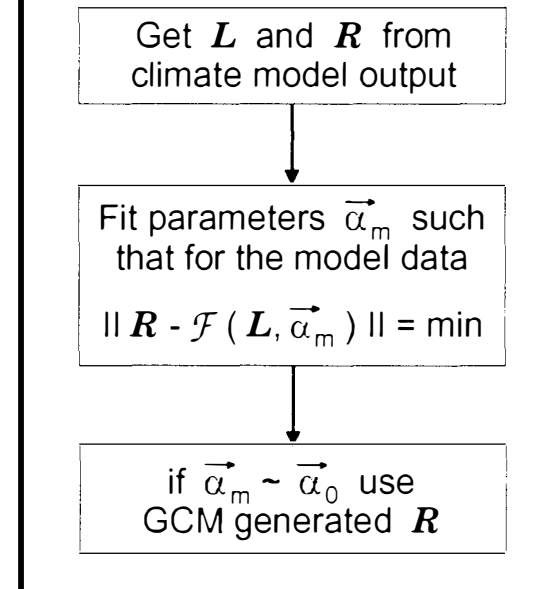


⇒ coast = contrast in some
box-averaged properties

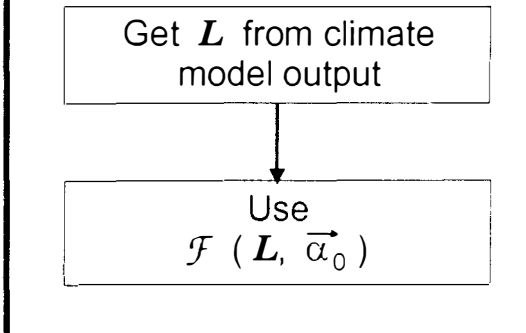
MODEL DESIGN



TEST CLIMATE MODEL



MODEL APPLICATION



Downscaling - relating a 'local' parameter of interest to well simulated 'large scale' parameters

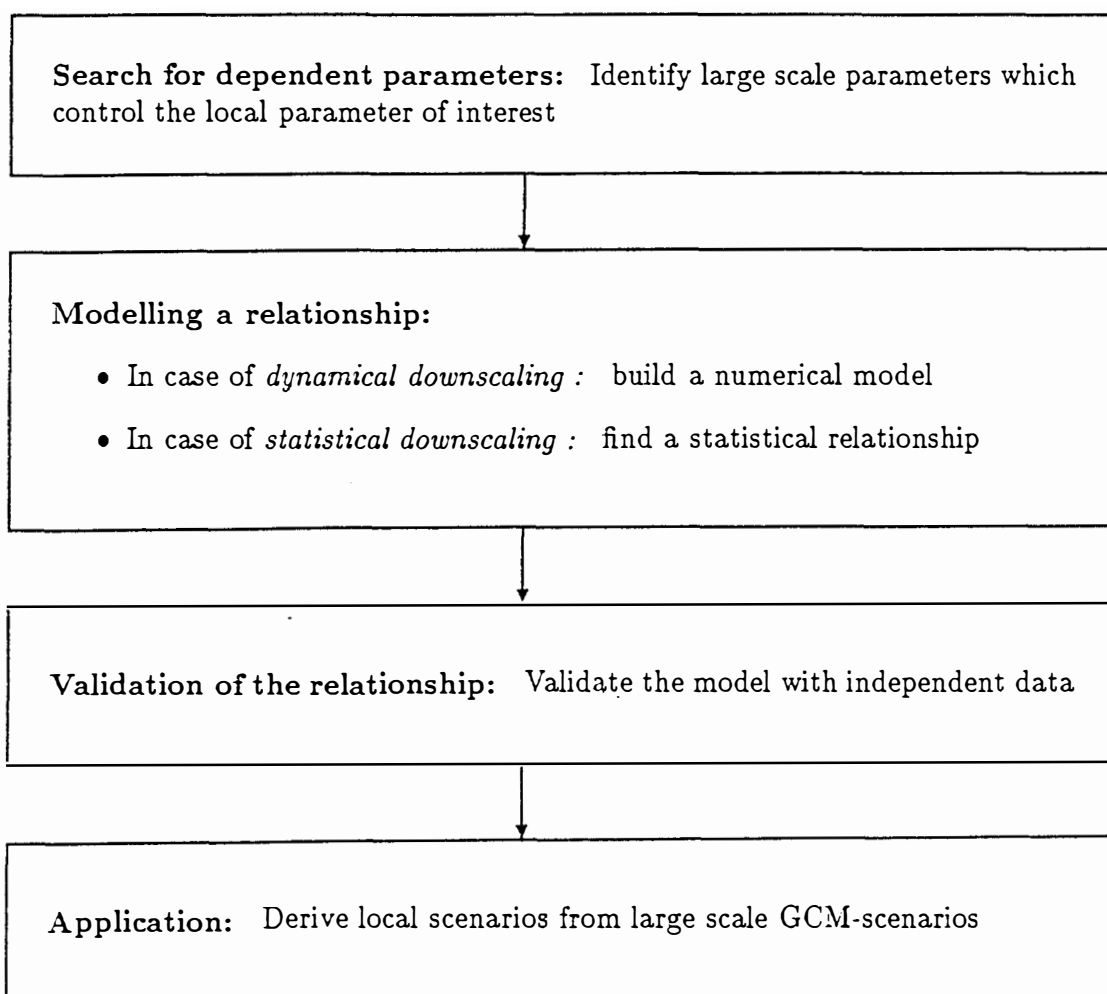
The necessity of downscaling:

In climate impact research downscaling techniques are required because

- GCMs reproduce 'large scales' but fail on 'small scales'
- spatially and temporally well resolved data is needed

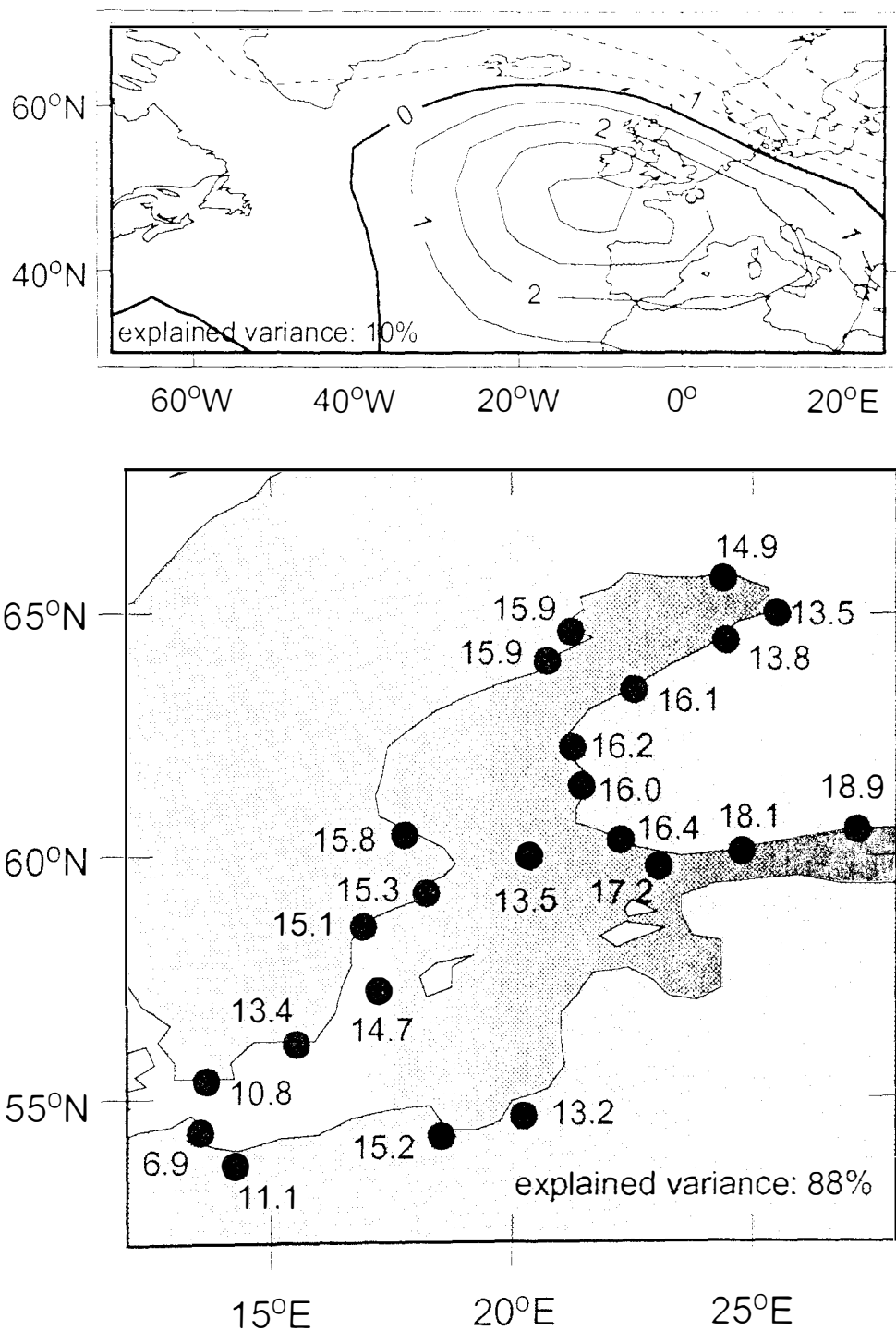
One distinguishes between '*dynamical downscaling*' (also called 'nesting') and '*statistical downscaling*' (e.g. 'analogue models', 'regression models', 'weather generators')

The concept of downscaling:

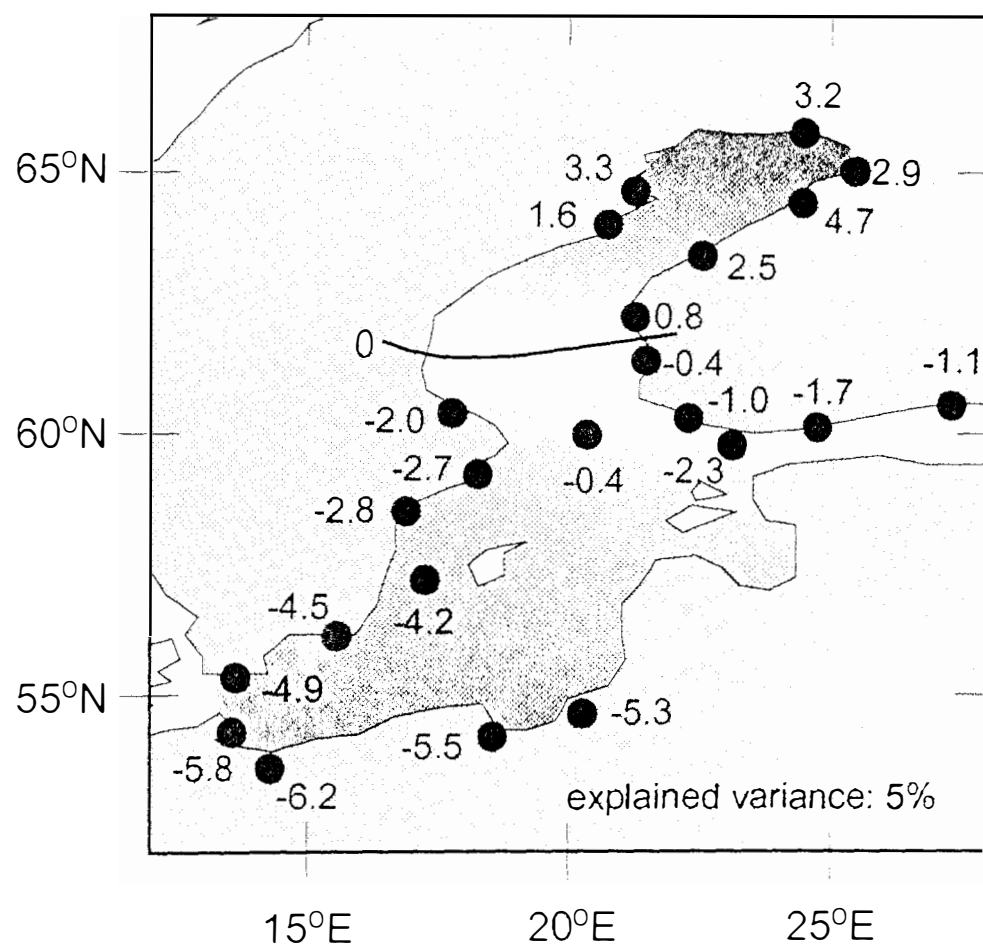
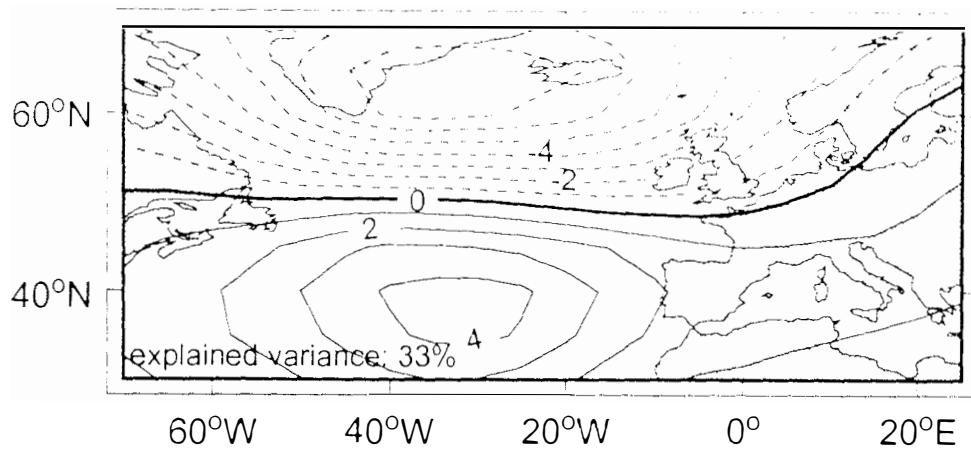


Example: BALTIC SEA

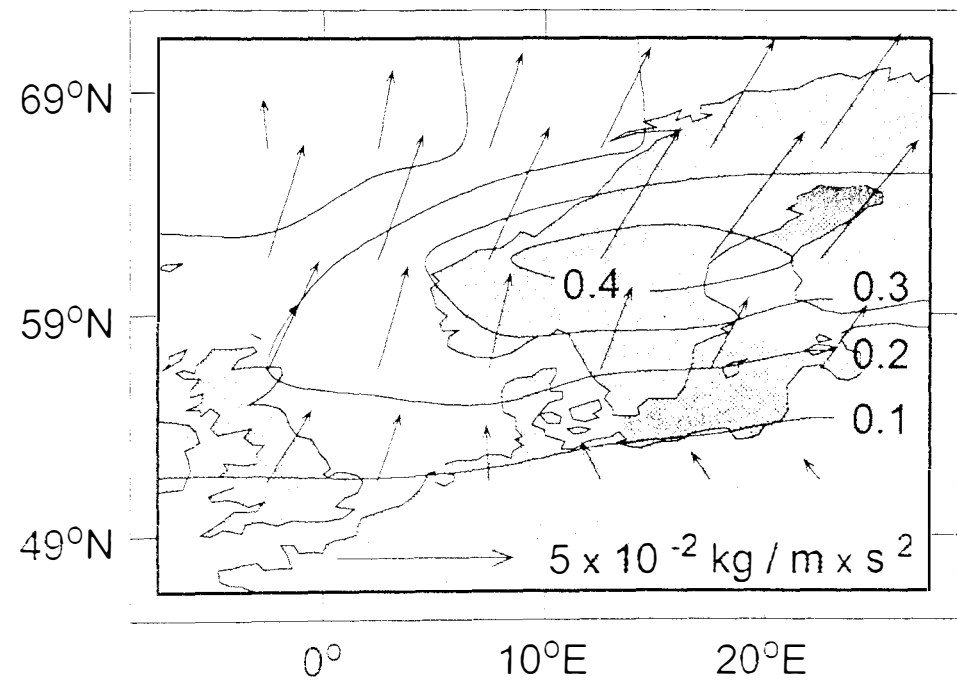
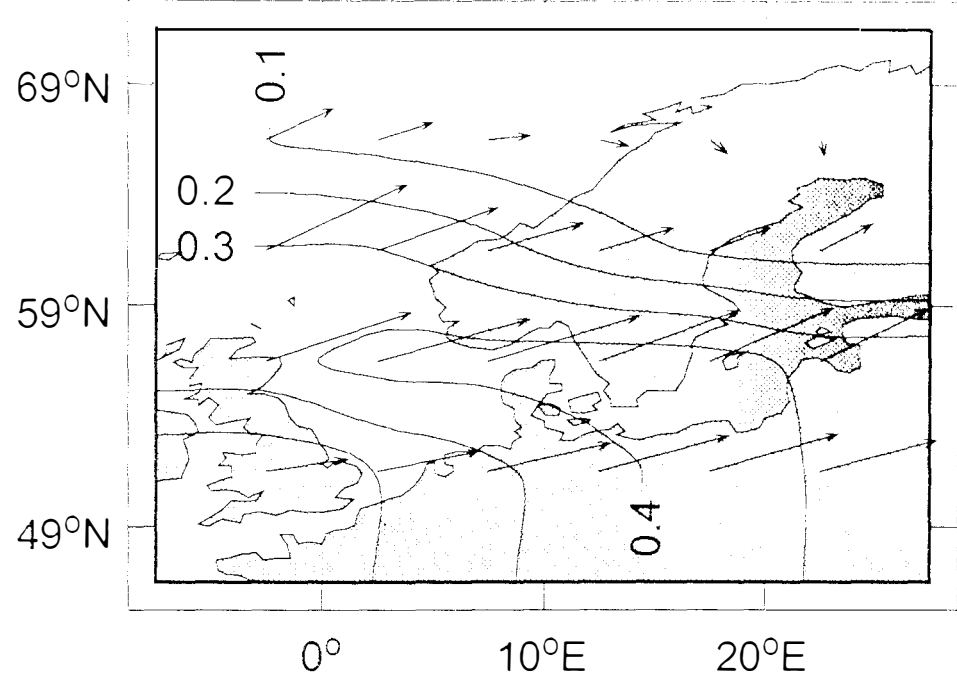
- **Regional Parameter R :**
 - Sea level at 14 stations along the coast of the Baltic Sea;
 - Detrended data (to avoid land sinking/rising signals);
 - Mean annual cycle subtracted;
 - Seasonal means (DJF) from 1905 - 1972.
- **Large-scale parameter L :**
 - North Atlantic sea level pressure $70^{\circ}W - 35^{\circ}E \times 30^{\circ}N - 85^{\circ}N$
 - Mean annual cycle and trend subtracted.
 - Seasonal means (DJF) from 1905 - 1972
- **Fit of CCA-model** with data from 1951-70.



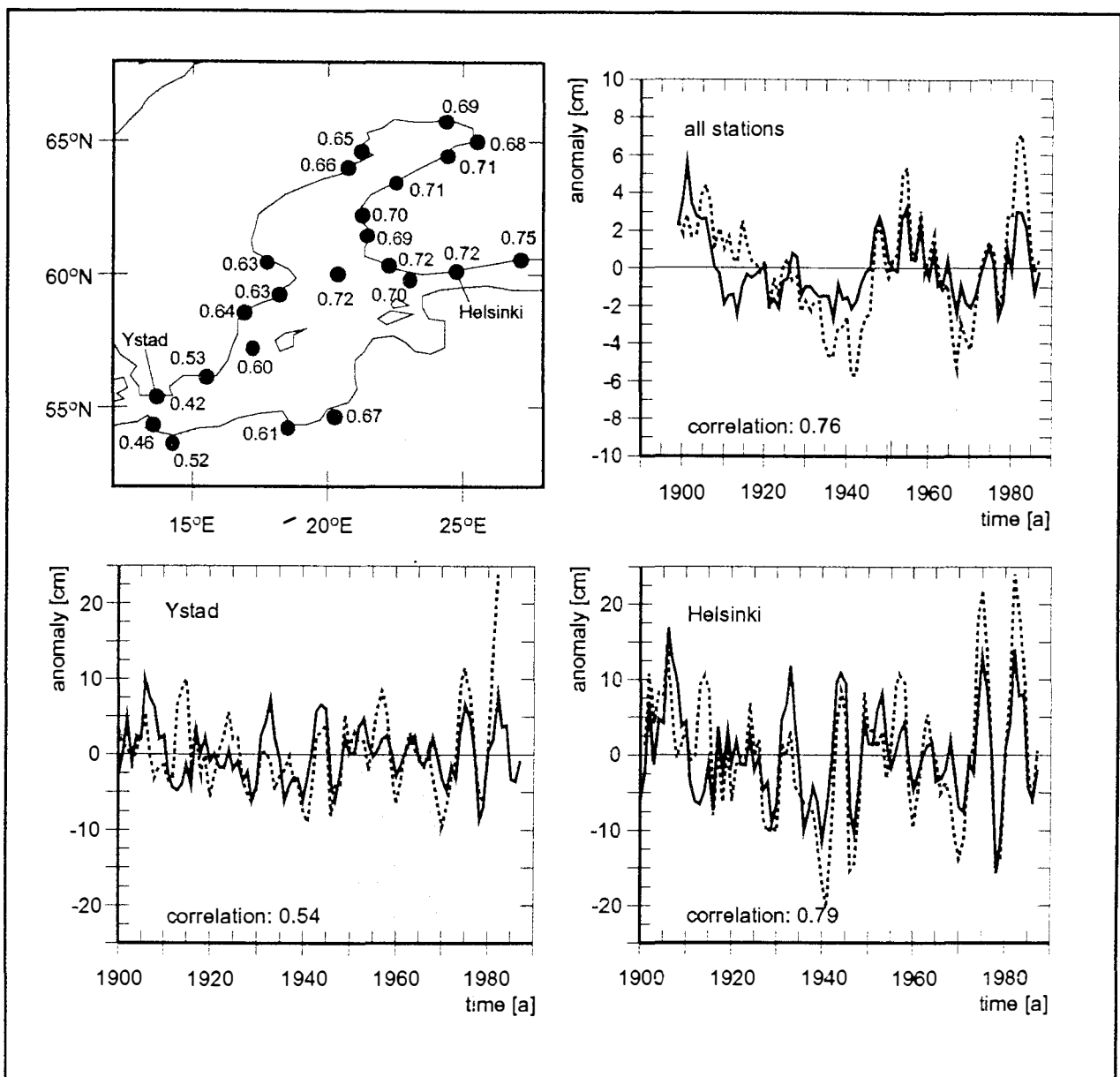
114Hg2.ds4



114HHAj1.ds4



1104A0203s4



tag1.ds4

Downscaling Coastal Sea Level

Limited Area Model (LAM):

- regional version of the GCM OPYC
- horizontal resolution 10km x 10km in the North Sea
- diabatic ocean GCM based on primitive equations
- isopycnals as Lagrangian coordinates in the vertical
- mixed layer model
- sea ice and snow model

Simulations:

The LAM is forced with atmospheric 12 hourly surface data from

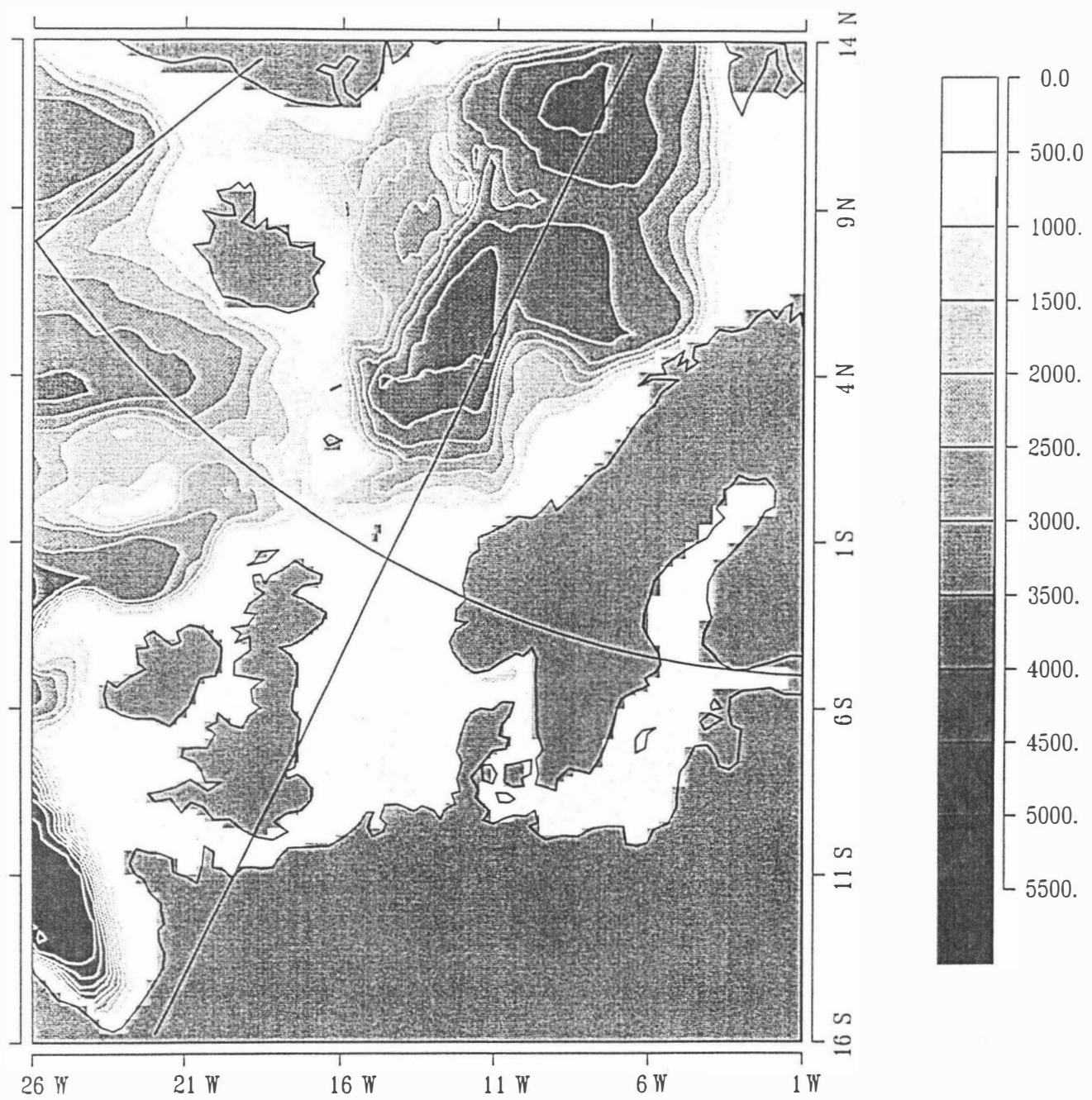
- the ECMWF-T106 re-analysis project.

Length of the integration: 13 years (1981-1993)

- the ECHAM3-T106 "time-slice" CTRL and 2xCO₂ runs.

Length of the Integration: 5 years + 1 winter

Figure 1: The topography [m] of the LAM.



Frank Kauker, GKSS

Figure 2: ECMWF run. The mean surface circulation in winter (DJF) in the North Sea.

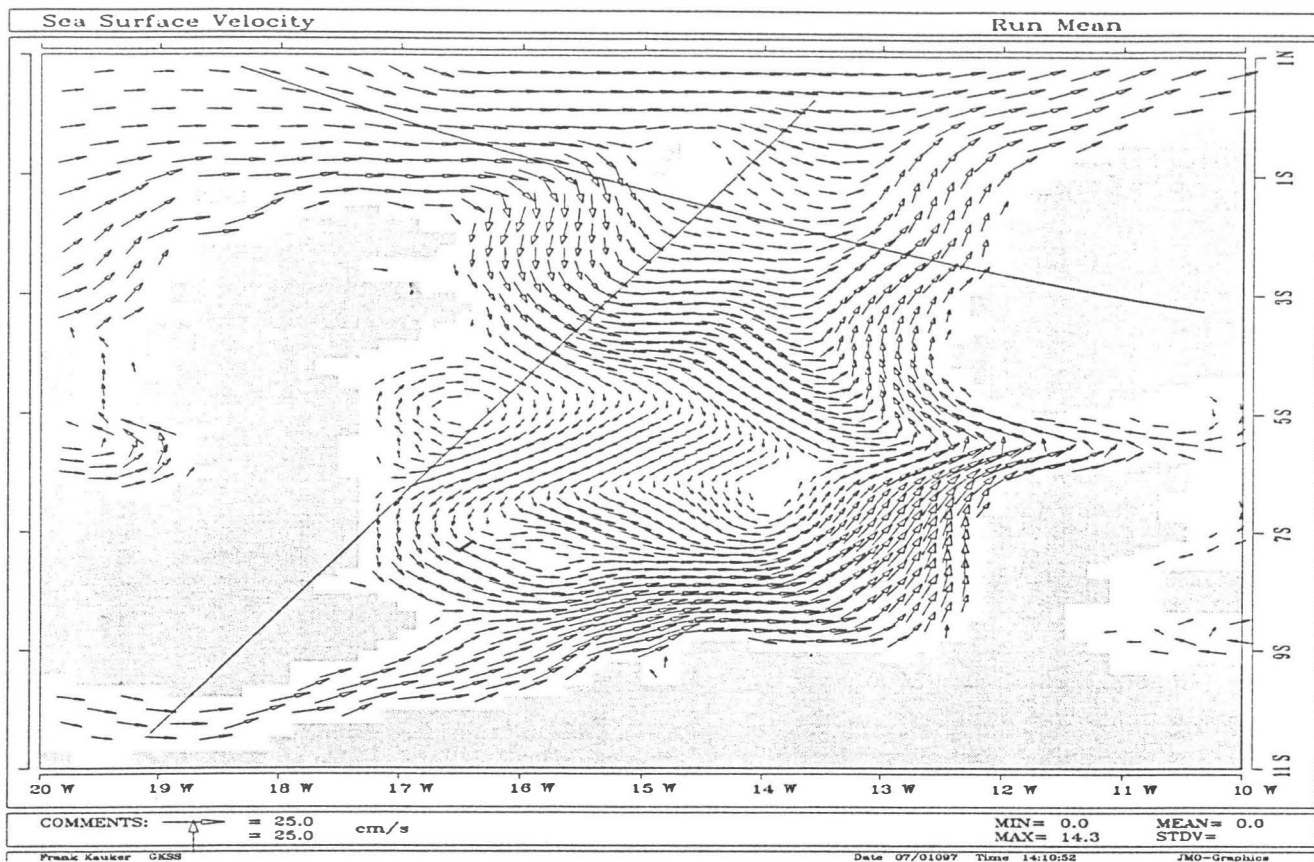


Figure 3: "time-slice" run. The mean surface circulation difference Scenario - Control in winter.

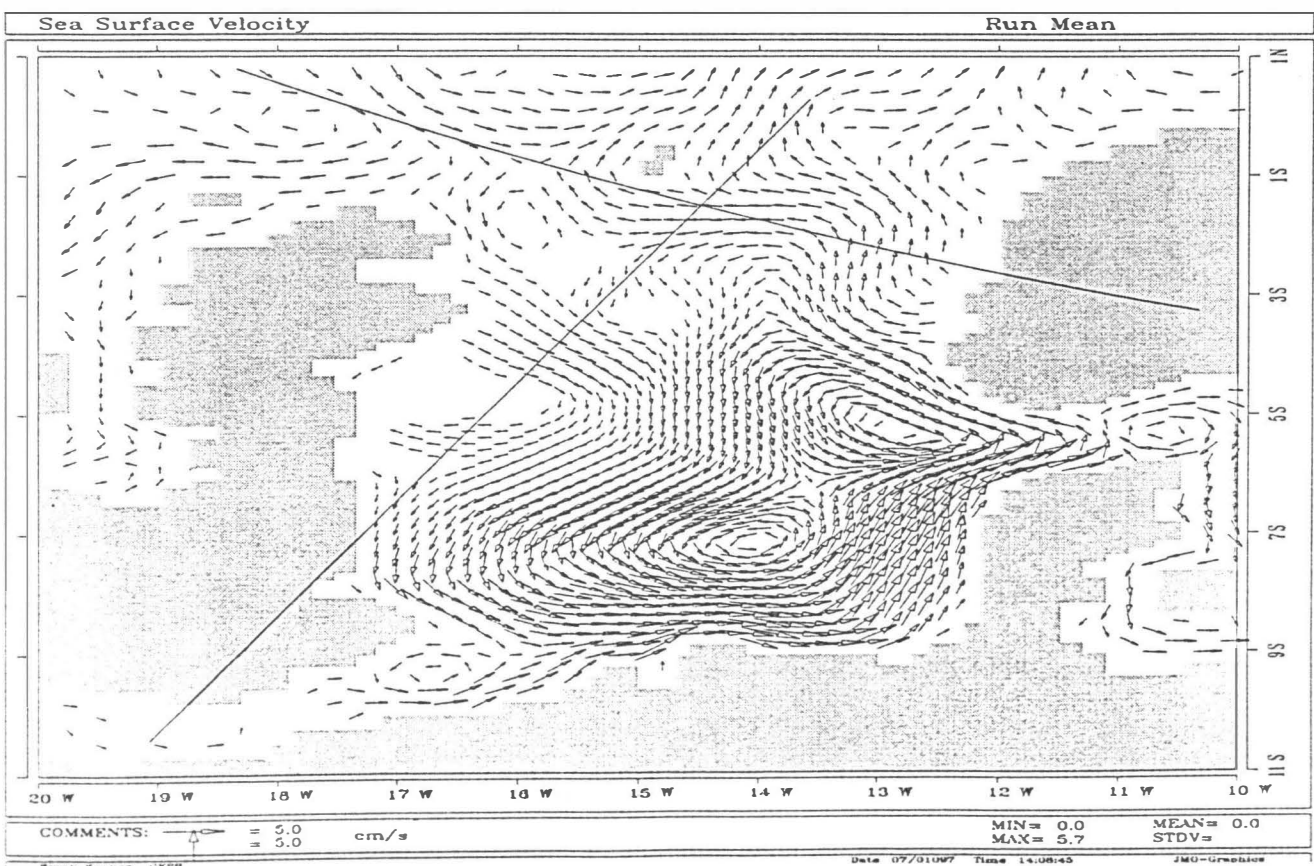


Figure 5: "time-slice"-Control run. The 1st EOF of the surface circulation in winter.

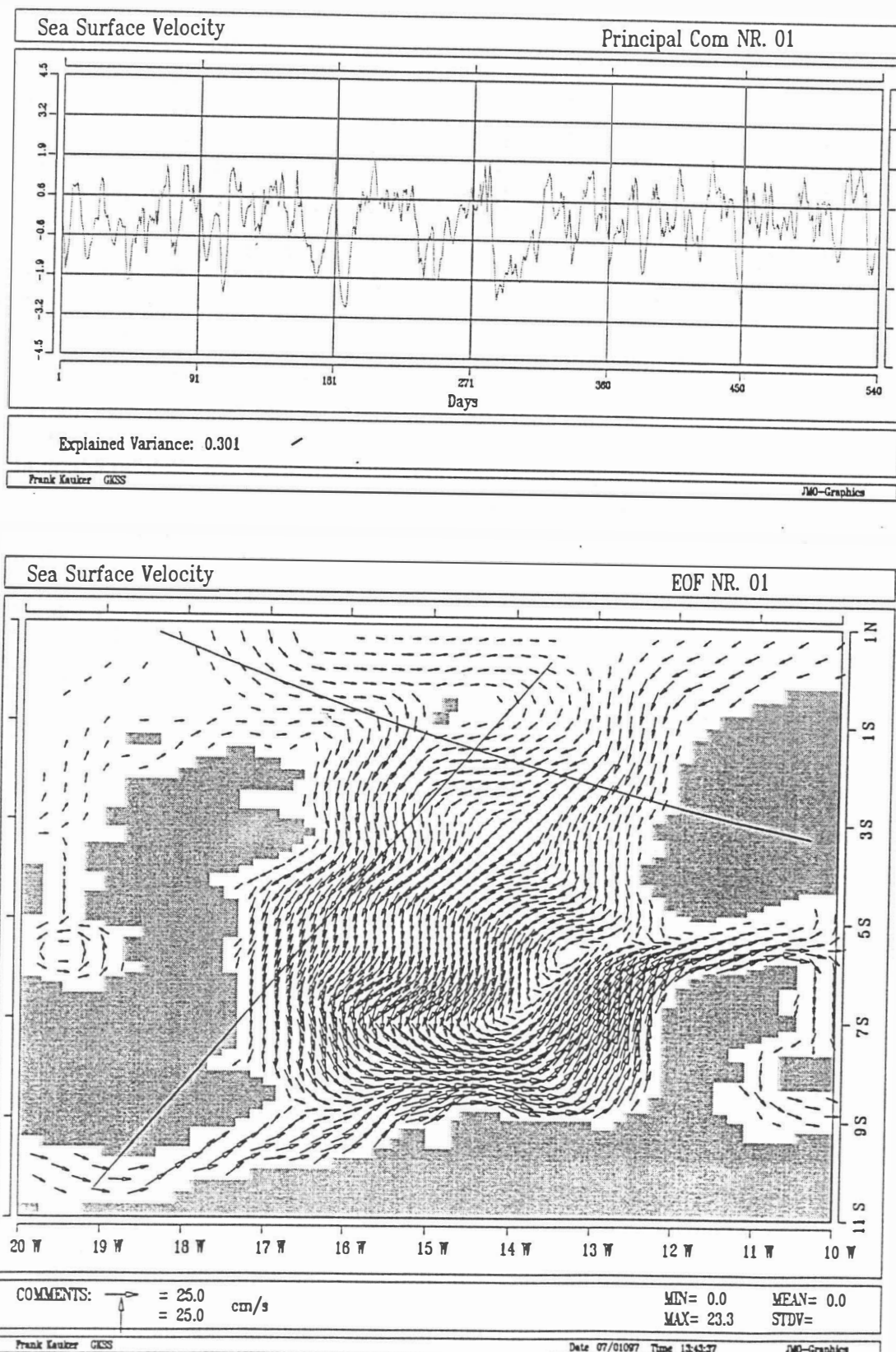
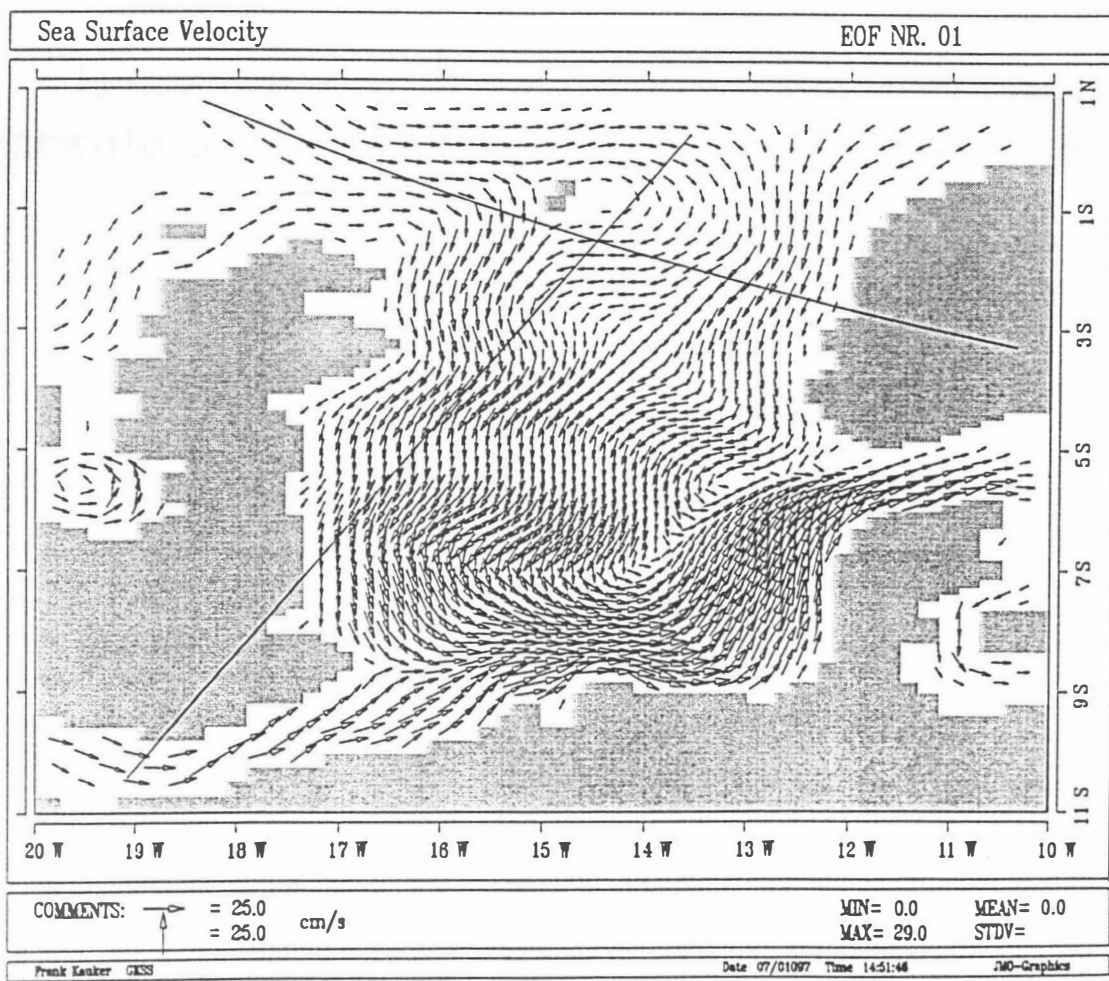
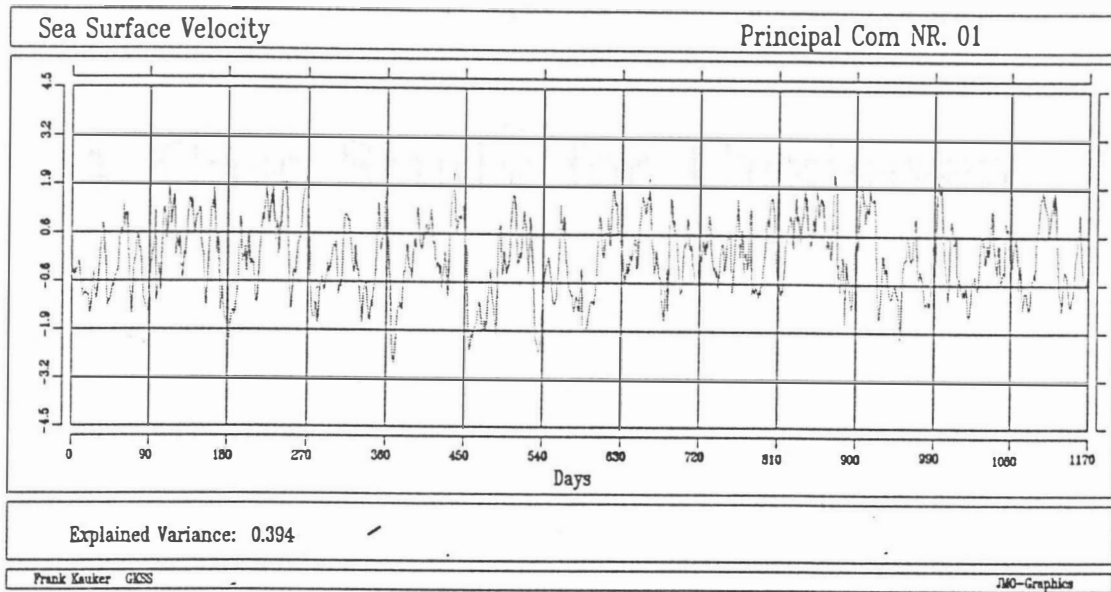


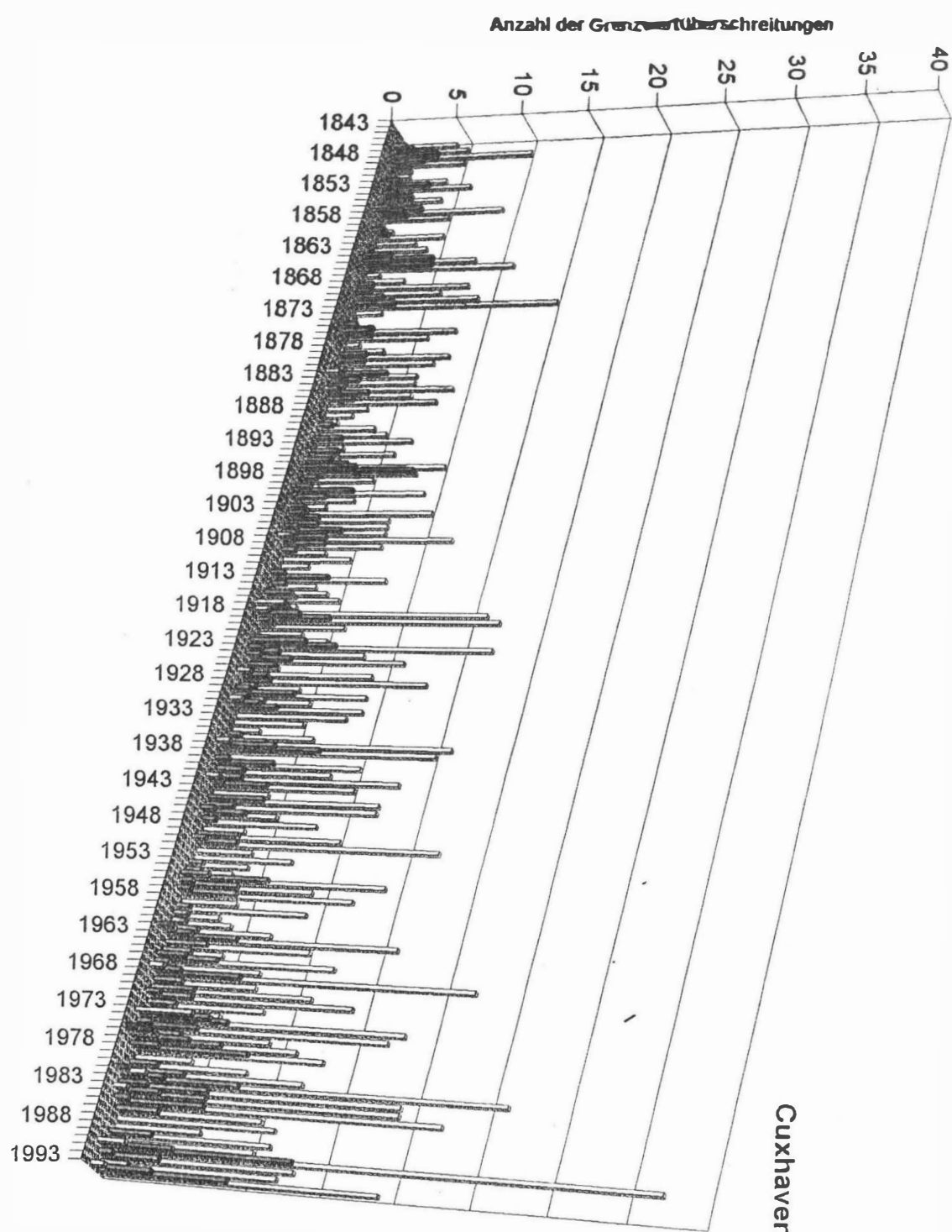
Figure 4: ECMWF run. The 1st EOF of the surface circulation in winter.



Changing Statistics of Storm Surges in the Recent Past and in the Foreseeable Future?

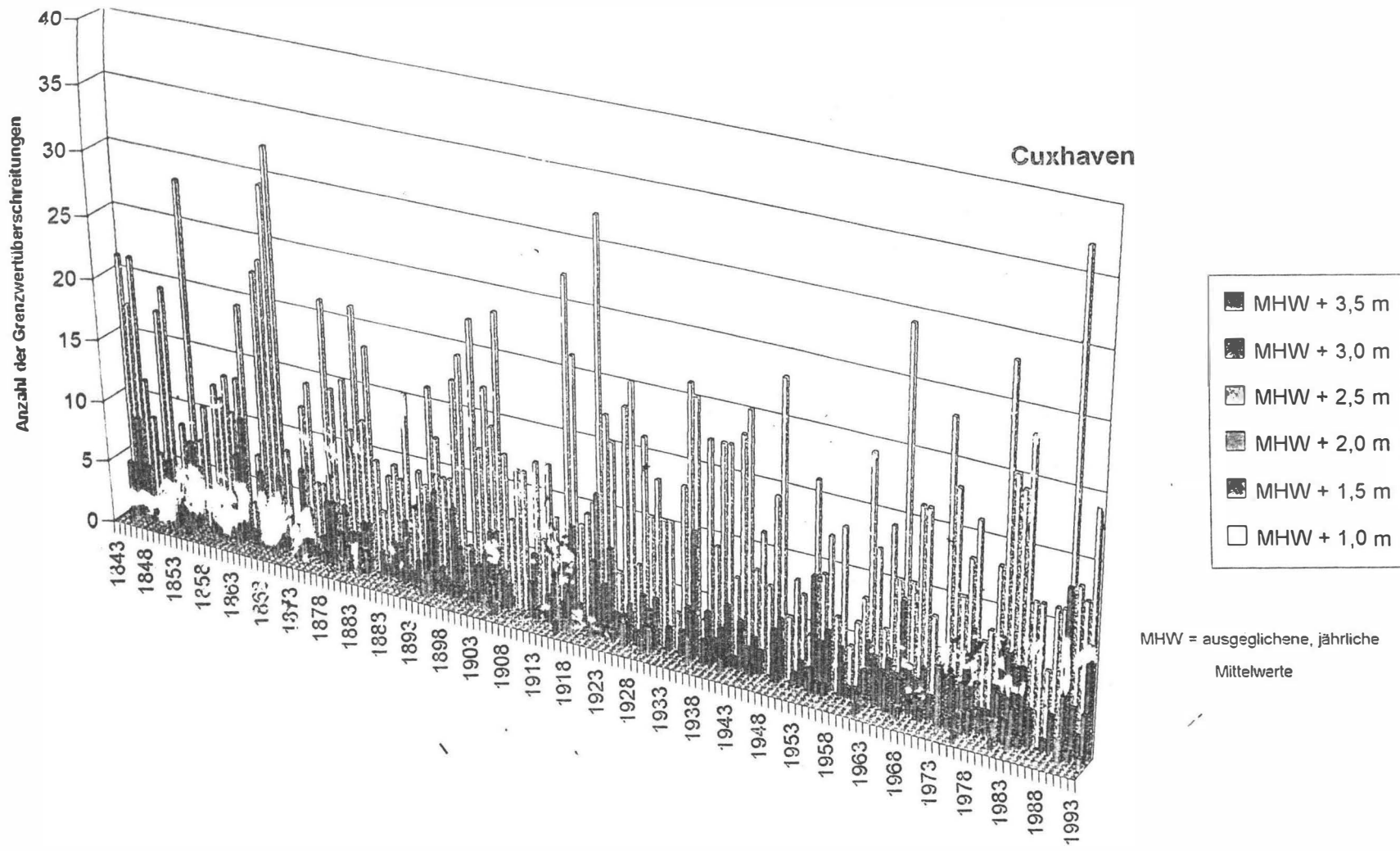
A Case Study for Cuxhaven.

Hans von Storch and Hinrich Reichhardt
Institute of Hydrophysics, GKSS Research Centre
PO Box, 21502 Geesthacht, Germany



Cuxdia.xls

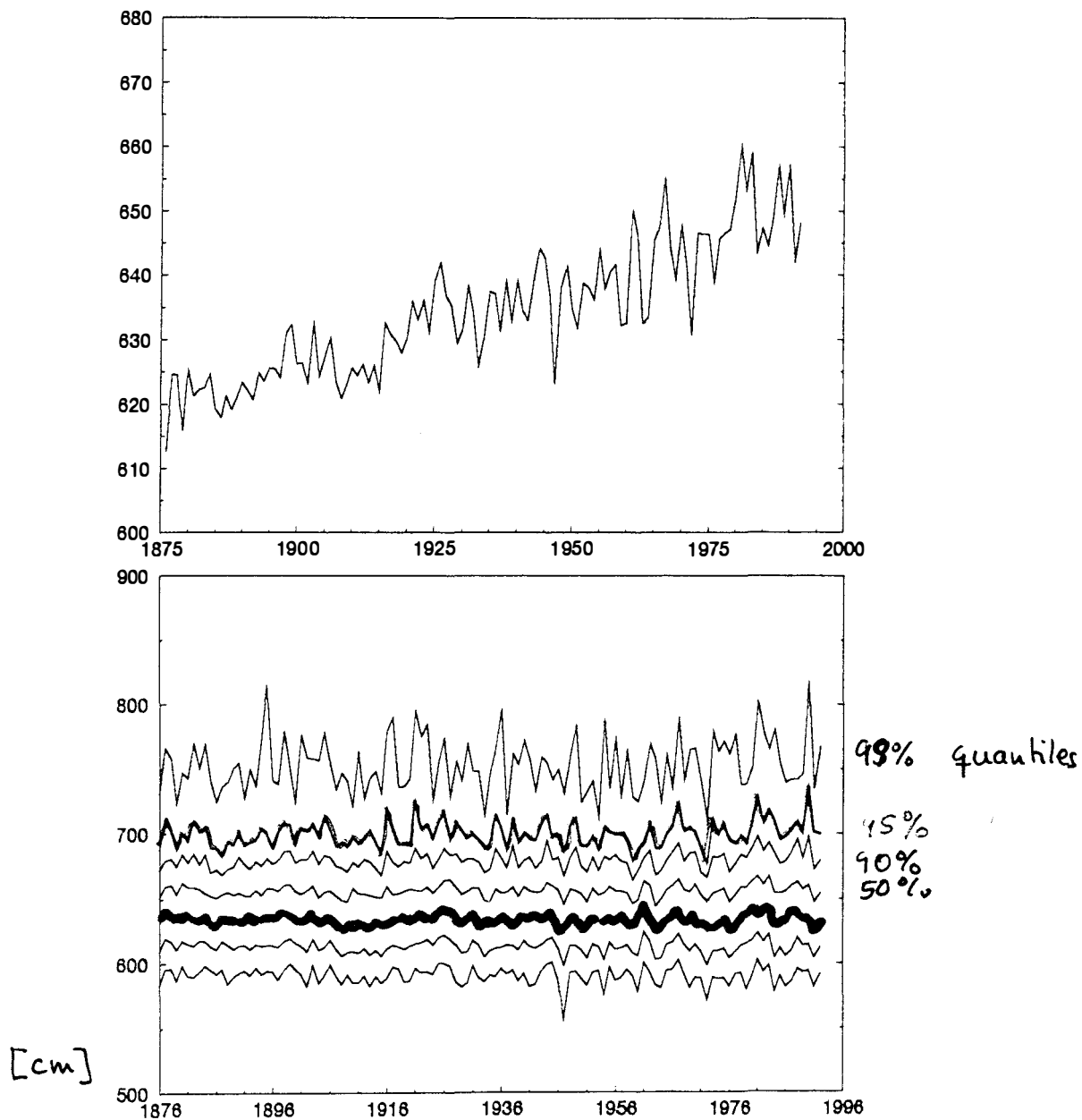
18.03.1994



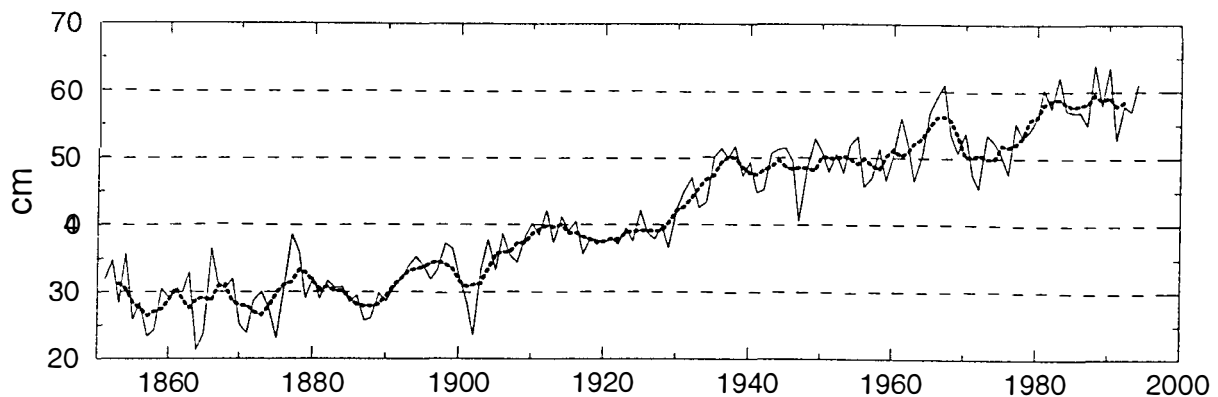
	Signifikanzniveau für Test		Bewertung Pegel "Cuxhaven" 1843 bis 1993 (MHW ansteigend)
	"keine Zufallsreihe"	"Trend vorhanden"	
MHW + 1.0	98%	52%	Datenfolge ist keine Zufallsreihe (möglicherweise ist ein periodischer Anteil enthalten), in ihr ist kein Trend nachweisbar
MHW + 1.5	94%	etwa 50%	"
MHW + 2.0	81%	etwa 50%	Datenfolge unterscheidet sich wenig von einer Zufallsreihe, in ihr ist kein Trend nachweisbar
MHW + 2.5	etwa 50%	etwa 50%	Datenfolge ist eine Zufallsreihe, in ihr ist kein Trend nachweisbar
MHW + 3.0	-----	-----	keine Aussage, nur 8 Werte vorhanden
MHW + 3.5	-----	-----	keine Aussage, nur 2 Wert vorhanden

Abb. 4

Figure 1: Time series of the annual mean of the sea level reported by the Cuxhaven (German Bight) tide gauge (top), and the time series of various percentiles (1%, 5%, 10%, 50%, 90%, 95%, 99% from bottom to top) of sea level relative to the annual mean (bottom). Units: cm

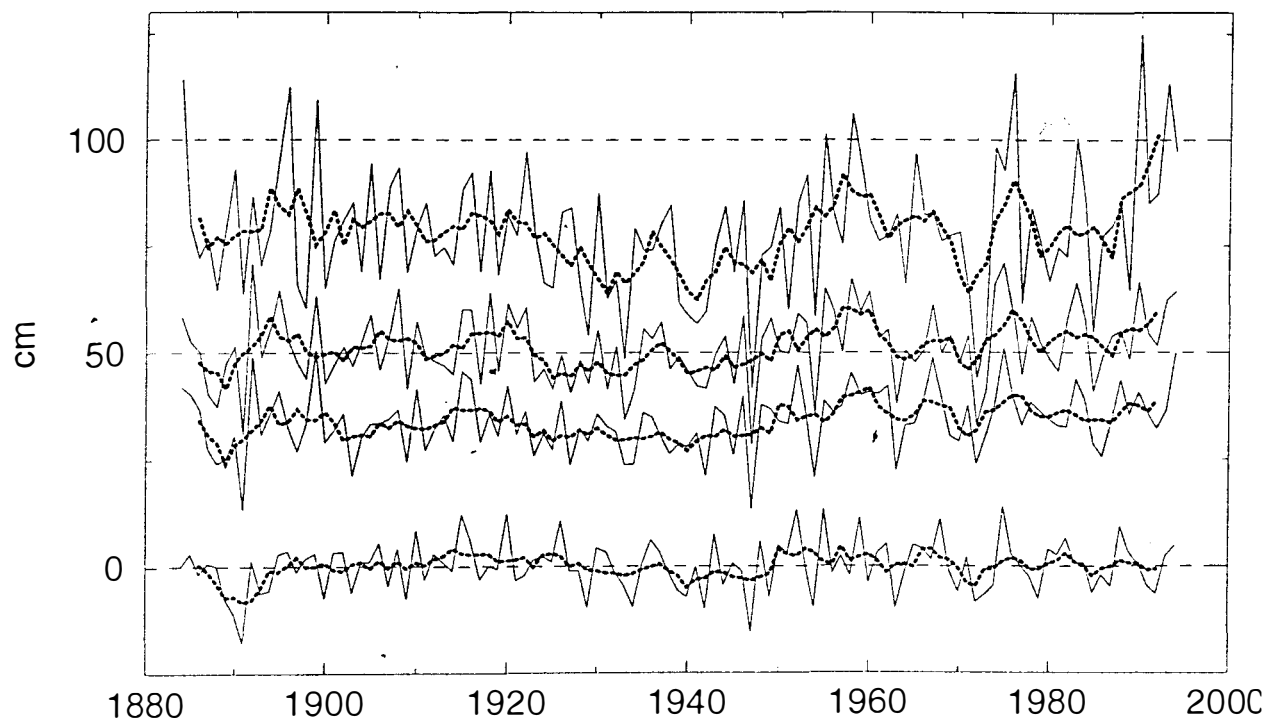


Den Helder



Jährliche Mthw und dazugehörige 5-jährige gleitende Mittel.

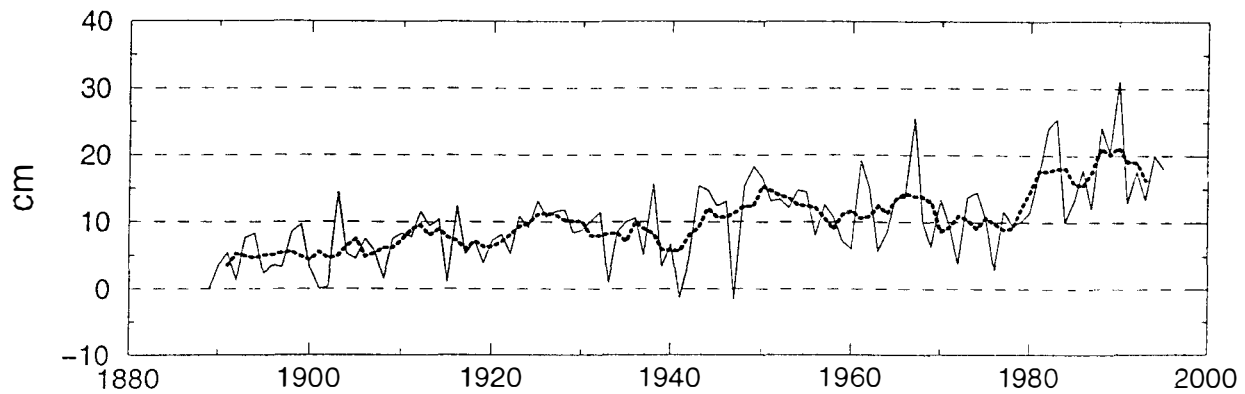
Annual mean high water and 5 year running mean.



Jährliche 50, 80, 95 und 97% Quantile des trendfreien Thw's in den Wintermonaten Dezember - Februar mit dem dazugehörigen 5-jährigen gleitenden Mittel.

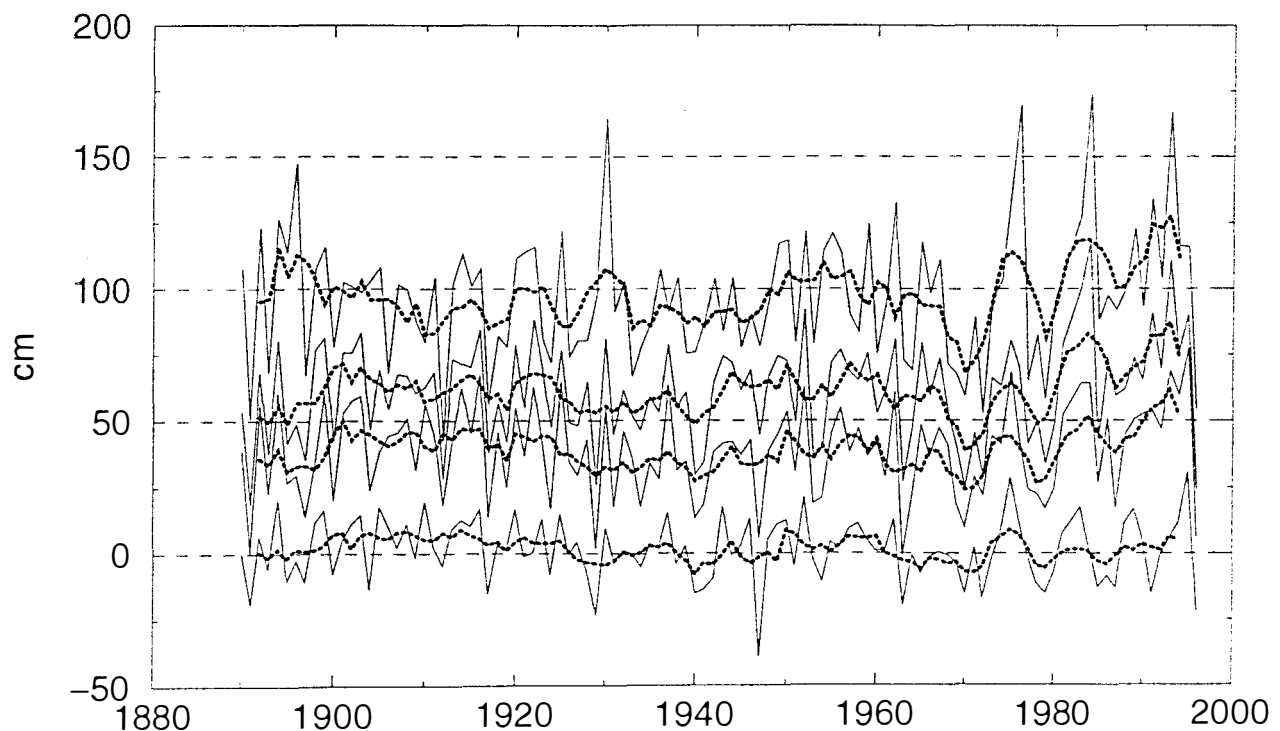
Annual 50, 80, 90 and 97% percentiles of trendless high water for the winter (DJF) and the 5 year running mean.

Esbjerg



Jährliche Mthw und dazugehörige 5-jährige gleitende Mittel.

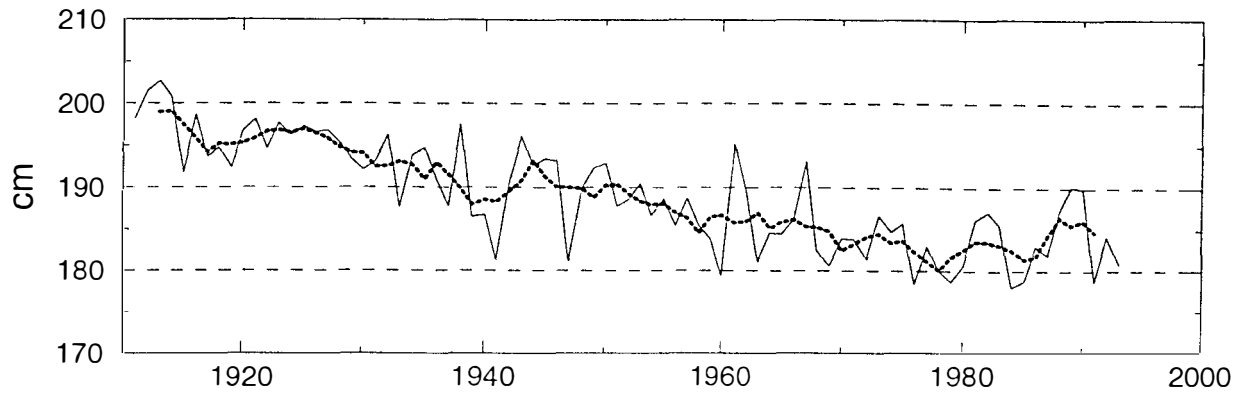
Annual mean high water and 5 year running mean.



Jährliche 50, 80, 90 und 97% Quantile des trendfreien Thw's in den Wintermonaten Dezember - Februar mit dem dazugehörigen 5-jährigen gleitenden Mittel.

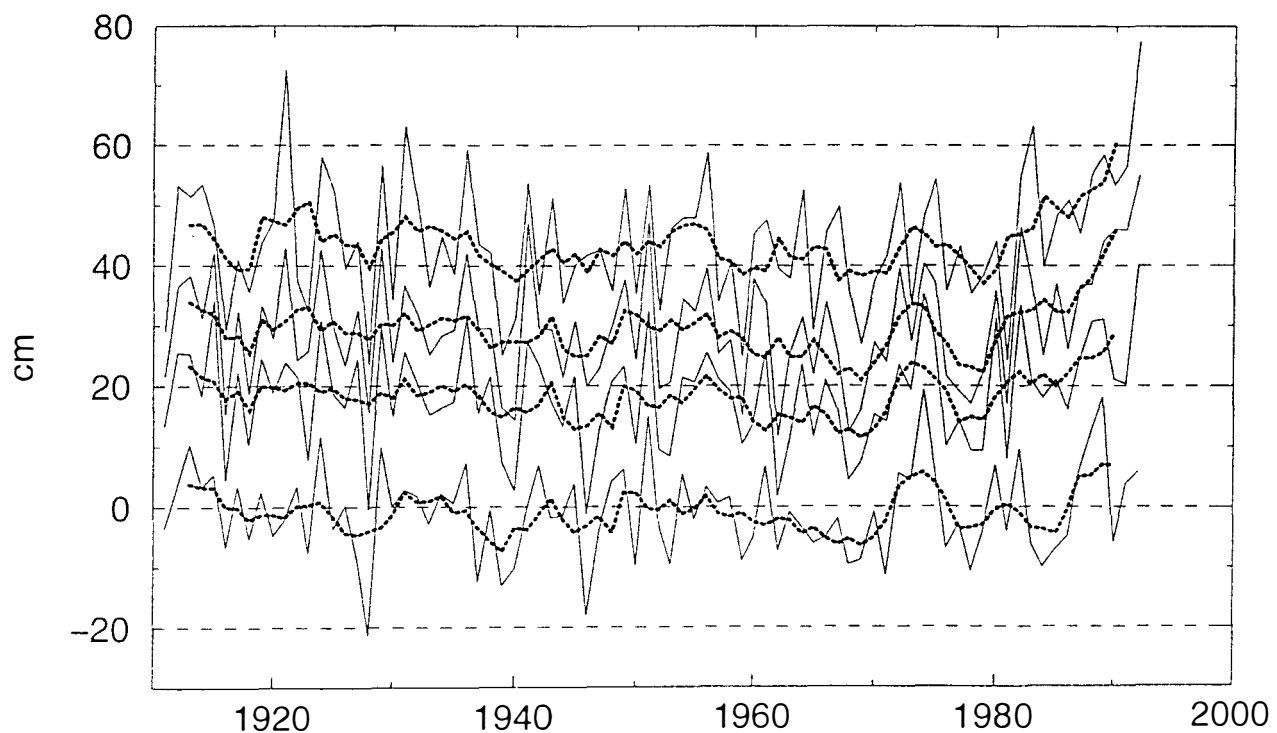
Annual 50, 80, 90 and 97% percentiles of trendless high water for the winter (DJF) and the 5 year running mean.

Smogen



Jährliche Mthw und dazugehörige 5-jährige gleitende Mittel.

Annual mean high water and 5 year running mean.



Jährliche 50, 80, 90 und 97% Quantile des trendfreien Thw's in den Wintermonaten Dezember - Februar mit dem dazugehörigen 5-jährigen gleitenden Mittel.

Annual 50, 80, 90 and 97% percentiles of trendless high water for the winter (DJF) and the 5 year running mean.

THE SHELF SEA CIRCULATION MODEL

- Resolution: 6'x 10', i.e. about 10 km x 10 km
- Area covered: North West European Shelf (including the Baltic)
- HAMSOM (IfM), 2-dimensional and baroclinic
- 'Frozen' salinity and temperature fields from climatological monthly means
- Wind data:
 - DNMI-Data (1955-82),
 - DNMI-Data + ECMWF Reanalyses (1984-93)

ECHAM3/T106 - time slice experiment:

2 x CO₂ und control - run

H. Langenberg

Past Variations

- Storm surges in Cuxhaven have lead to higher and higher water levels in the past 100 years.
- The increase of high tides in Cuxhaven is mostly due to a rise of 30 cm/100 years the mean level of high tides.
- The storm-related variations, around the overall trend in the mean water level, has remained stationary in the past 100 years. A slight increase has taken place since about 1960, but this increase may well be a swing reflecting natural variability.

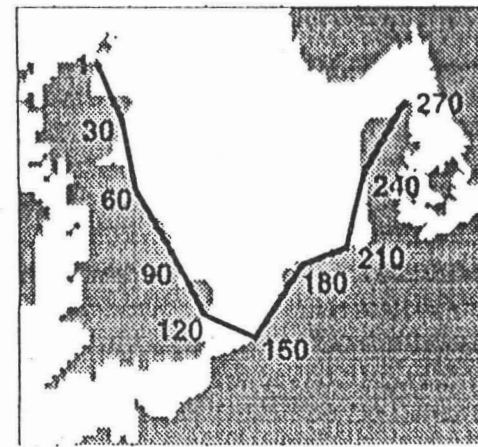
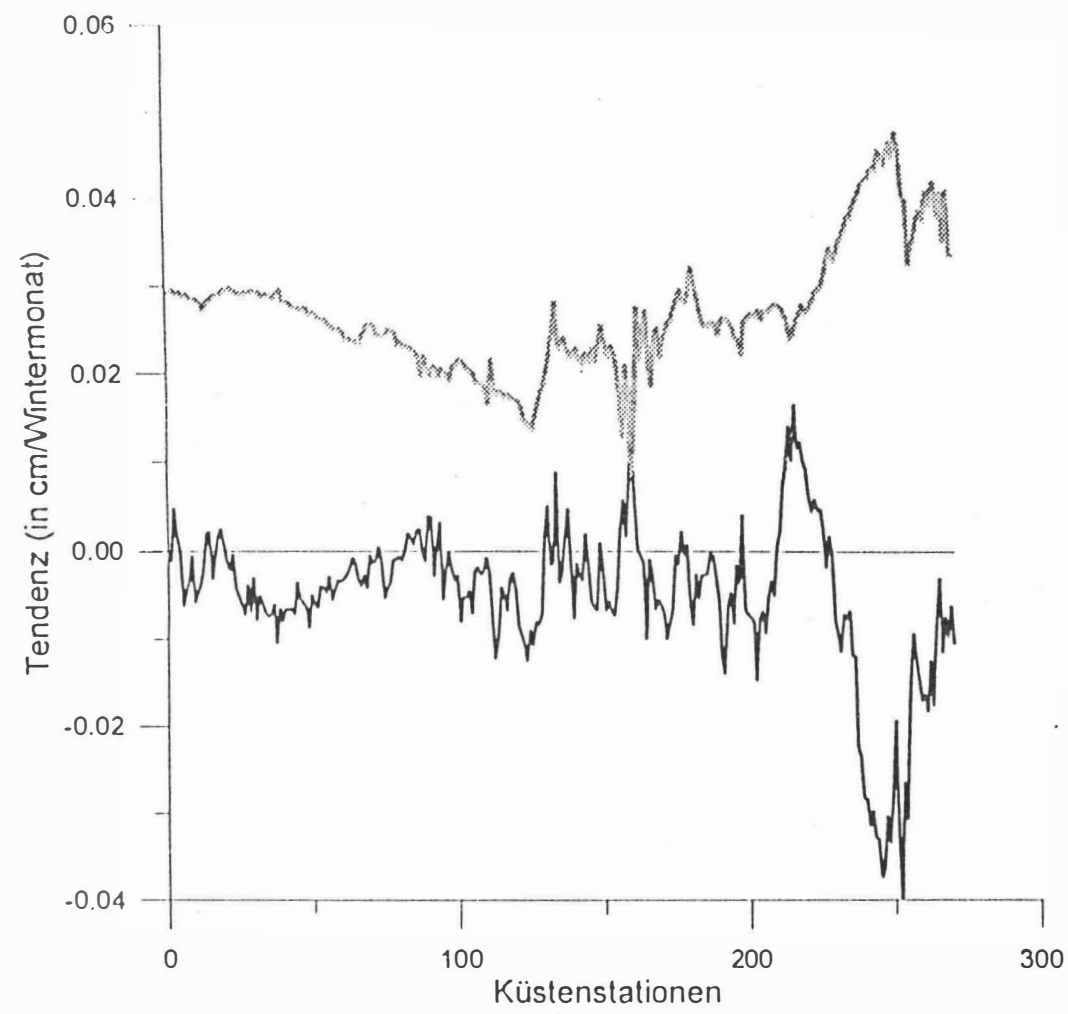
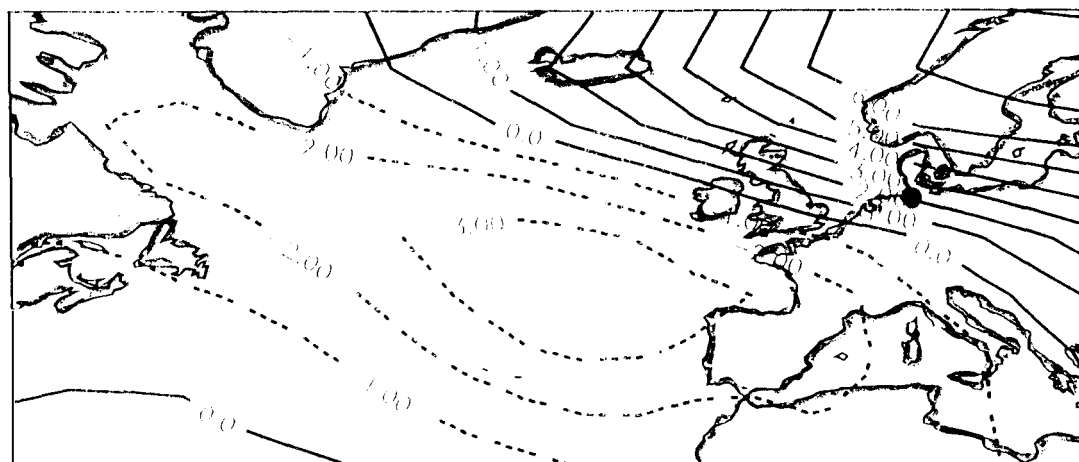


Abbildung 1: Trends der mittleren Hochwässer (grau) und intramonalichen 90% Quantile (schwarz) der Hochwässer für die Monate November bis März 1955-82 rund um die Nordsee; für die Lage der Küstenspunkte siehe oben links

The Statistical Downscaling Model

- The statistical downscaling model is a multiple regression model based on a Canonical Correlation Analysis which links the anomalous monthly mean air pressure distribution over the Northeastern North Atlantic and Europe to the three-dimensional vector of anomalous intramonthly 50%, 80% and 90% percentiles of storm-related (de-trended) high tide level variations in Cuxhaven.
- The model is fitted with data from 1970 to 1988. The CCA identifies two "good" pairs of patterns.
- The first pair describes an uniform shift of the water level distribution in Cuxhaven. Its anomalous air pressure distribution describes an northwesterly flow across the North Sea; the storminess, in terms of the intramonthly standard deviation of band-pass filtered pressure variations are enhanced.
- The second is associated with a broadening (or shrinking) of the distribution. The 50% percentile is reduced but the 90% percentile is enhanced. The anomalous monthly mean air pressure distribution has a weak local southeasterly component; the overall configuration leads to an intensification of storm activity in the North Sea area.

monthly mean SLP anomaly



intramonthly
percentiles of
high freq. water
level anomalies

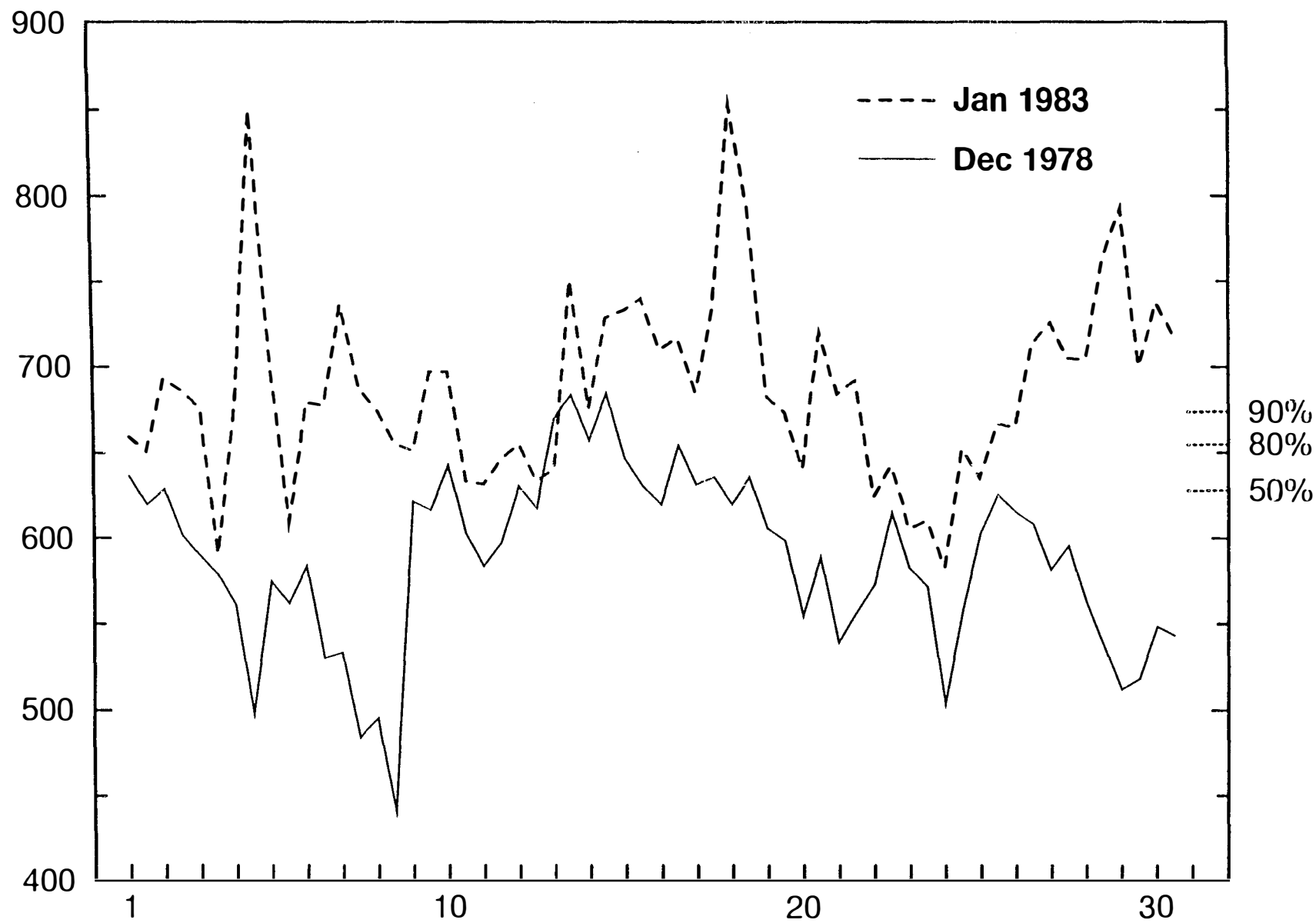
$$q_{50\%} = +21 \text{ cm}$$

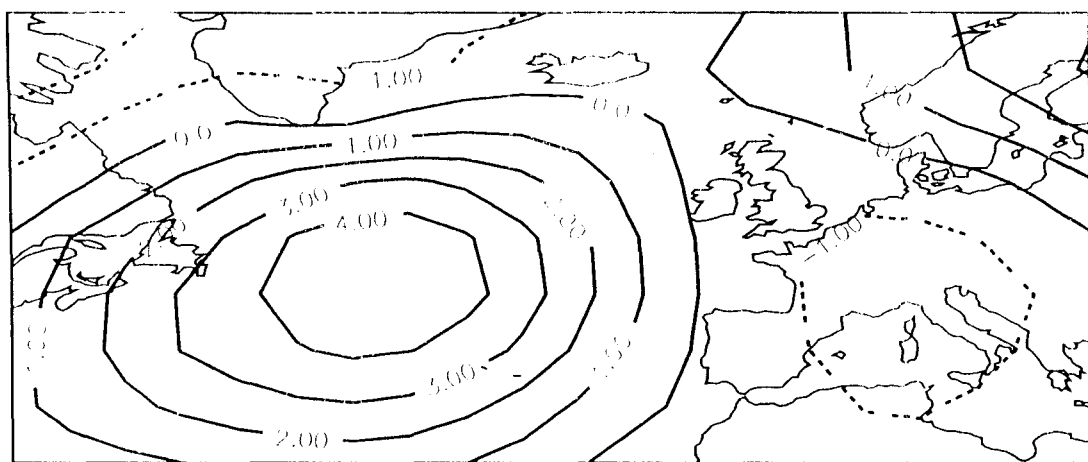
$$q_{80\%} = +16 \text{ cm}$$

$$q_{90\%} = +13 \text{ cm}$$

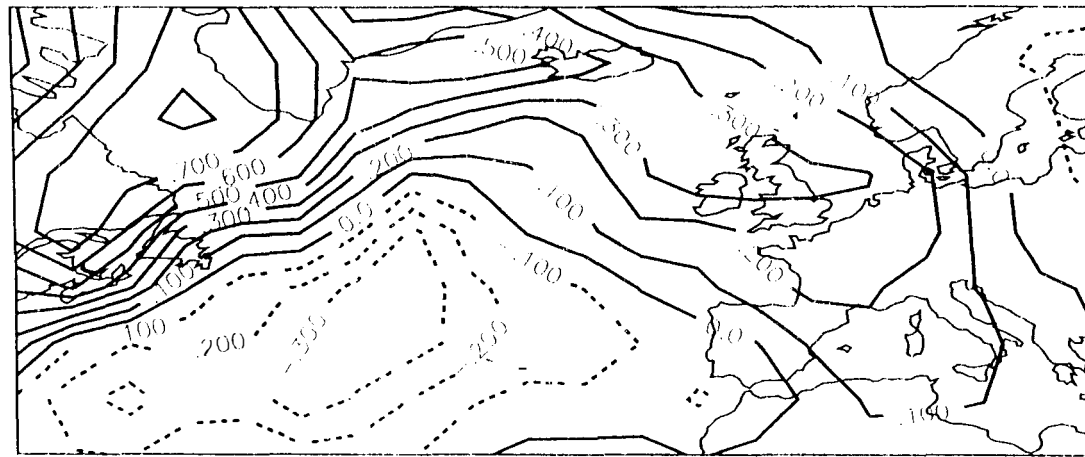
at Cuxhaven.

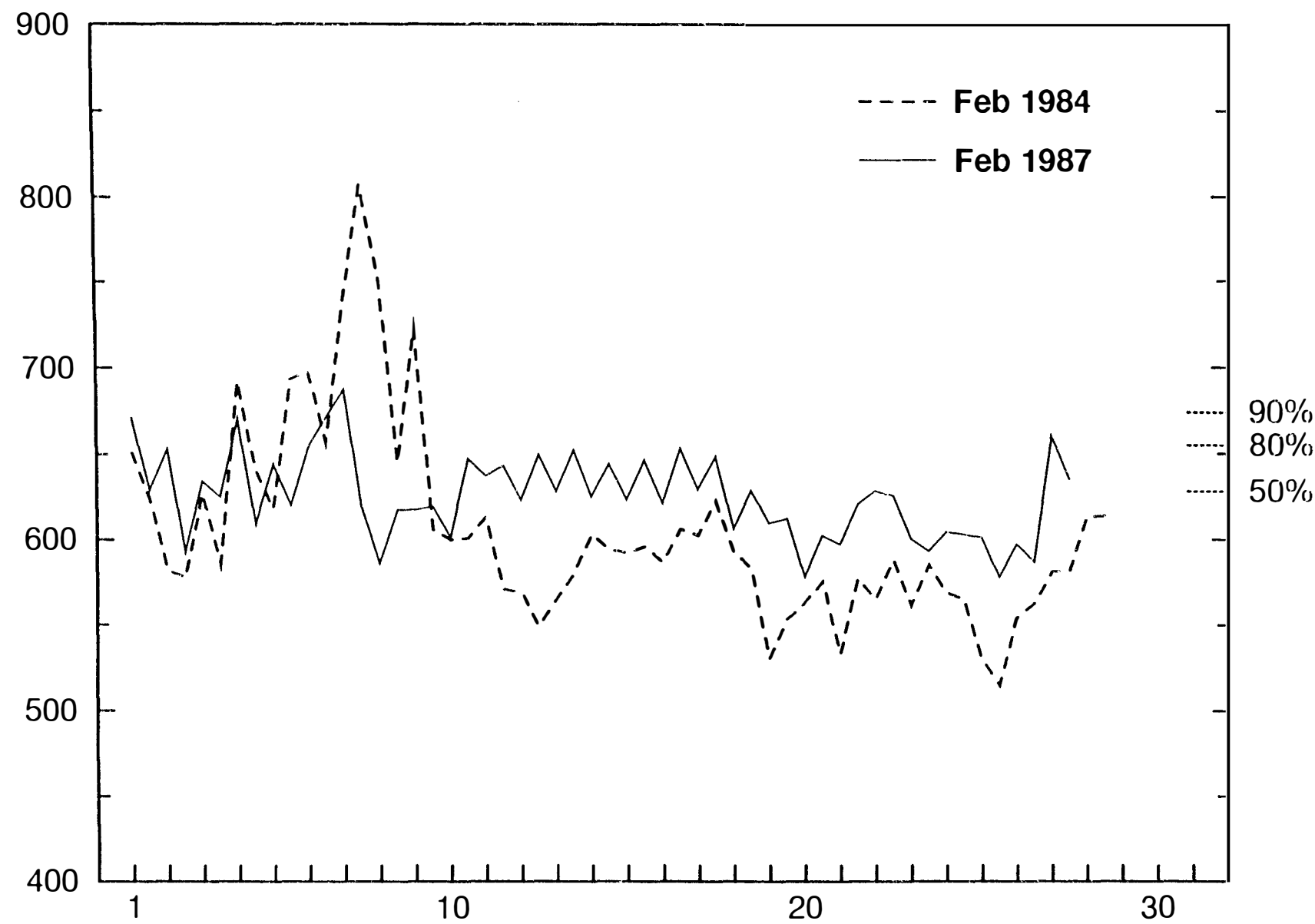






U.S.S.R. - 10
80 °C.
90 + 10





Verification of the Statistical Model

- The model is verified with independent data from 1899 to 1969.
- The *skill* of the resulting regression model is measured by the correlation of in-situ intra-monthly 50%, 80% and 90% percentiles and the estimated percentiles.

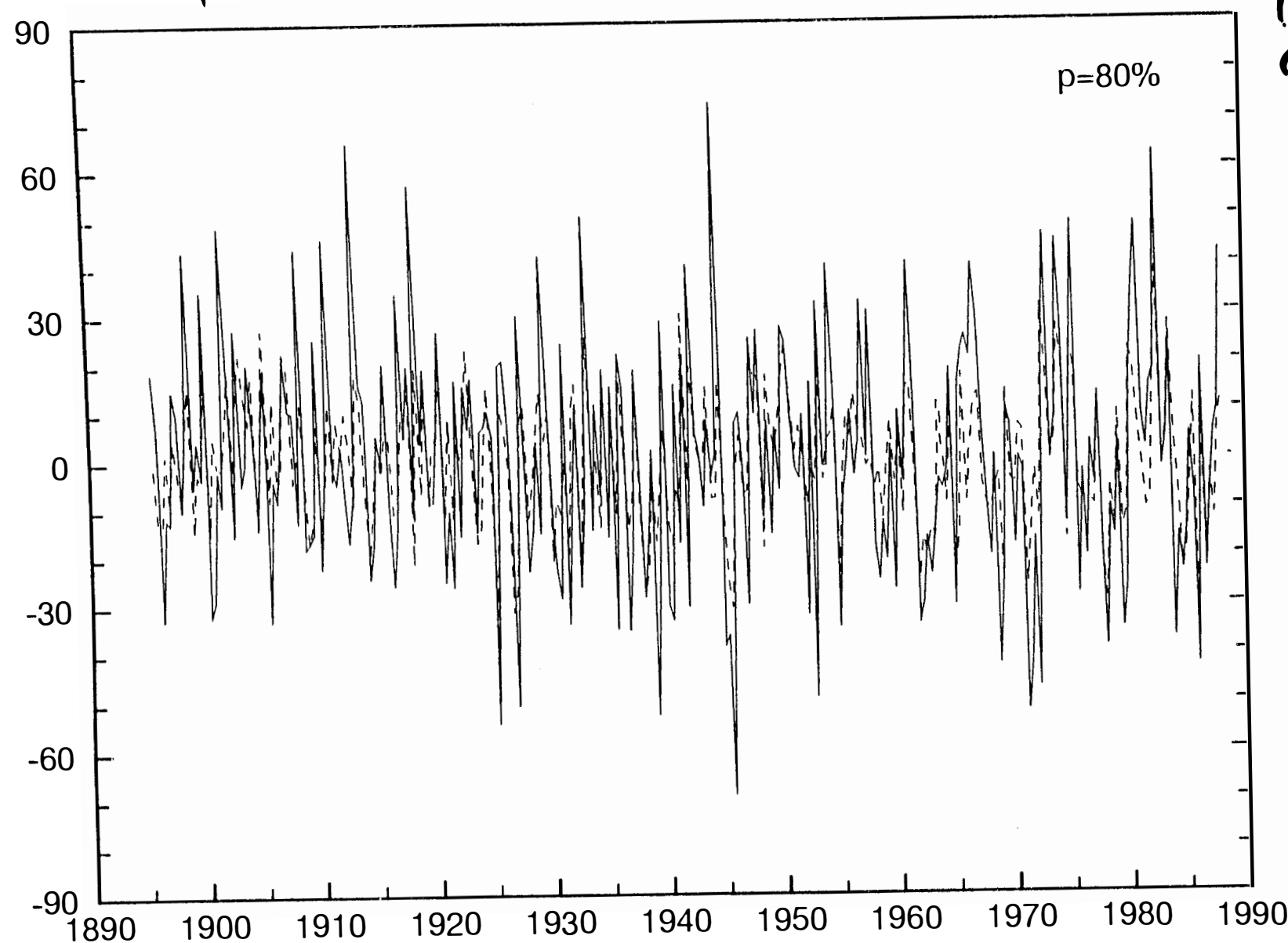
50%	80%	90%
.79	.72	.63

- Another measure of skill is the *percentage of explained variance*:

50%	80%	90%
62%	50%	40%

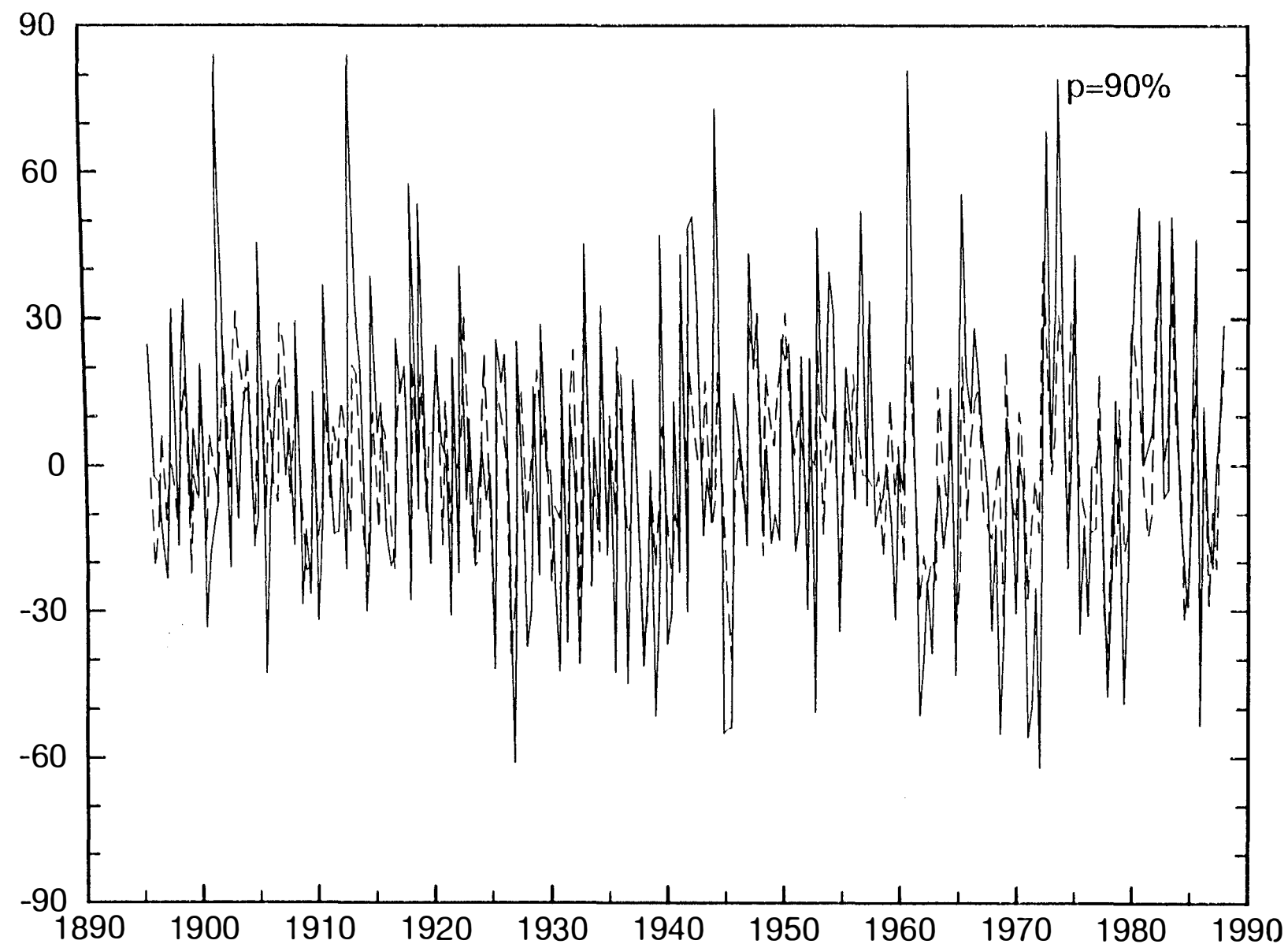
- An inspection of the time series indicates that the statistical model is skillful in reproducing the low-frequency variations. The differences between in-situ data and estimated data are mostly white in time.
- **Byproduct:** The conclusion of no systematic increase of storm-related variability is supported by air-pressure data.

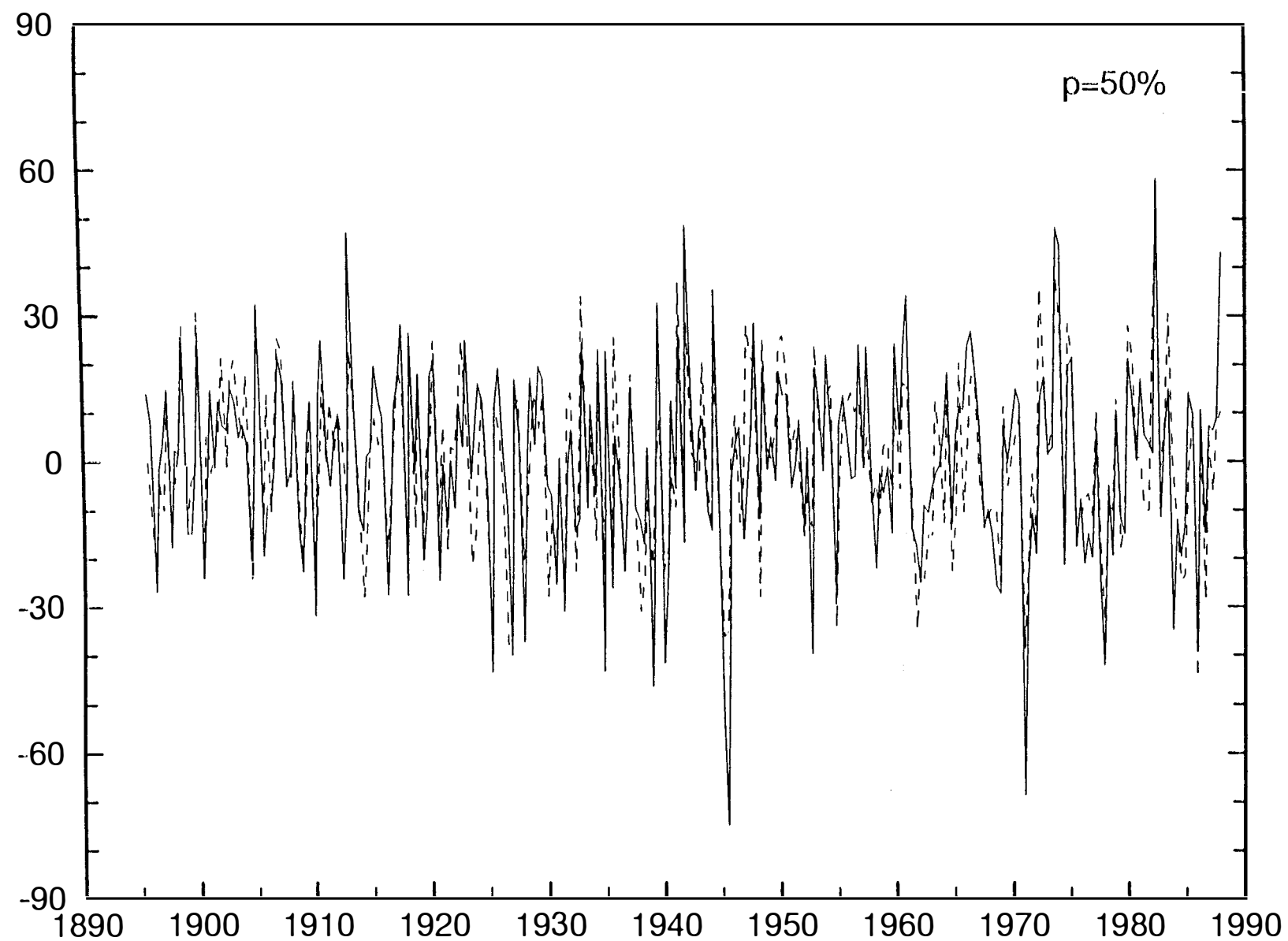
80% percentile of storm related intramonthly variability of water level in Cuxhaven.



p=80%

$\Delta_{\text{CO}_2} \sim 7 \text{ cm.}$





Scenario for Future Changes due to Global Warming for the Time of Doubled CO₂ Concentrations

- Standard climate models are too coarse to simulate regional details. Therefore *downscaling strategies* are required.

- We pursue a two-step downscaling strategy.

First, a scenario derived from a coarse (T21) resolution coupled ocean-atmosphere climate model is dynamically downscaled by means of a *T106 time slice experiment*.

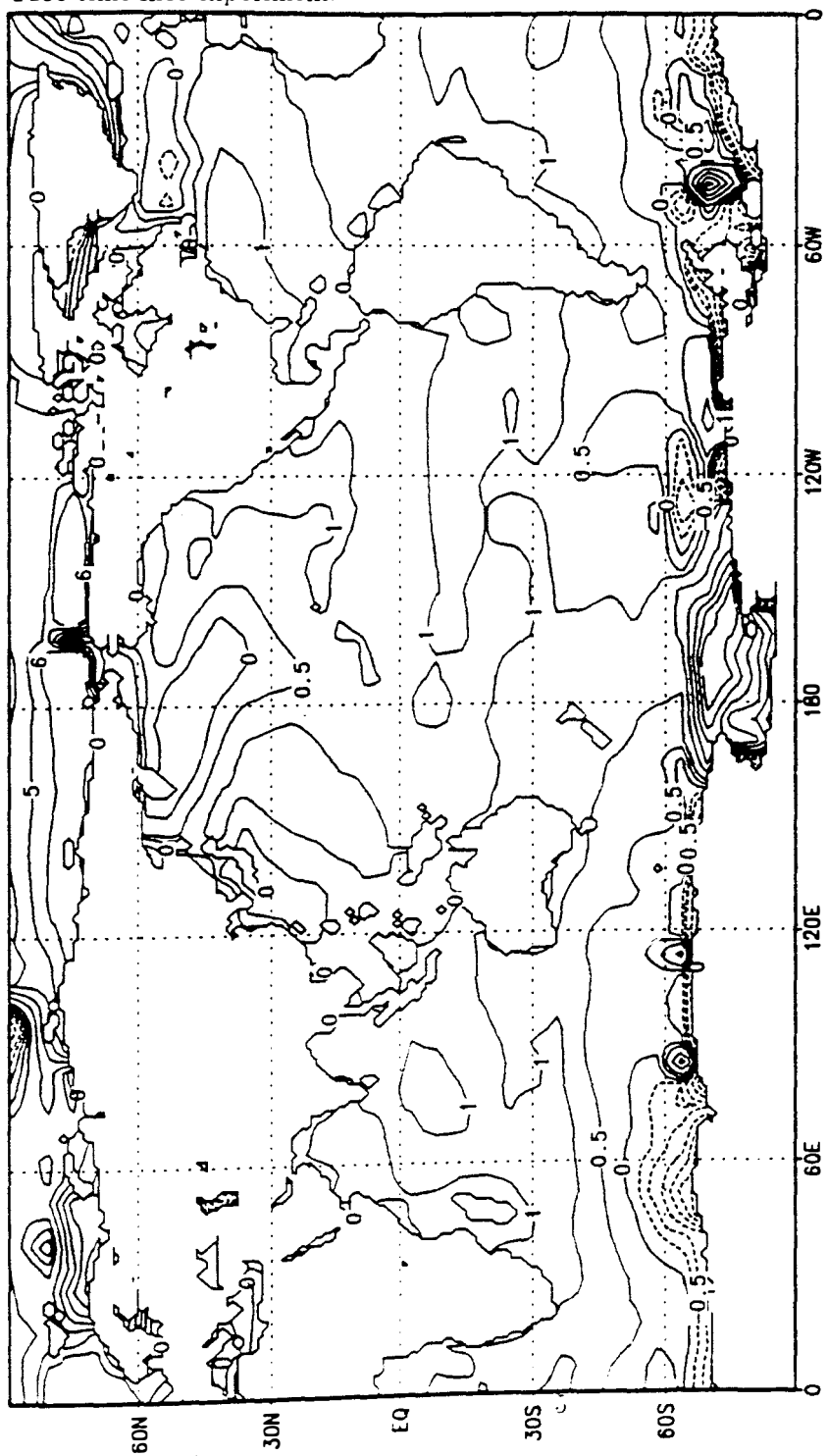
Then, in a second step, a *statistical model* is designed which relates intra-monthly percentiles of storm-related high tide variations to the monthly mean air pressure distribution.

- The T106 scenario indicates for the expected time of doubled CO₂ concentrations, in about year 2035, an intensification of the mean northwesterly flow across the North Sea.
- The statistical model interprets the large-scale T106 air pressure distribution change as a tendency towards higher tide levels in Cuxhaven. The increase of storm related high tides in Cuxhaven is rather small. The 50% percentile is expected to rise by 10 cm whereas the 90% percentile is expected to rise by 12 cm.
- The storm related increase of water level extremes has to be added to the mean sea level rise, due to ongoing land sinking and thermal expansion of the sea water, of some decimeters.

The Combined Two-Step Dynamical/Statistical Downscaling

- The T106 time slice experiment has been integrated with doubled CO₂ concentrations and SST/sea ice distributions taken from the “transient” base ECHAM T21/LSG coupled climate change experiment. A total of 6 winters has been integrated so that 18 anomalous (= difference to control run) monthly (DJF) mean air pressure distributions are available.
- The mean anomalous pressure distribution indicates an enhanced mean northwesterly air flow across the North Sea. This distribution has CCA coefficients $\alpha_1 = -0.40$ and $\alpha_2 = 0.26$.
- The regression model transforms these α 's into anomalous percentiles of about 7 cm.
- The estimated systematic change is comparable with the model generated standard deviations. Thus, the evidence supplied by the model fails to reject the null hypothesis of “no change of storm related percentiles”.

Figure 3: Sea surface temperature obtained in the base climate change run for the "time slice" 2035. This anomalous distribution is superimposed on the present SST distribution in the T106 time slice experiment.

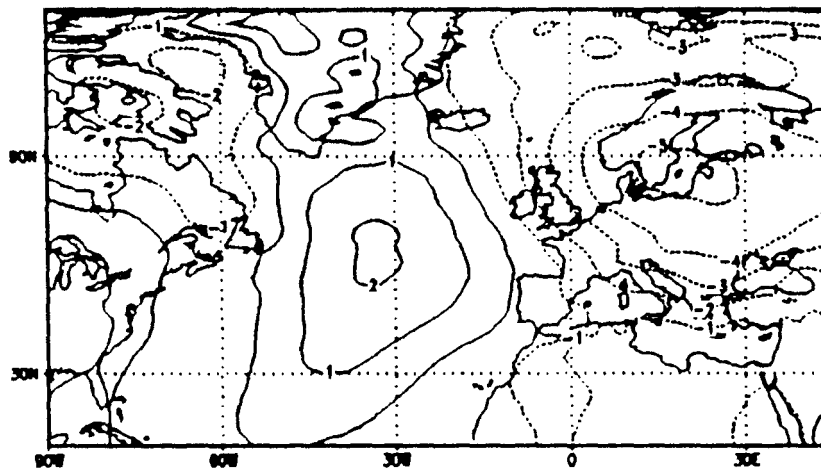


orfh (1993) who found no indication towards a systematic worsening of storm climate in a long time series of synoptic winds in the German Bight (see WASA, 1995).

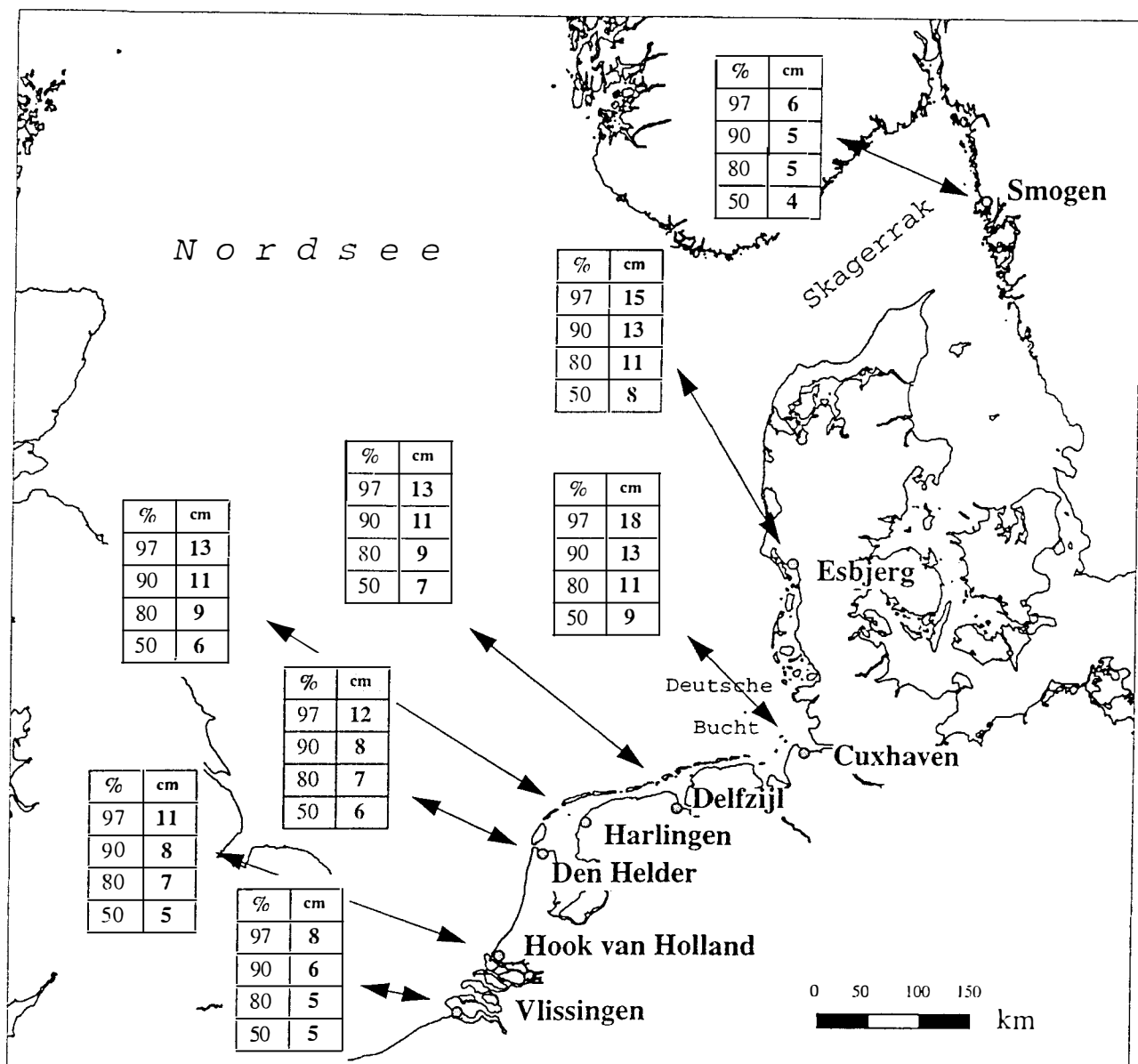
Another observational data set comes from monthly analyses of the distribution of air pressure over Western Europe and the Northern North Atlantic ($20^{\circ} - 25^{\circ} E, 30^{\circ} - 70^{\circ} N$) since 1899 until 1988. These analyses have been prepared by different weather services. The analyses have continuously been improved, so that the daily analyses are increasingly homogeneous, containing a spurious signal of a roughening storm climate. The monthly analyses, however, are believed to be mostly homogeneous and unaffected by significant inhomogeneities (Trenberth and Paolino, 1980).

Monthly mean air-pressure maps for the Northern European / Northern North Atlantic area are also available from a time slice GCM experiment (see below in Section 4). This GCM experiment was

Figure 4: Anomalous winter (DJF) mean air pressure anomaly simulated in the time slice experiment as a response to modified SST and doubled CO_2 concentrations.



(Hewitson and Crane, 1992; von Storch et al., 1993). The paradigm behind this approach is that the large-scale climate of the atmosphere is determined by planetary scale features such as the distributions of continents and mountains and the latitudinal variation of incoming radiation. Then, the local climate appears as the result of an interplay of the large-scale climate and the local details such as the details of a coast, of landuse and smaller orographic

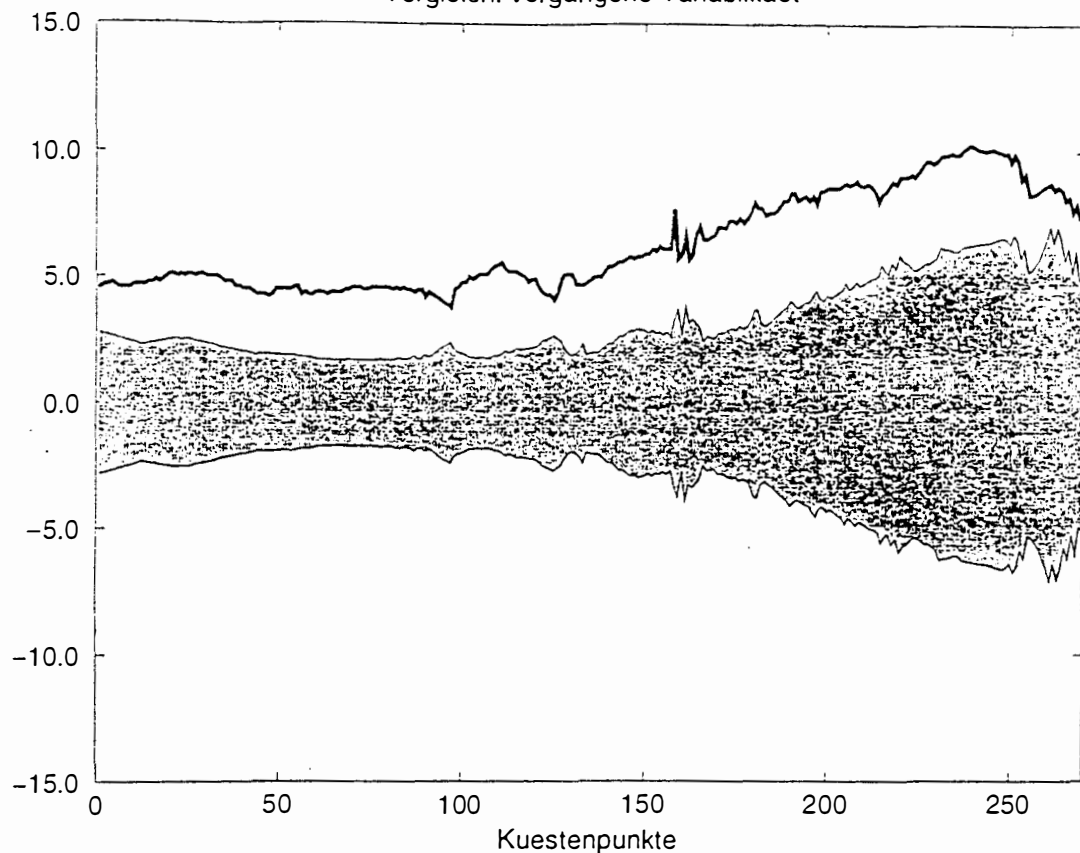


Mittlere Änderung der Quantile des Thw's an den Pegelstandorten. Berechnet aus dem 2*CO₂ - T 106 Lauf für die Wintermonate Dezember - Februar.

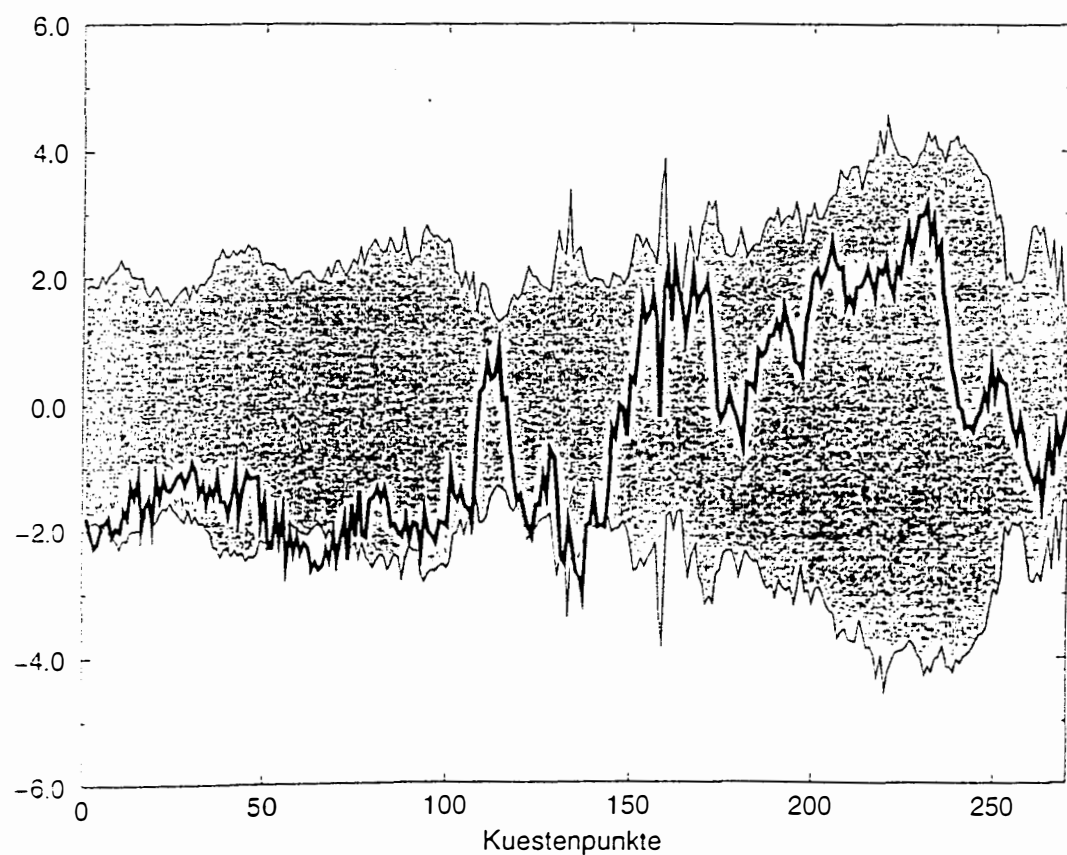
Changes of percentiles of high water. Calculate from the 2*CO₂ scenario for the winter (DJF).

Mittlerer Wasserstand durch 2 x CO₂

Vergleich: vergangene Variabilität



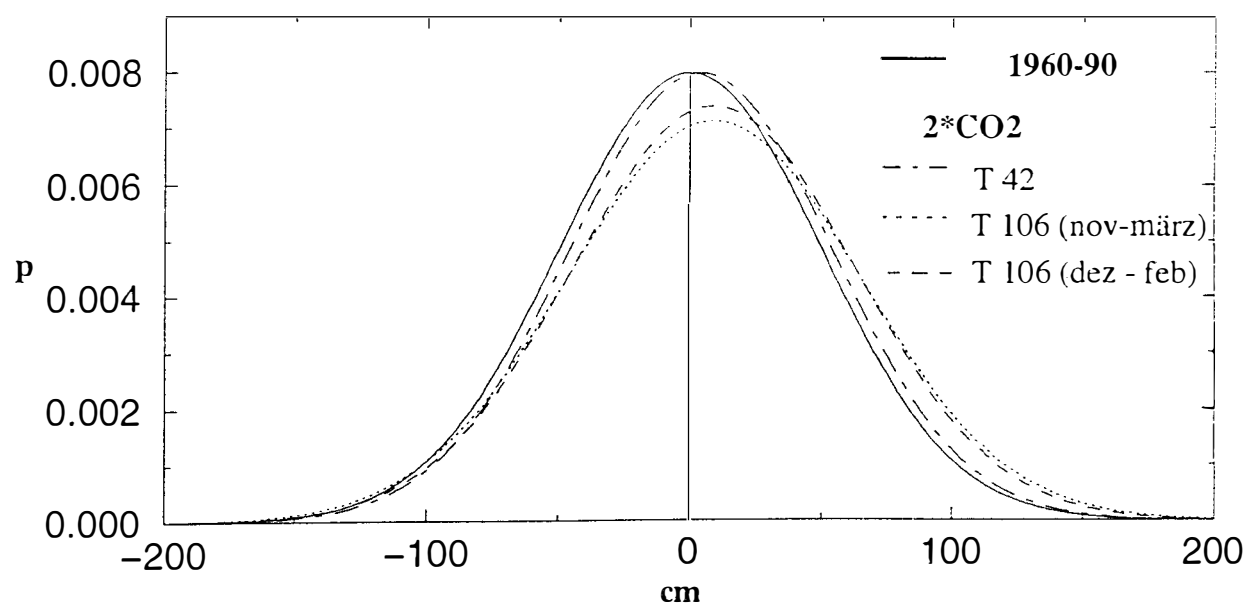
90% Quantile durch 2 x CO₂



Zunahme in cm pro Meter des Thw's unter 2*CO₂ Bedingungen gegenüber 1972-92 für die Monate dez - feb, sowie nov - märz.

2*CO ₂ Zunahme	dez - feb cm/m	nov - märz cm/m
Smogen	0	3
Esbjerg	3	10
Cuxhaven	7	12
Delfzijl	8	12
Harlingen	5	10
Den Helder	4	9
H.v.Holland	5	8
Vlissingen	4	5

Cuxhaven

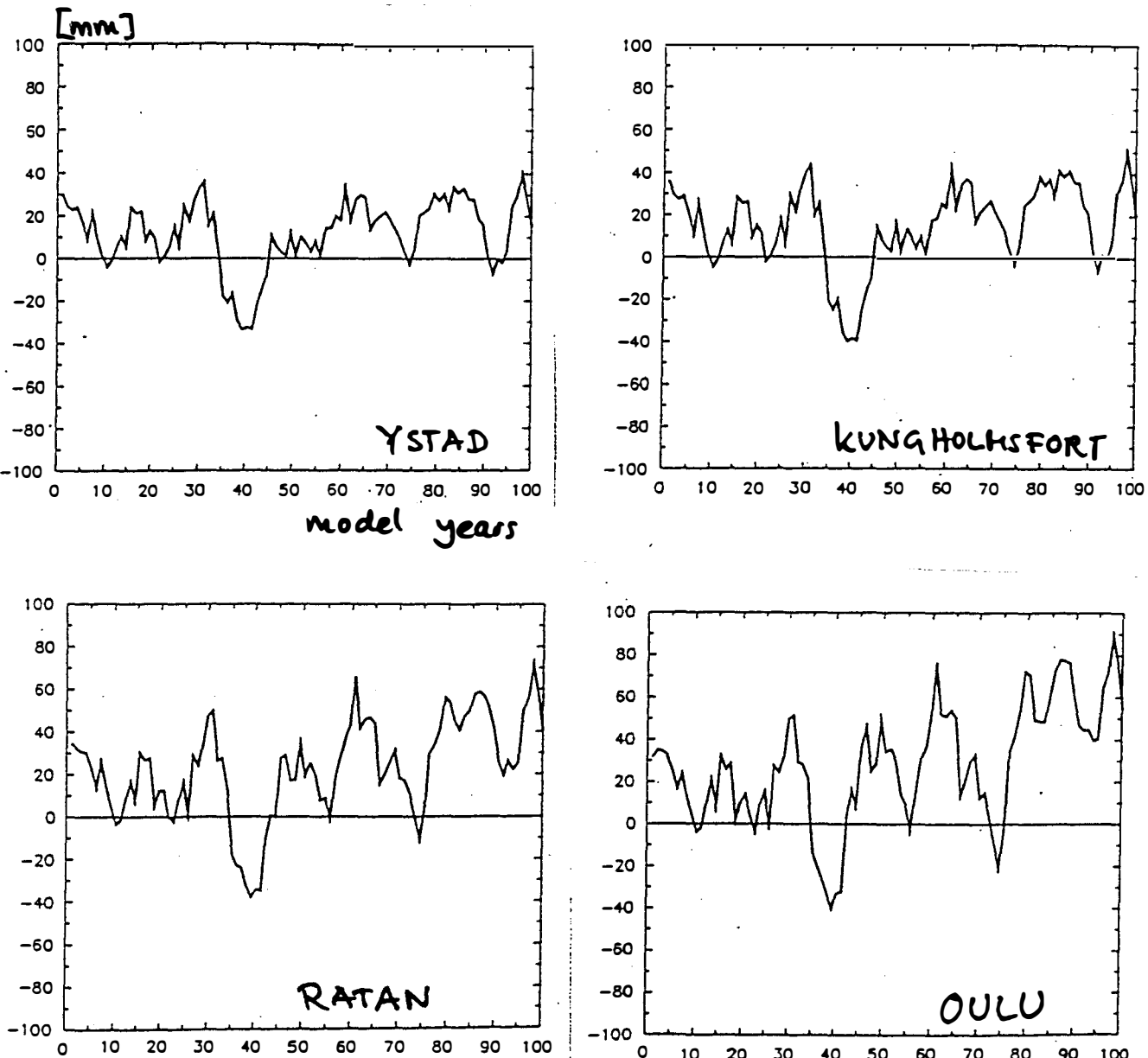


Verteilung Thw's

Distribution of high water

sea level rise according
to the "downscaled" scenario A

Abb.11) Ergebnis des Downscalings für "Scenario A":



Die Kurve stellt die aus dem Luftdruckfeld ermittelten Wasserstandsano-
malien in mm dar, saisonal und durch ein 5-jähriges laufendes Mittel
gemittelt. Die x-Achse zeigt die Jahre des Klimamodellaufs.

HEYEN, 1984

Figure 8.d

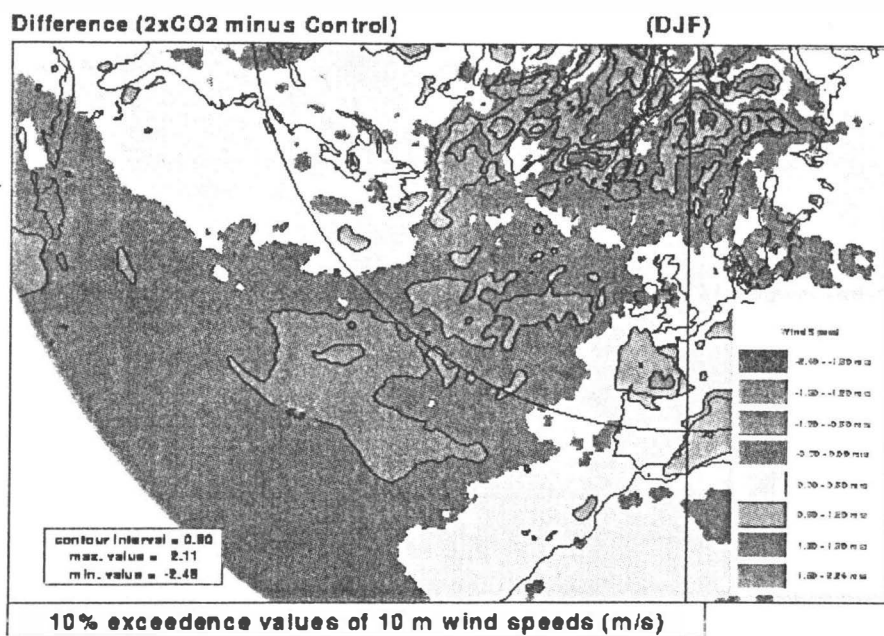
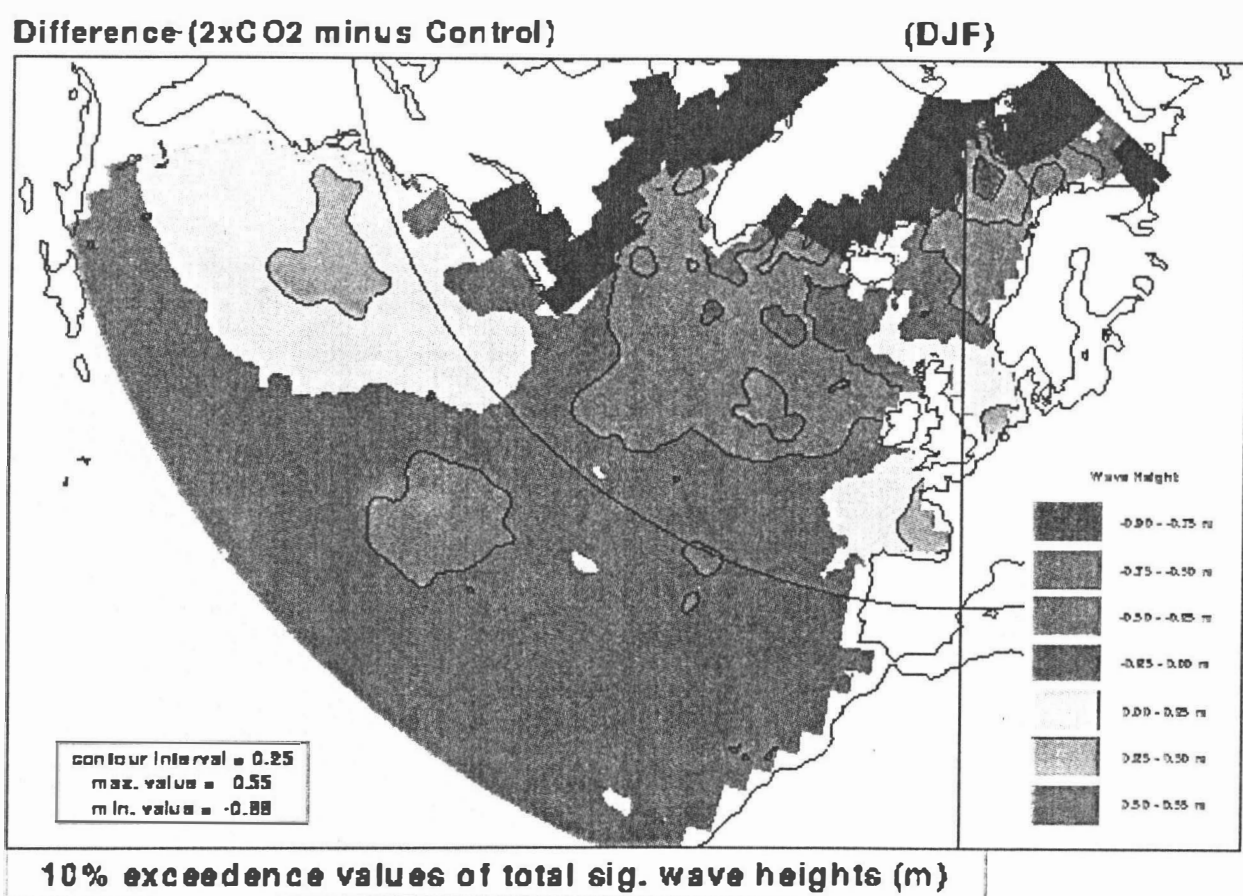


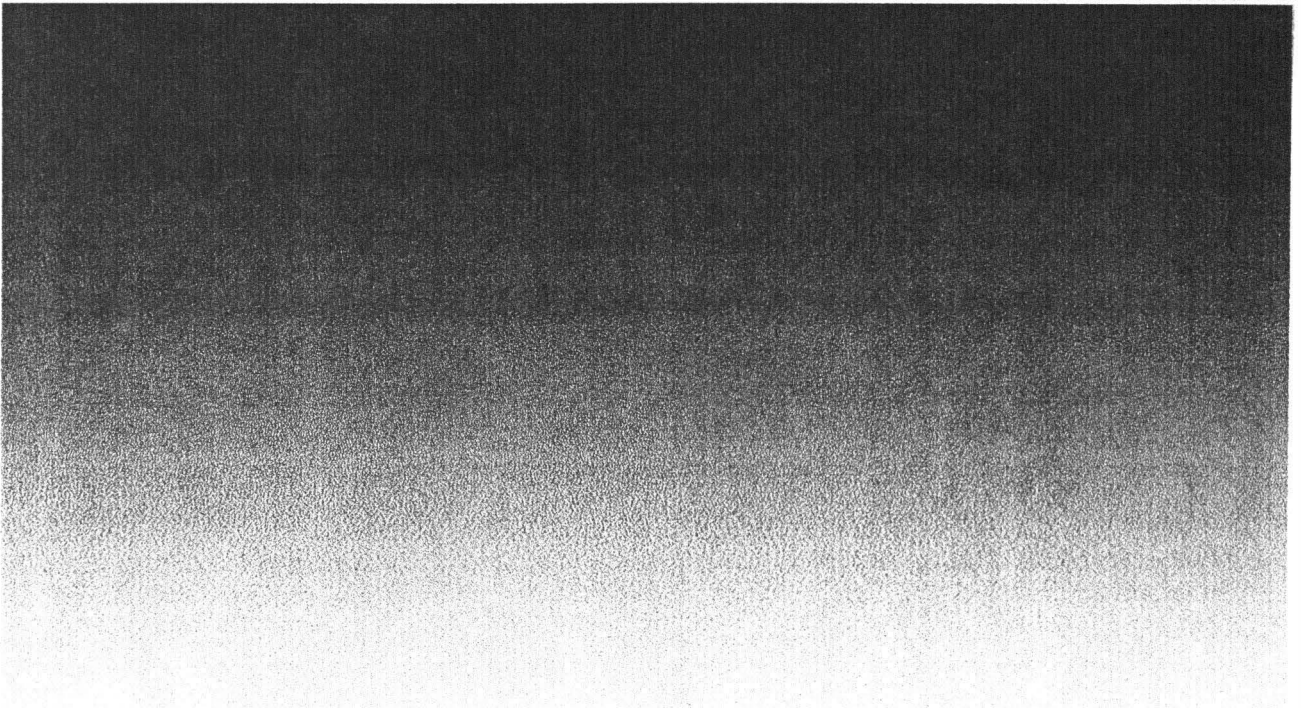
Figure 18.c



FEW degrees of freedom
DETAILS matter
described by dynamical
models

Many DGFs,
statistics matter
not completely resolved by dynamical models

TRUNCATION



The Local modifying the Global - PARAMETERIZATIONS of sub-grid scale processes

Let's consider a climate model

$$\frac{\partial \phi}{\partial t} = R(\phi)$$

and a spatial truncation $\phi = \bar{\phi} + \phi'$

Then

$$(*) \quad \frac{\partial \bar{\phi}}{\partial t} = R_{\Delta x}(\phi) = R(\bar{\phi}) + R'(\phi')$$

Equation (*) is not closed and cannot be integrated.

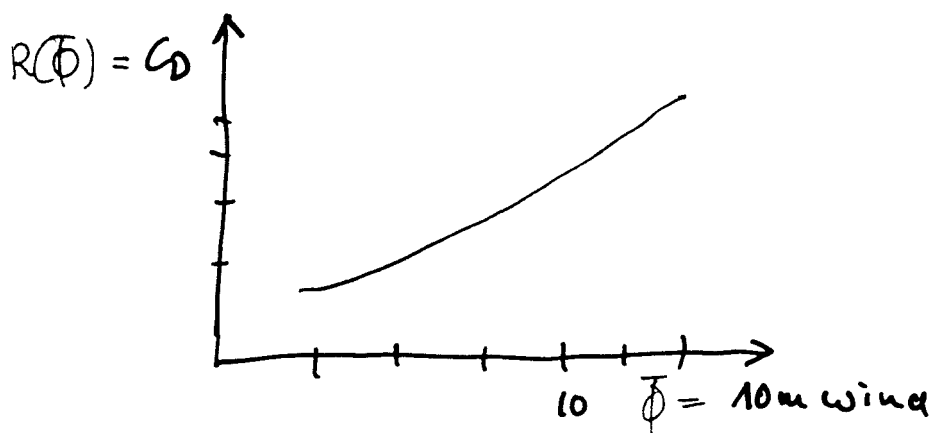
Options

(a) $R'(\phi') = 0$ in many cases done

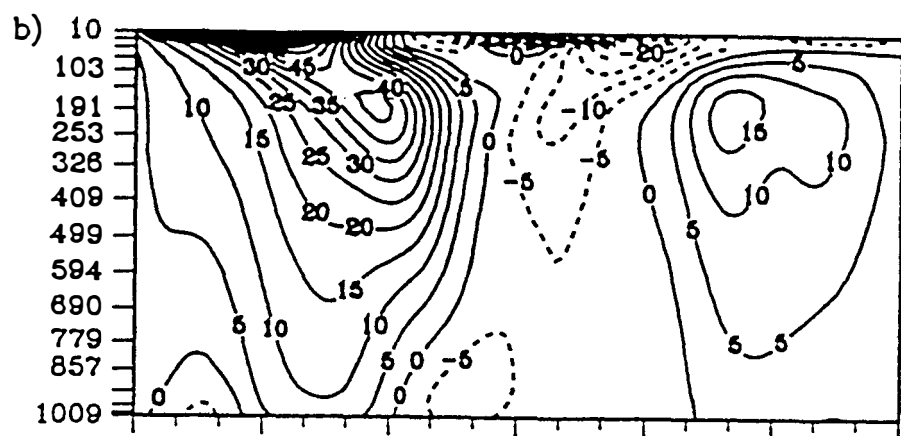
(b) $R'(\phi') = Q(\bar{\phi})$ called "parameterization"

This ansatz implies that all variability on sub-grid scales unrelated to the resolved scale dynamics, $\bar{\phi}$, is irrelevant.

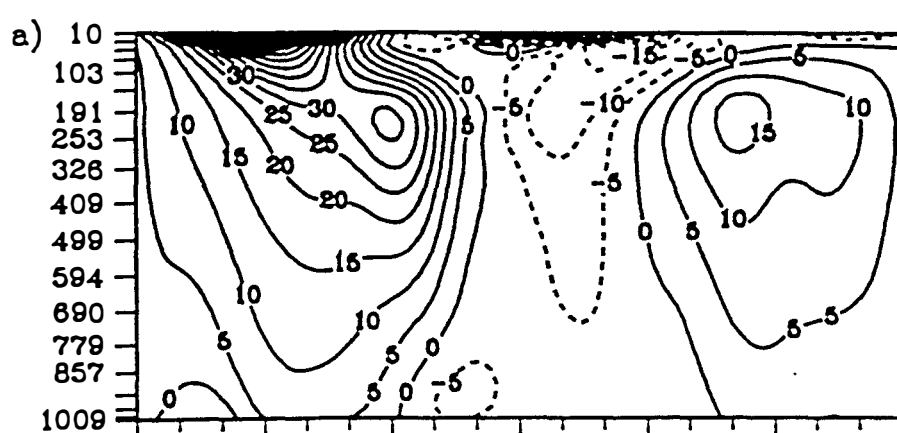
Example



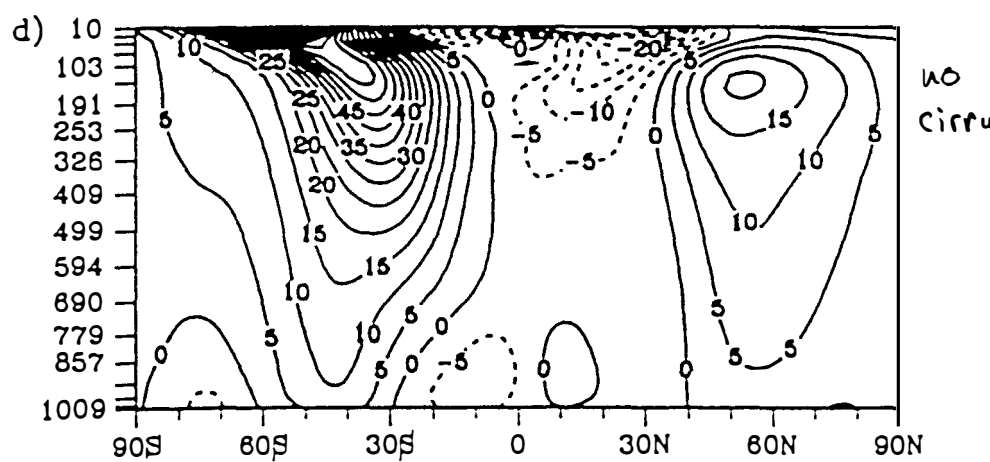
Different parameterizations of Cirrus clouds



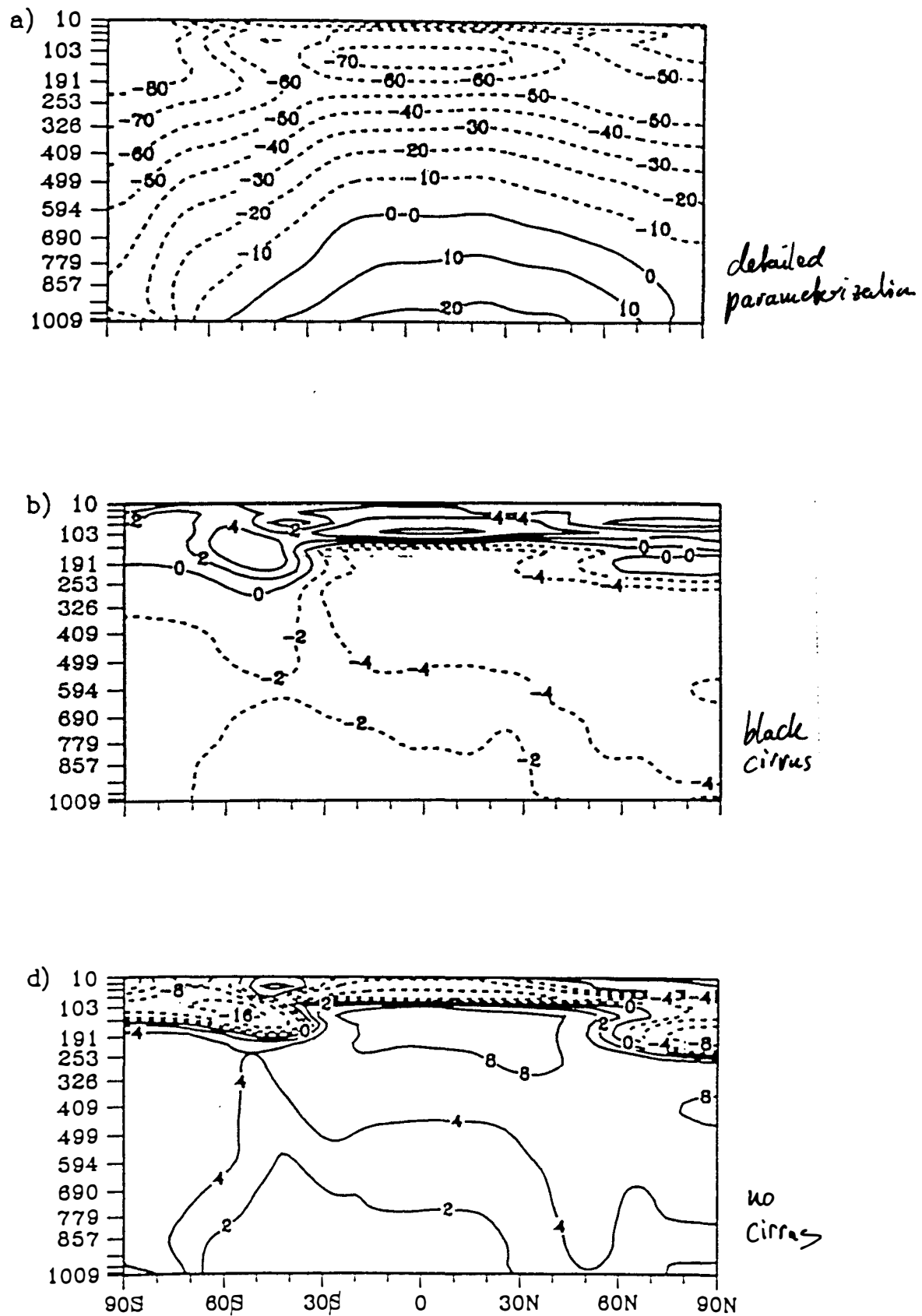
detailed parameterization



black Cirrus-



no Cirrus



(c) randomized parameterization

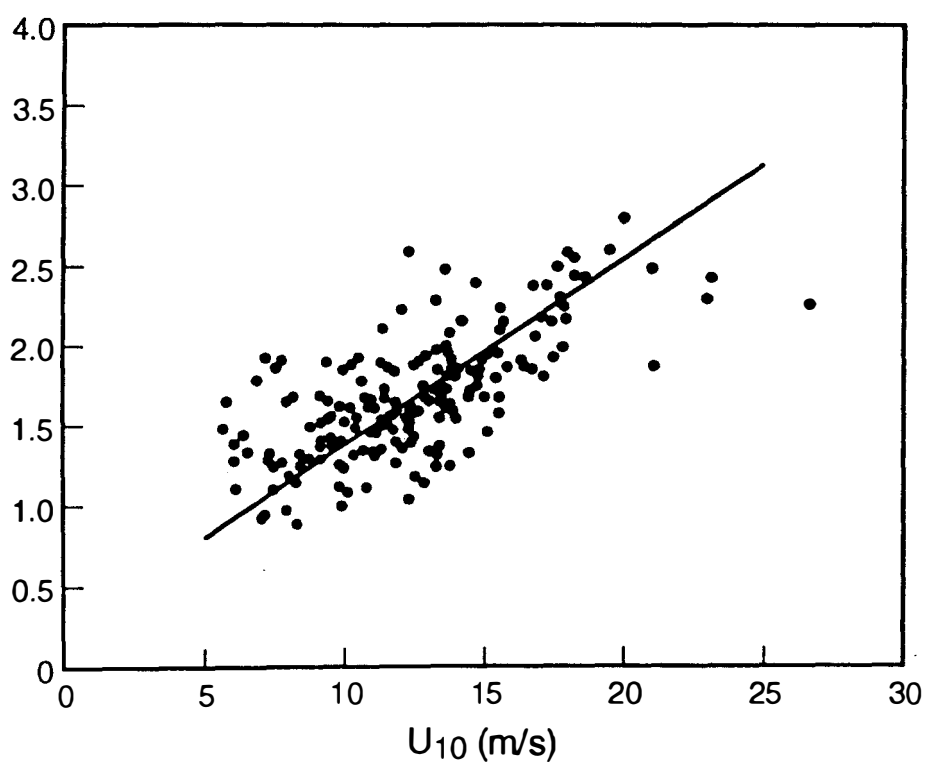
$$R'(\phi') \sim \mathcal{P}(\vec{\alpha})$$
$$\vec{\alpha} = \mathcal{F}(\bar{\phi})$$

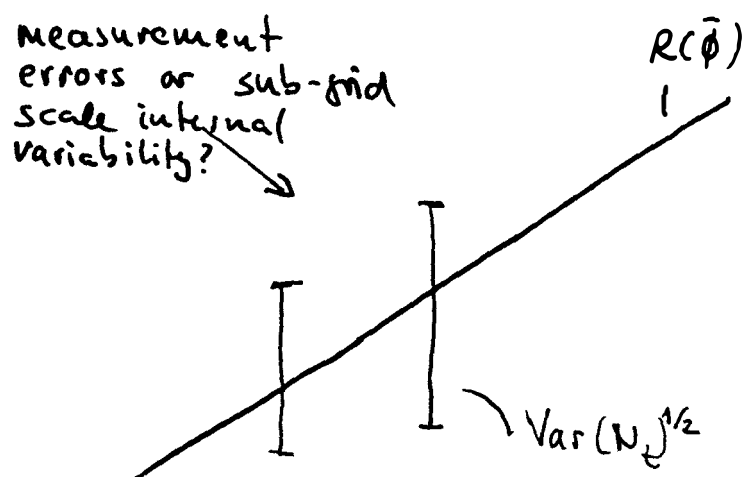
$$\Rightarrow R'(\phi') \sim \mathcal{P}[\mathcal{F}(\bar{\phi})]$$

and often: $= Q(\bar{\phi}) + N_L$ }
with N independent of $\bar{\phi}$
and adequately distributed.

(**) is a randomized parameterization as it returns different values for the same resolved scale state.

[It is formally identical with the randomized downscaling, with $\bar{\phi} \neq g$.]





DOES IT MATTER ?

A demonstration with an Energy Balance Model

$$\frac{\partial \bar{T}}{\partial t} = c_w [S + L]$$

↑
short

↑
long wave radiation

; \bar{T} = global mean temp

option b) conventional

$$S = \bar{S} = (1 - \alpha) S_0, \quad \alpha \text{ a function of } \bar{T}.$$

$$L = \bar{L} = b \bar{T}^4$$

$$\Rightarrow \frac{d\bar{T}}{dt} = \zeta(1 - \alpha(\bar{T})) S_0 + b c_w \bar{T}^4$$

two stable solutions, no "real" variability
after initial adjustment phase.

option c) randomized

$$S = \bar{S} + S_0 N_t$$

$$N_t \sim \mathcal{N}(0, 5\%)$$

two dynamical equilibria, full spectrum
of variability, stationary dynamics
Considerably richer than option b.

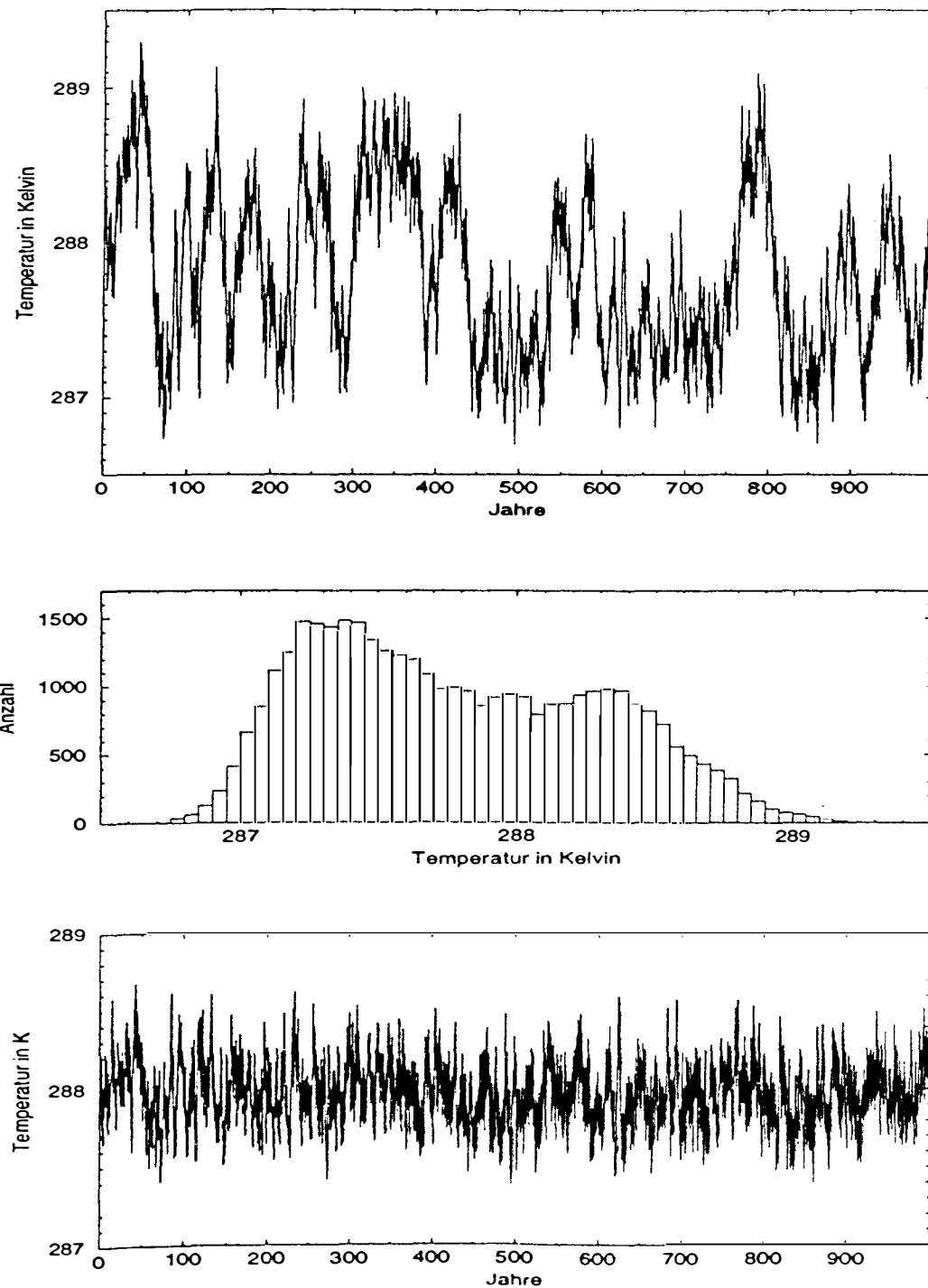
... this of course just Hasselmann's stochastic climate
model ...

Yes, it matters, at least in certain situations.
Nonlinearity is not a needed ingredient.

Abbildung 5.7: Oben: Langfristverhalten des EBM bei temperaturabhängiger Albedo (aus Abbildung 5.6).

Mitte: Die Häufigkeitsverteilung des Ergebnisses.

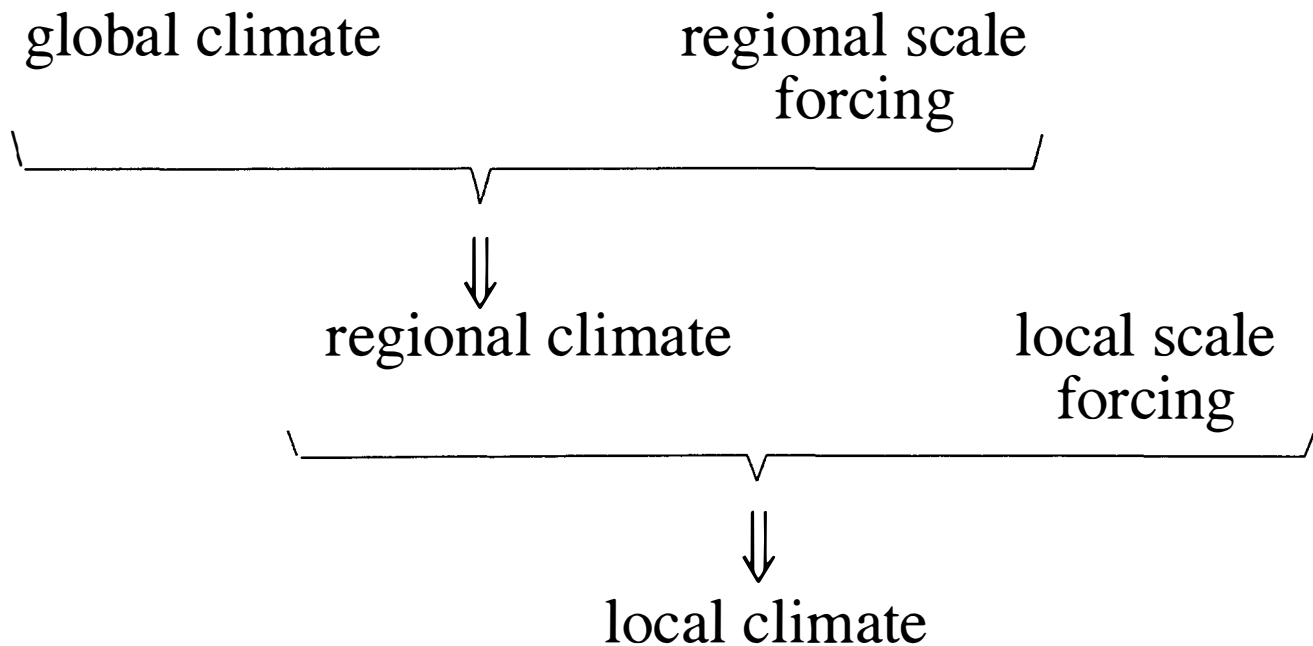
Unten: Als Vergleich das Langzeitverhalten des EBMs bei konstanter Albedo.



Main Conclusions

a) global climate $\neq \sum_{\text{regions}}$ regional climates

b) planetary scale
forcing



c) statistics of local features, and not details
of specific localized features, matter for the
formation of the global climate

Climate Variability and Change

Outline

- ⇒ **Notion of Climate Variability and Climate Change**
- ⇒ **Dynamics of Climate Variability- Nonlinear Dynamics and Integration of Noise.**
Multiple equilibria of the North Atlantic circulation and in the terrestrial biophere; low-frequency modes in the ocean excited by random forcing; low-frequency modes in the atmosphere unrelated to the ocean.
- ⇒ **Modelling Climate Change** with Coupled Ocean-Atmosphere-Cryosphere models.
- ⇒ **The Signal-to-Noise Problem in Detecting Climate Change.**

Climate Variability
fluctuations
of natural origin

Climate Change
systematic change
man-made

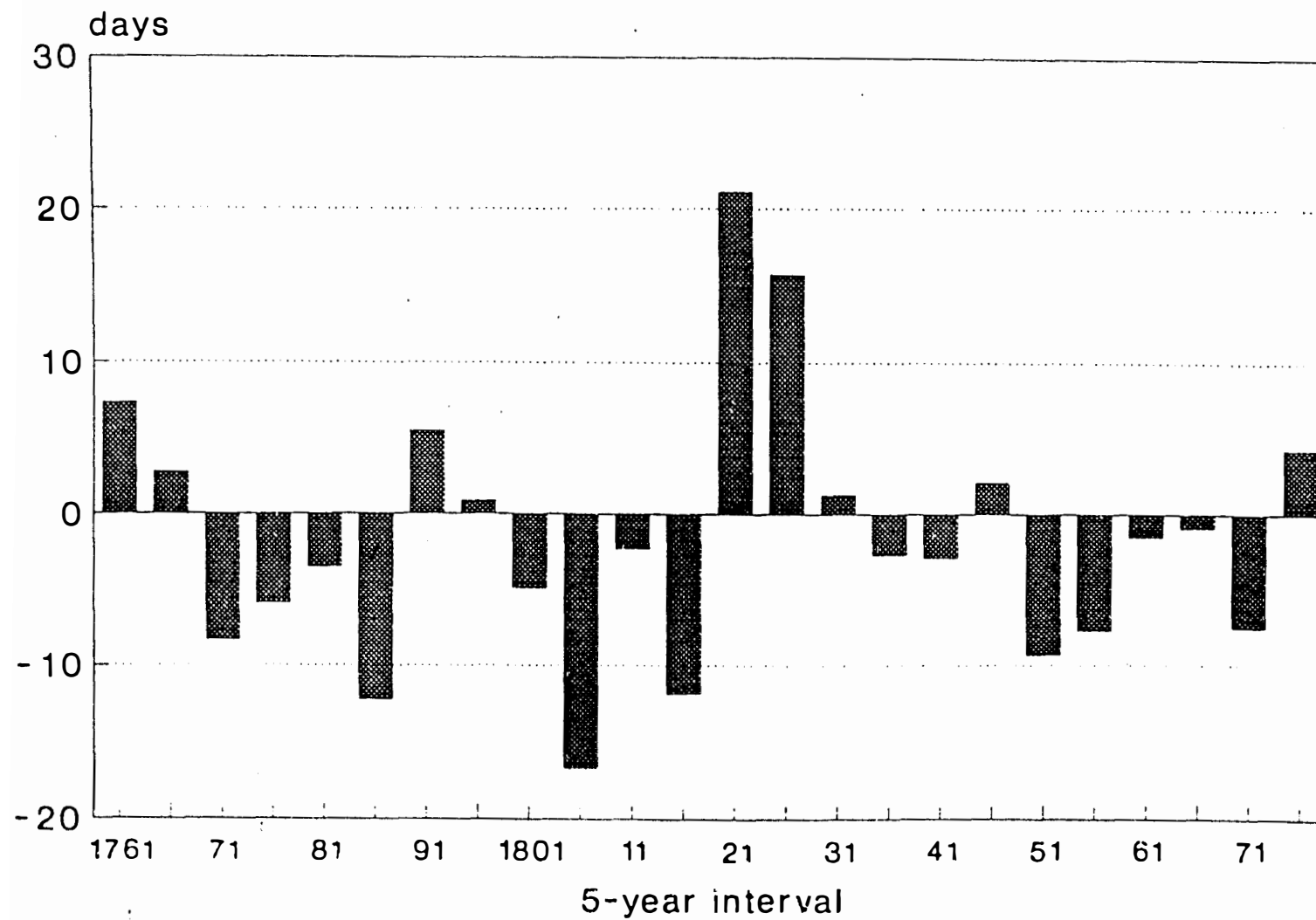


Figure 1. 5-year mean anomalies of the number of ice-free days on the river Newa at St. Petersburg (Russia) from 1761-1880. The anomalies are formed relative to the 1816-80 mean. Adapted from Brückner, 1890.

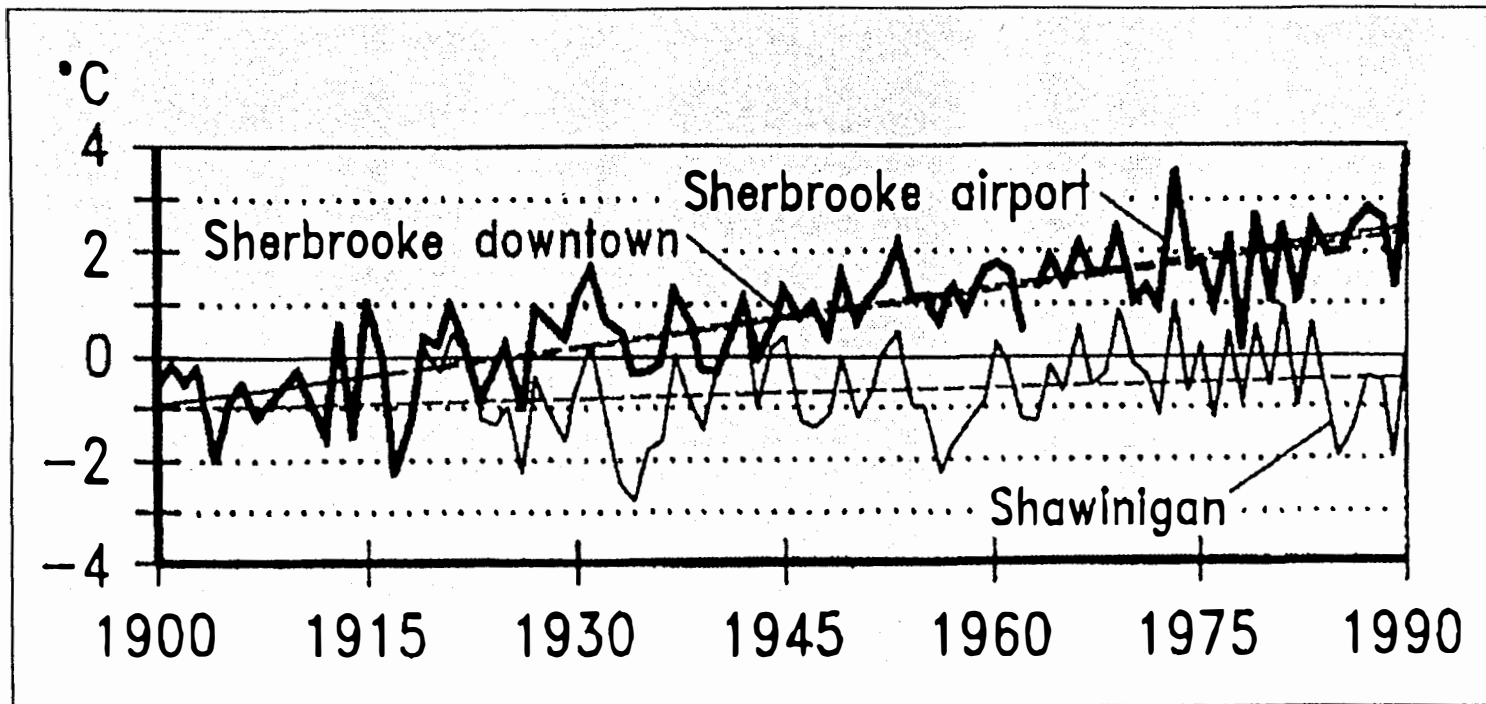


Figure 2. Mean temperature at two neighbouring weather stations in Quebec (Canada). The urban station Sherbrooke exhibits a marked trend due to urbanization whereas the rural station Shawinigan is almost trend-free. From von Storch and Zwiers, 1996.

Climate Variability

bifurcation

- Atlantic circulation
- Biome distribution

**integration of
high-frequency noise**

- in the ocean
 - in the atmosphere
-

Figure 3: Transport of the meridional overturning cell in the North Atlantic for different numerical experiments involving moderate injections of freshwater at high latitudes. (See also Figure 4.)
 From Rahmstorf (1995).

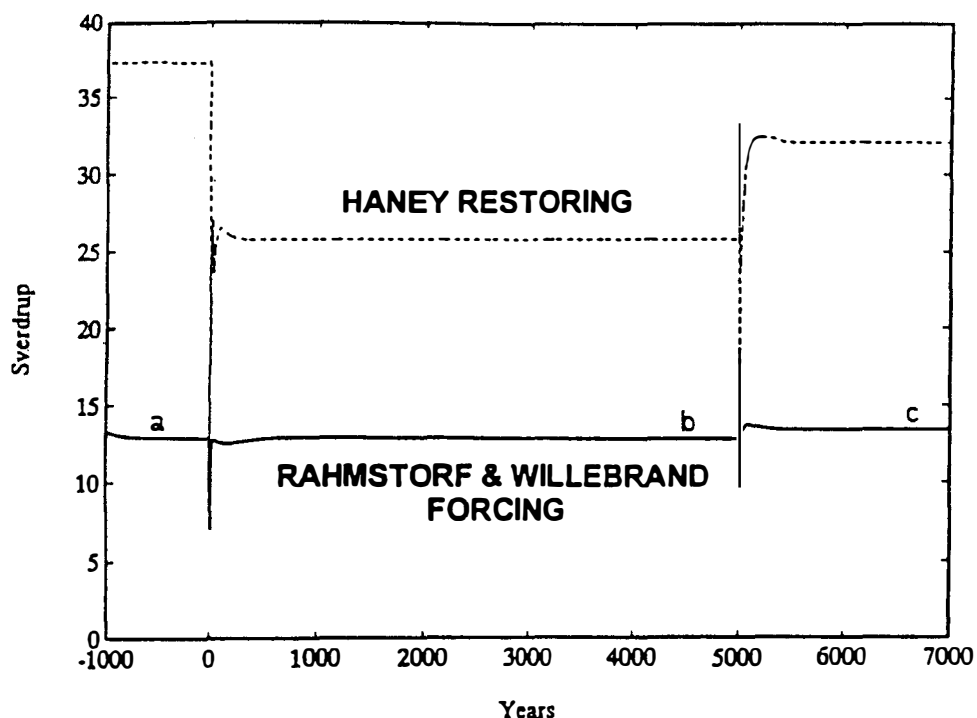
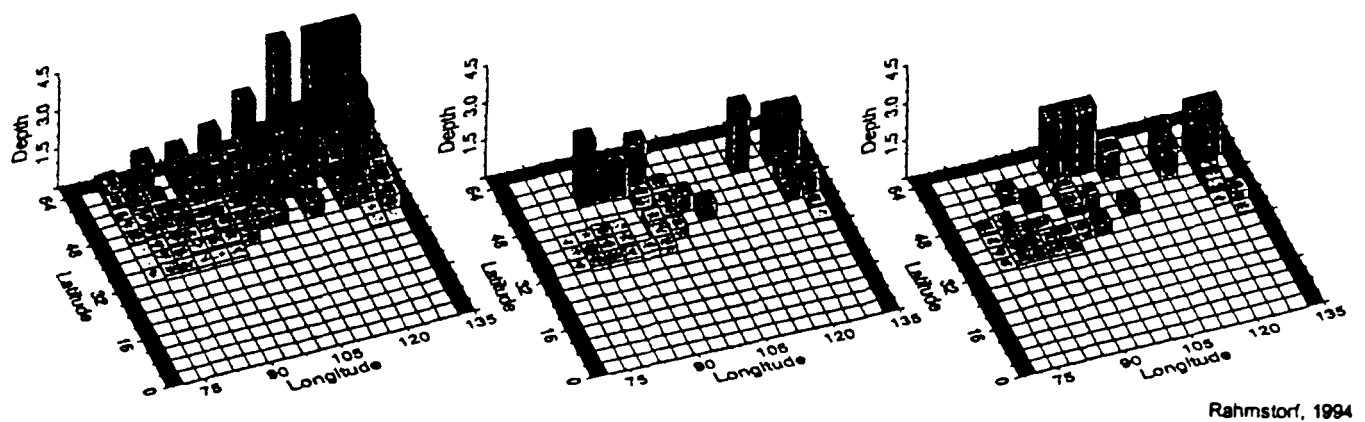
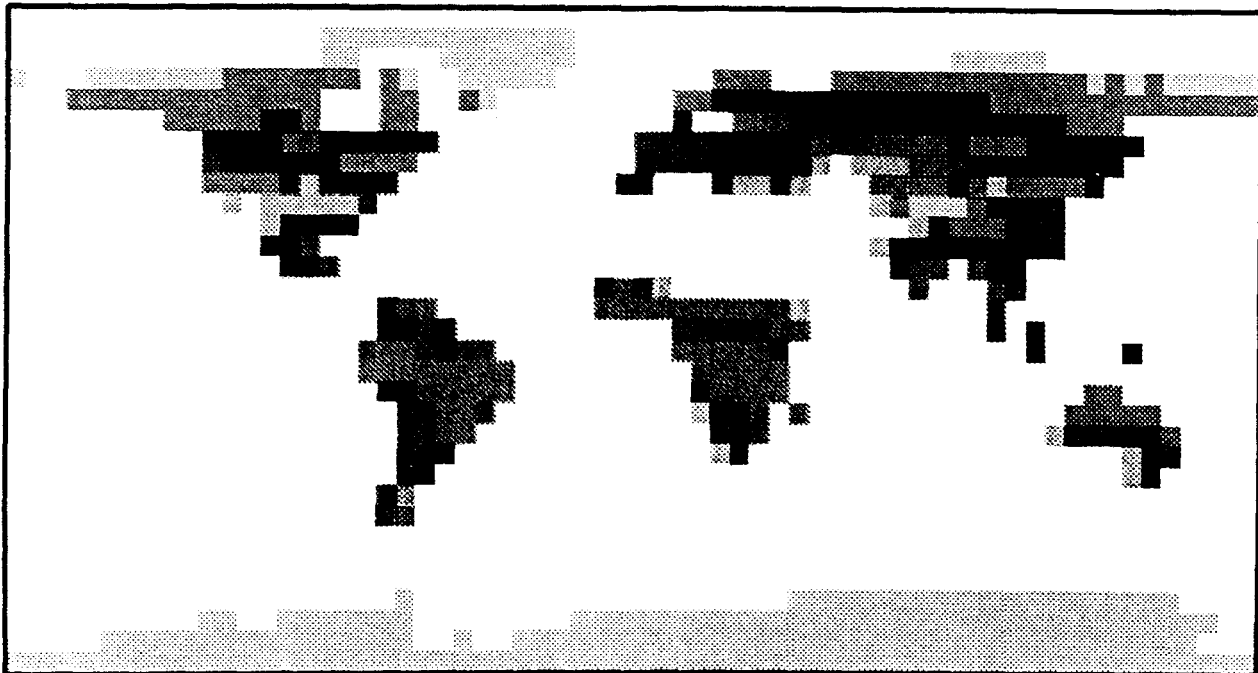


Figure 4: Patterns of convection in a numerical experiment with an ocean general circulation model after the injection of a moderate amount of freshwater at high latitudes during phases a, b, and c of the lower curve in Figure 3. The depth (km) of convection in each grid cell is plotted as a vertical bar.
 From Rahmstorf (1994).

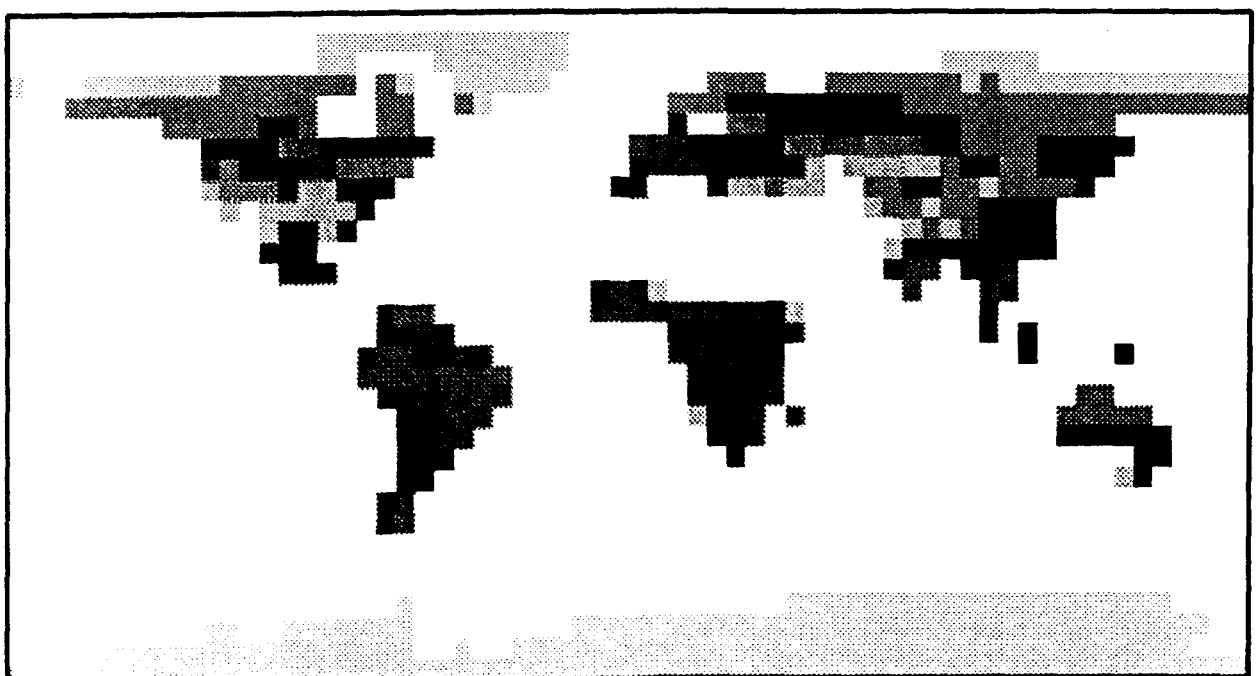


Distribution of Biomes

specified according to present model climate

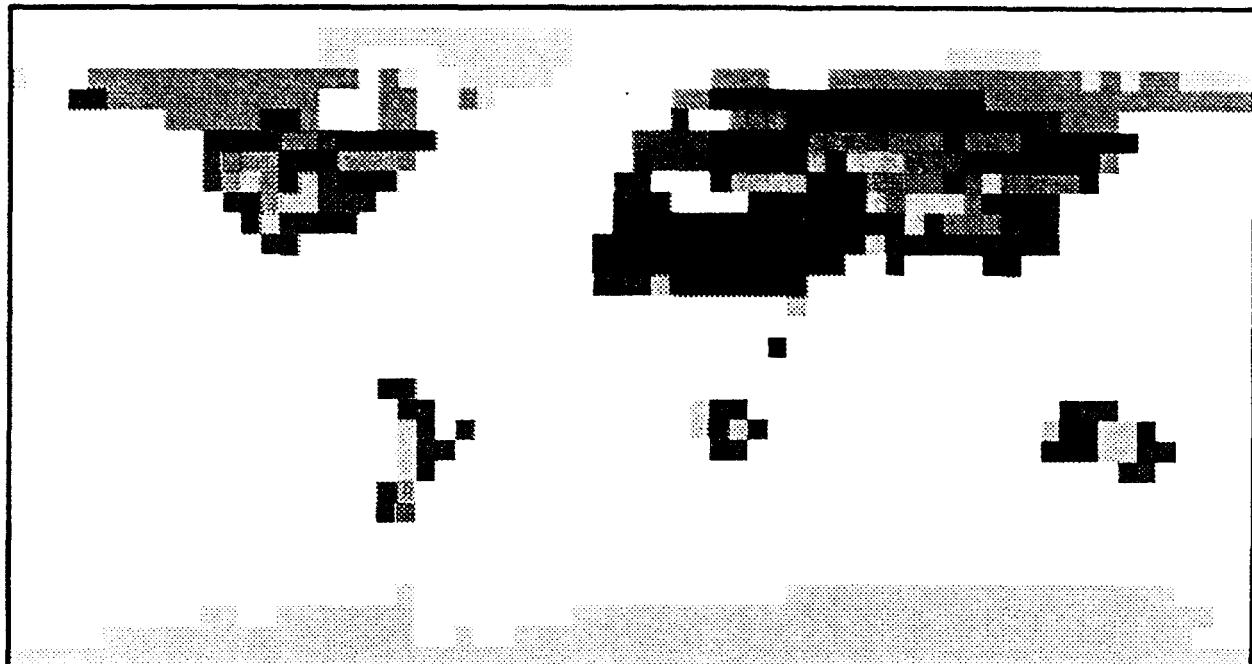


equilibrium

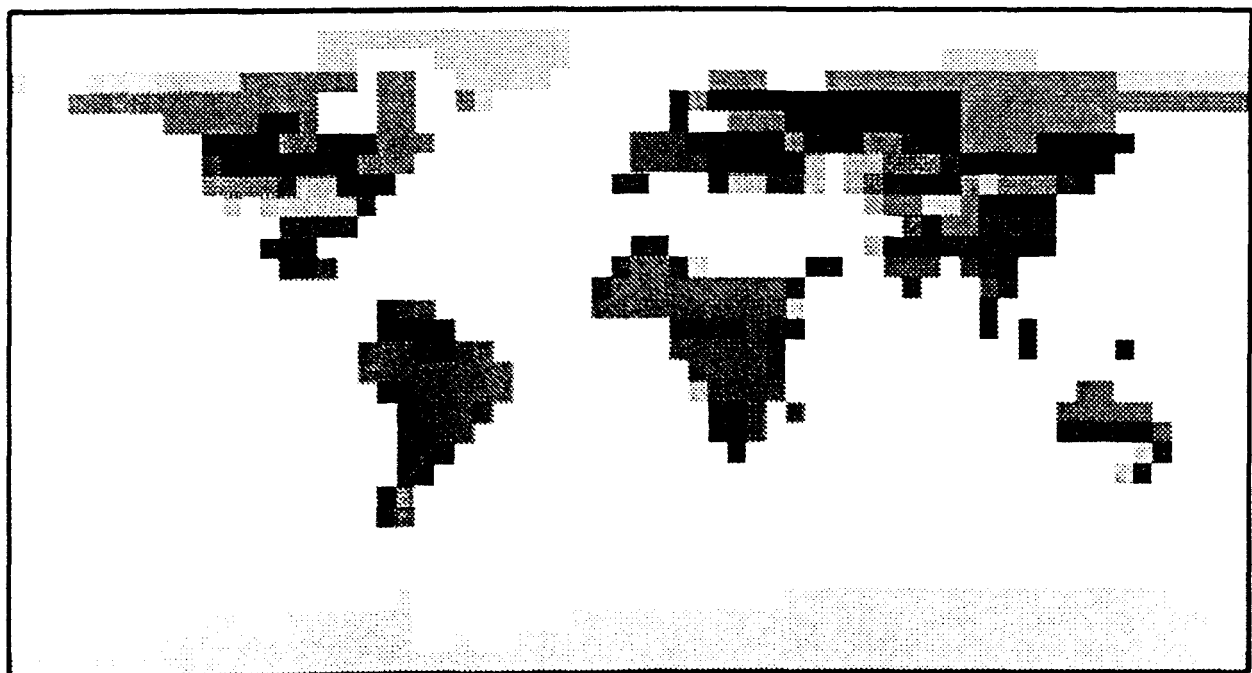


Distribution of Biomes

anomalous initial state



equilibrium



from Claussen, 1994

Figure 7: Intensity of the mass transport through the Drake Passage in a numerical experiment with an ocean GCM forced with white-noise freshwater flux.
From Mikolajewicz and Maier-Reimer (1990).

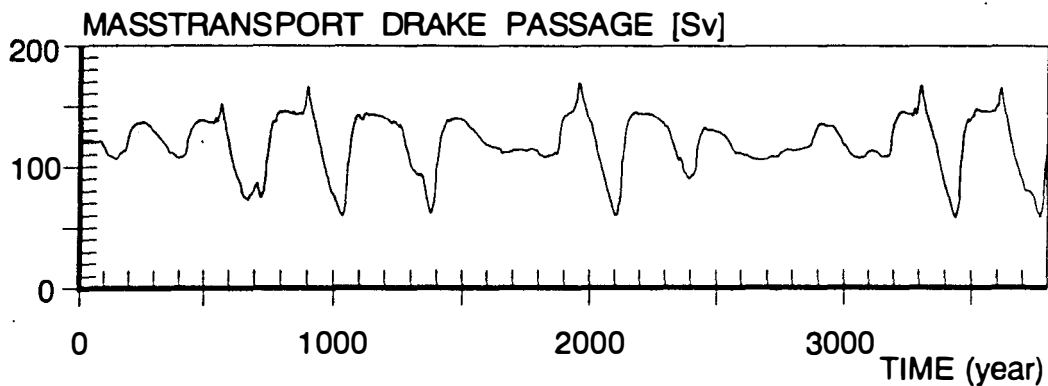
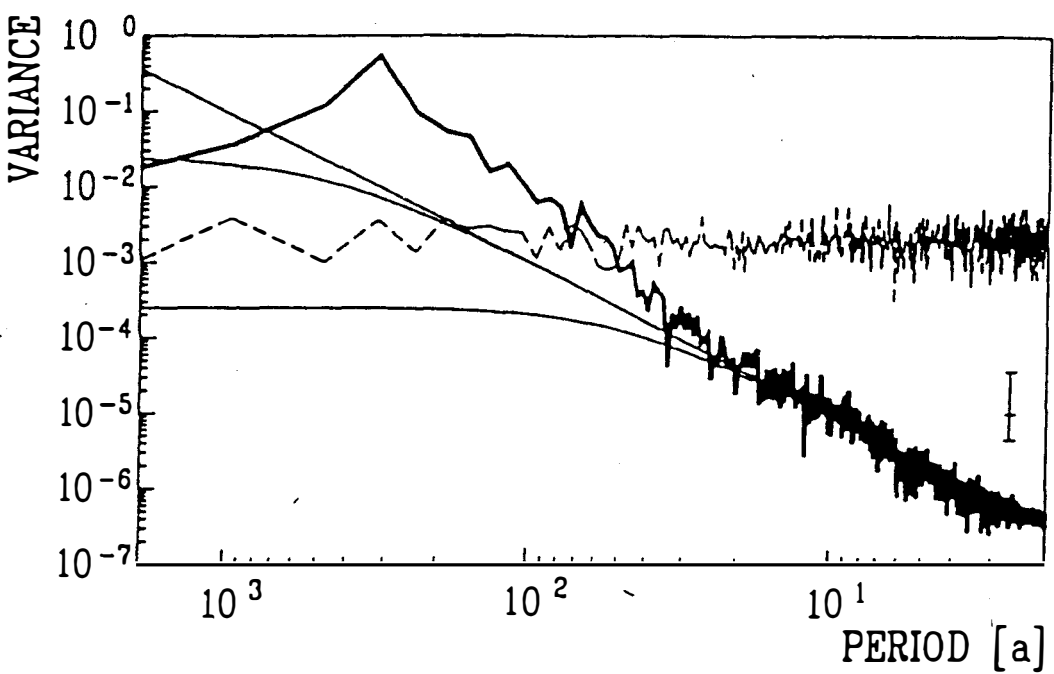
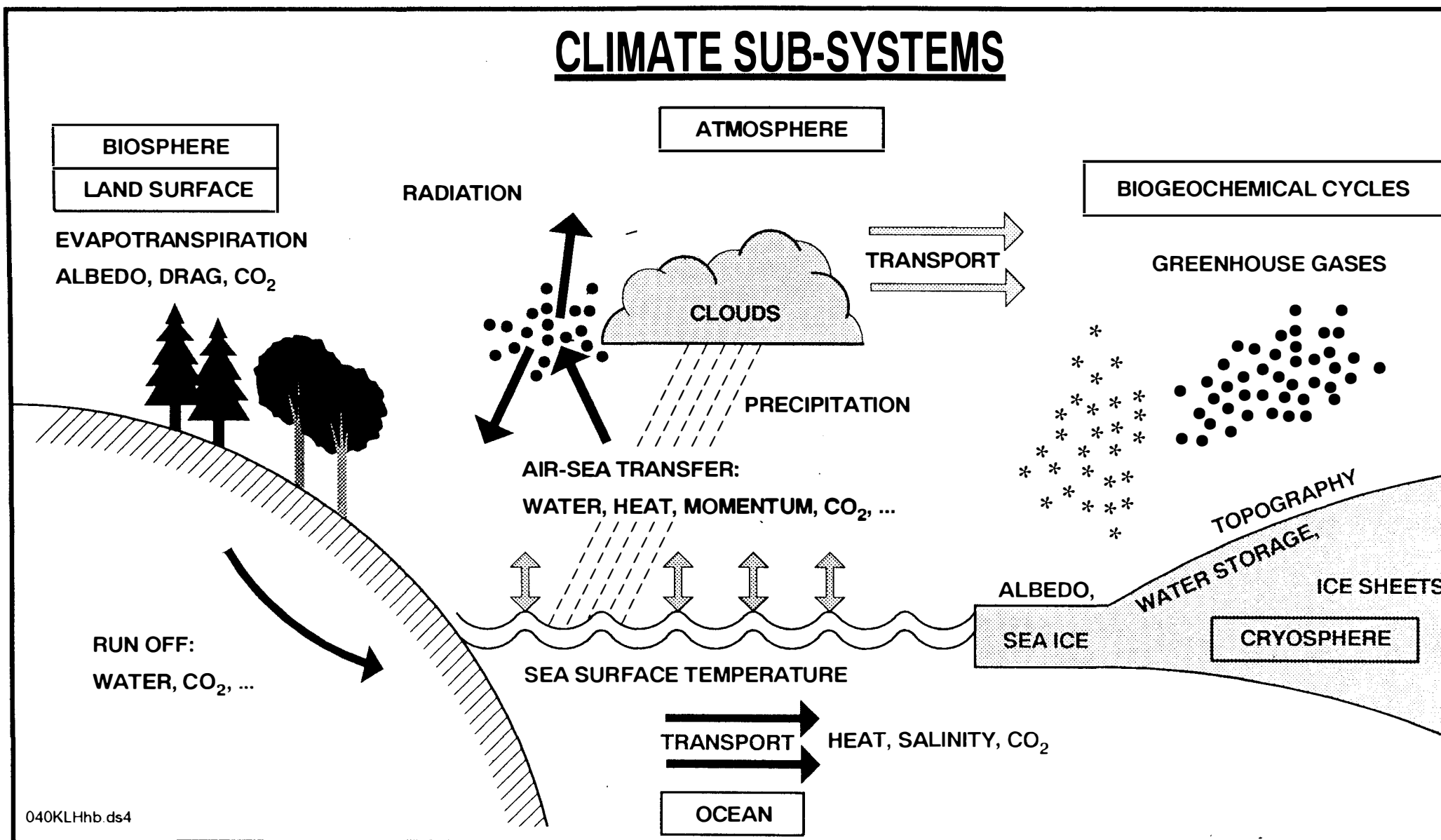


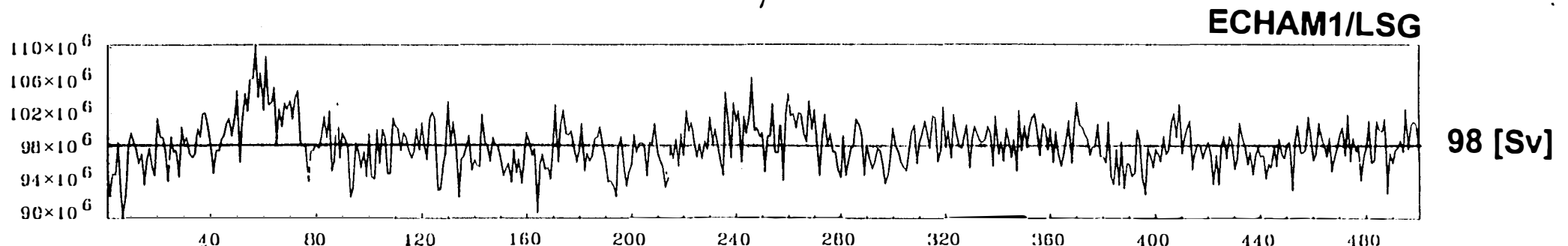
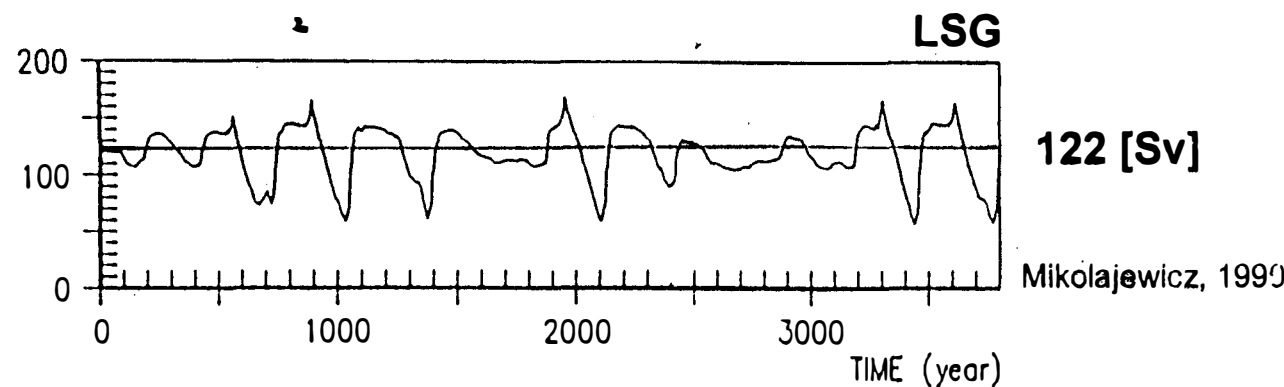
Figure 8: Spectrum of the variability represented in Figure 7. For comparison spectra of red-noise processes (pure integrator and Markov process) are also shown. The flat spectrum (dashed line) represents the driving white noise forcing.
From Mikolajewicz and Maier-Reimer (1990).



CLIMATE SUB-SYSTEMS



Intensity of the Mass transport through the Drake Passage



from J. von Storch (1994)

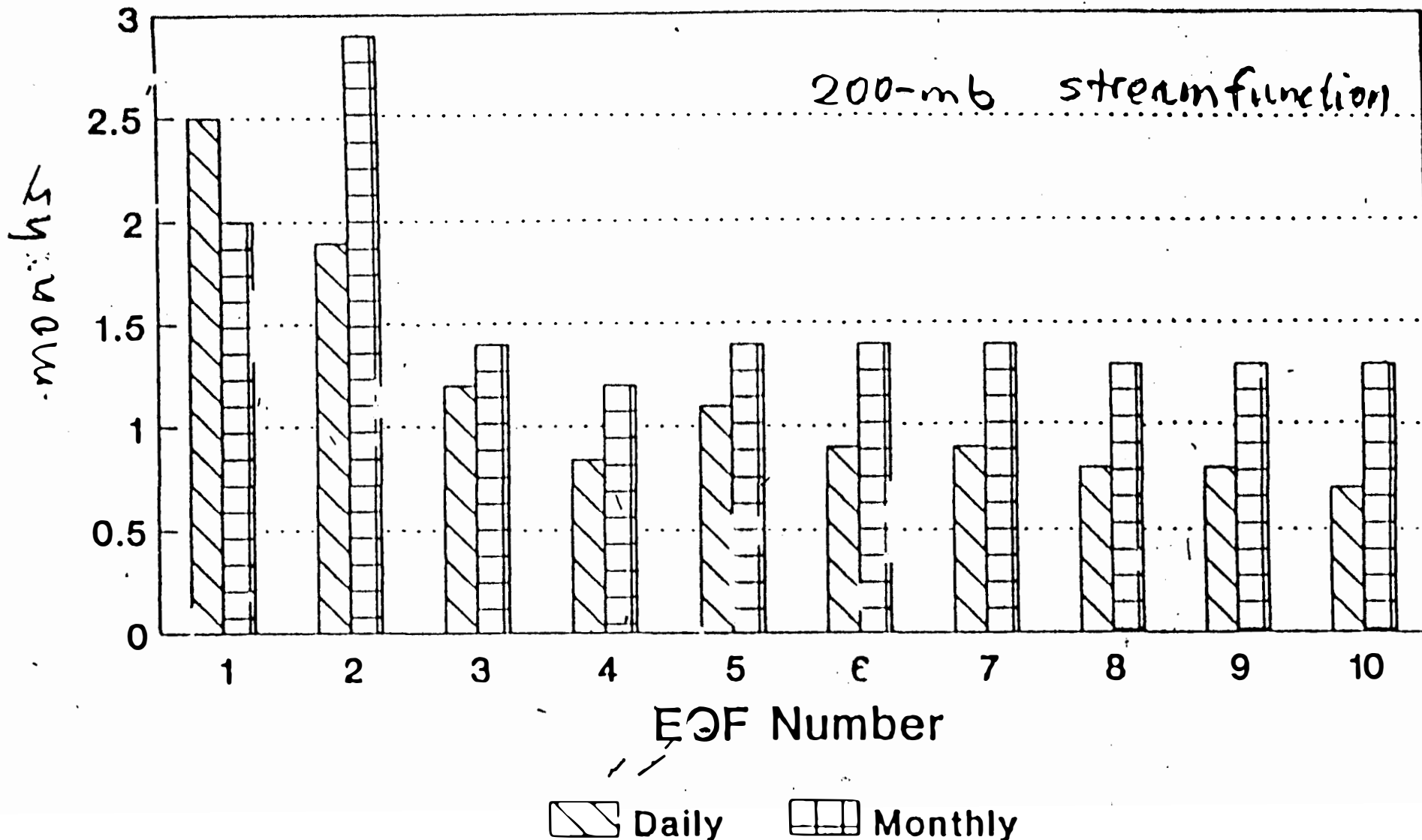
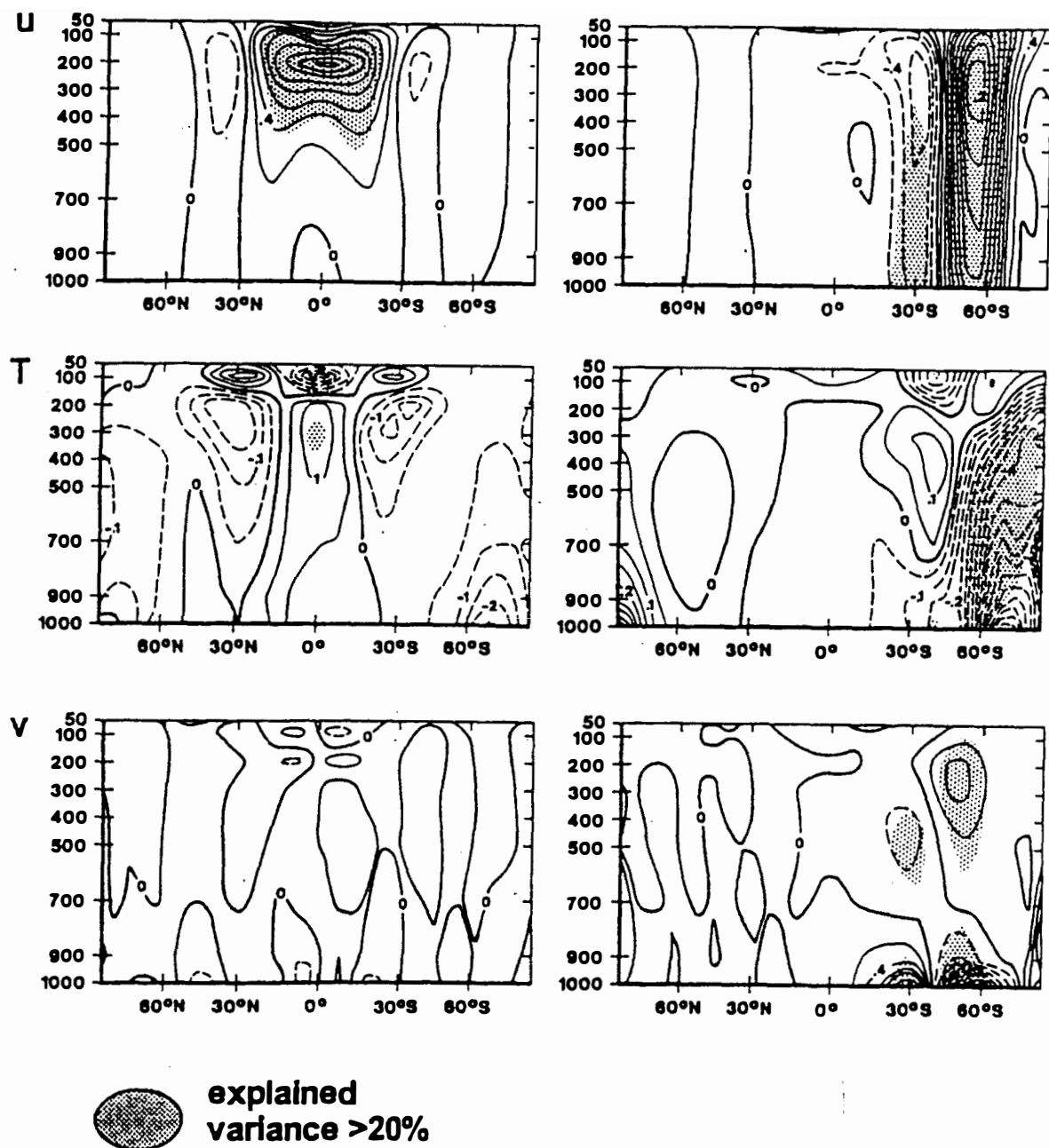
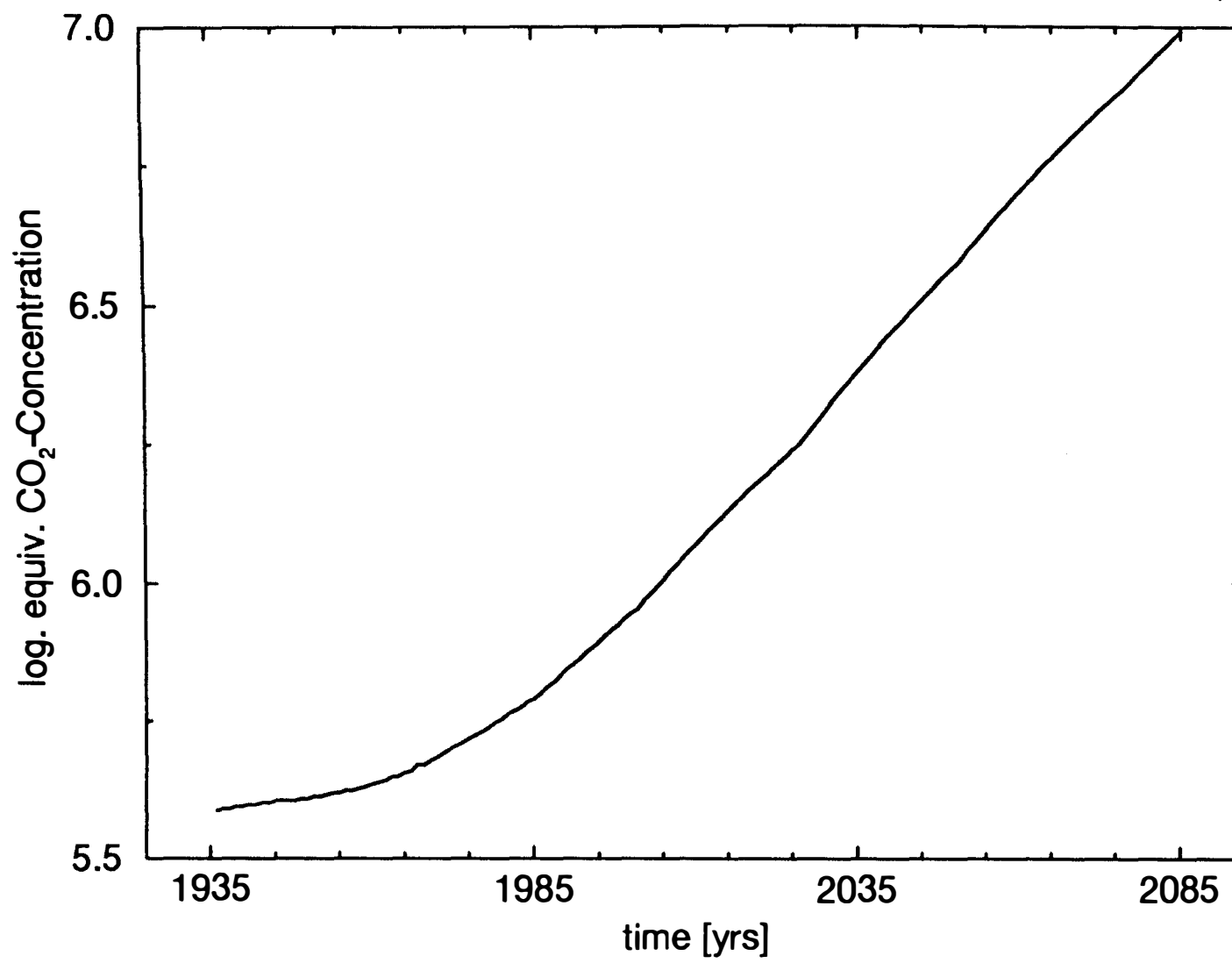


Figure 13: Characteristic patterns of the dominant two modes in the LSG/ECHAM1 T21 coupled run for zonally averaged zonal wind, temperature and vertical velocity. From J. von Storch (1994).



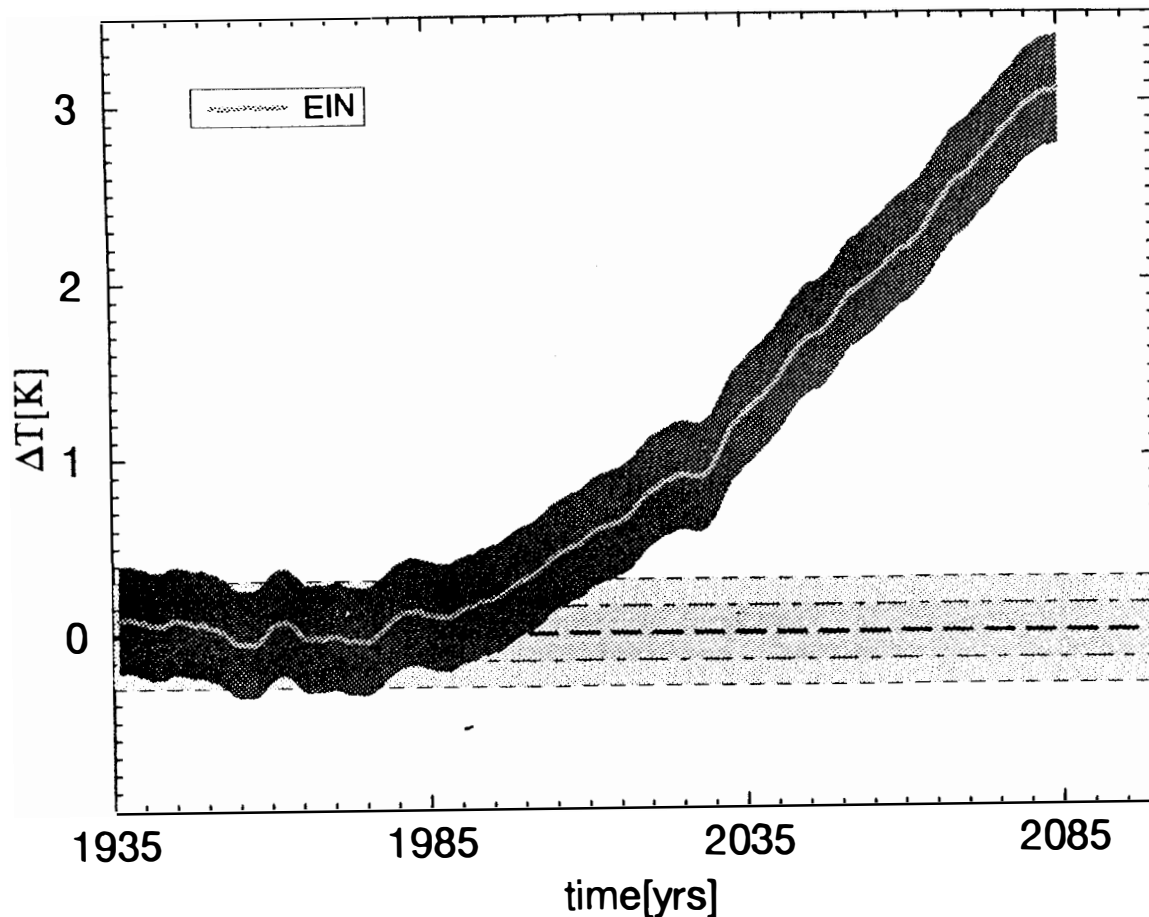
Prescribed CO_2 concentration in "ErN"-experiment



Cubasch et al., 1994

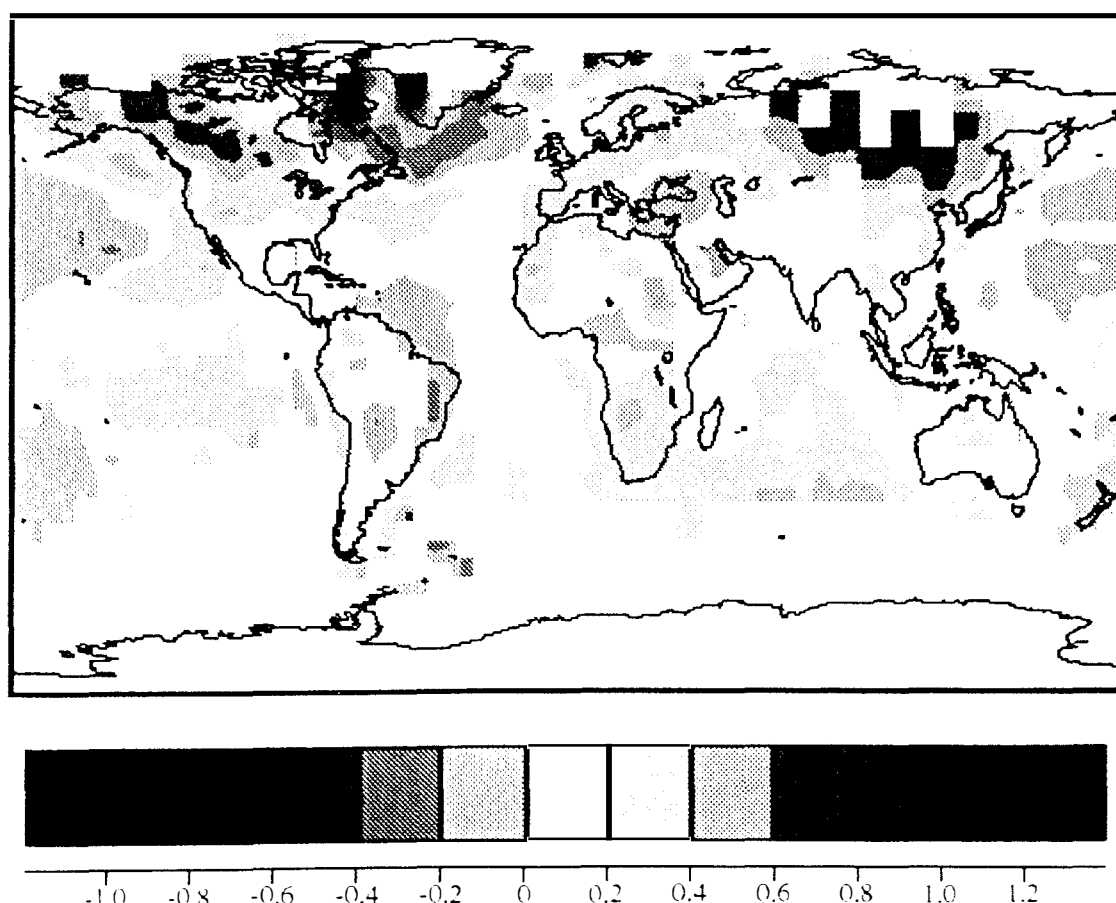
LSG/ECHAM 2m Temperature

global

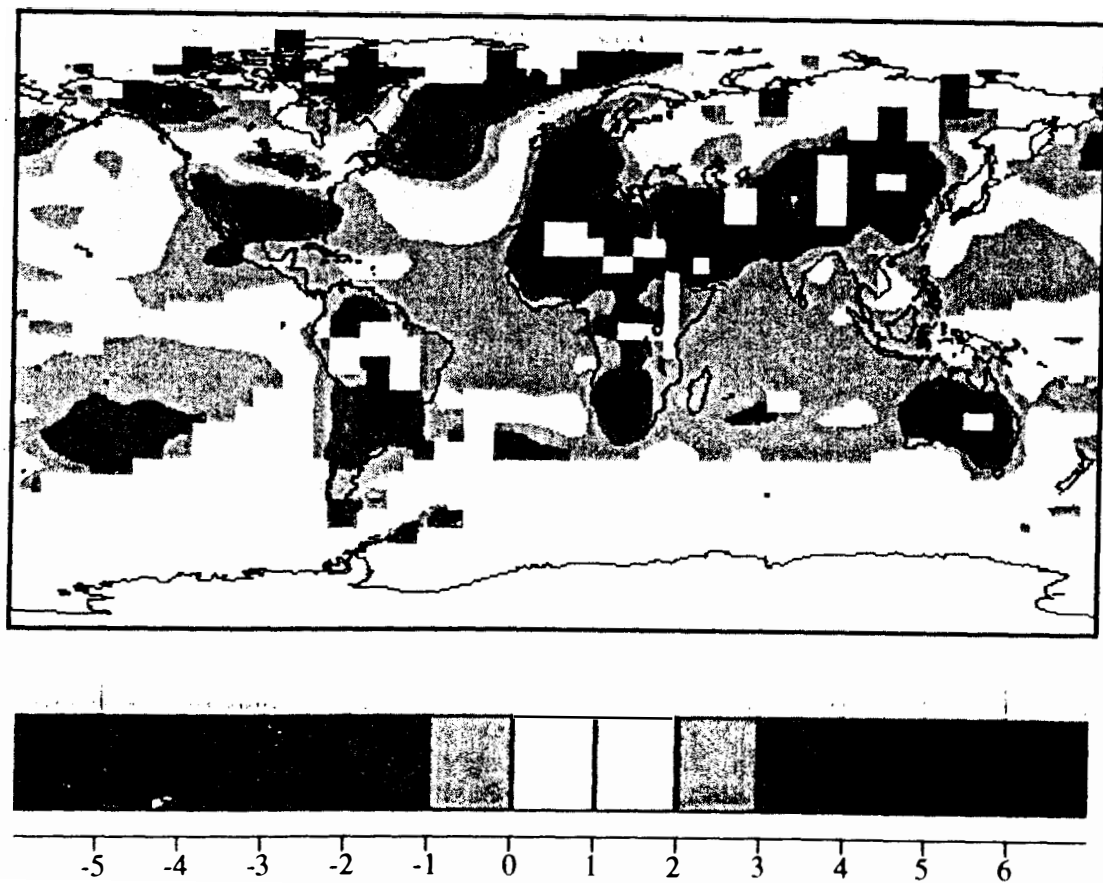


Cubasch et al, 1994

Observed 30-Year Trends: 1965-1994 [C/dec]
Data by Jones + Briffa

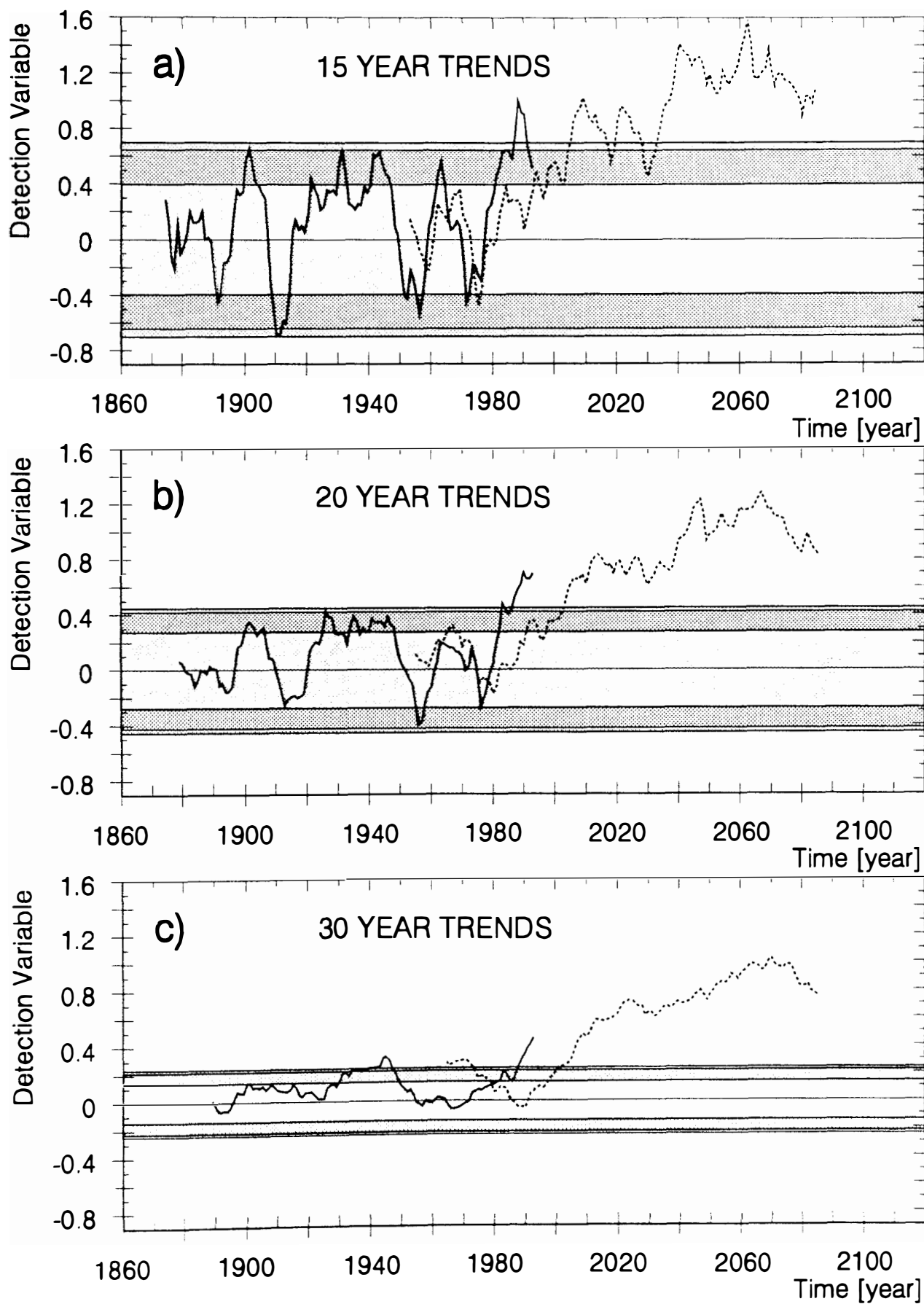


Optimal fingerprint for 30-year trends
(data: 1000 yrs ECHAM/LSG; space: 8 EOFs "EIN")

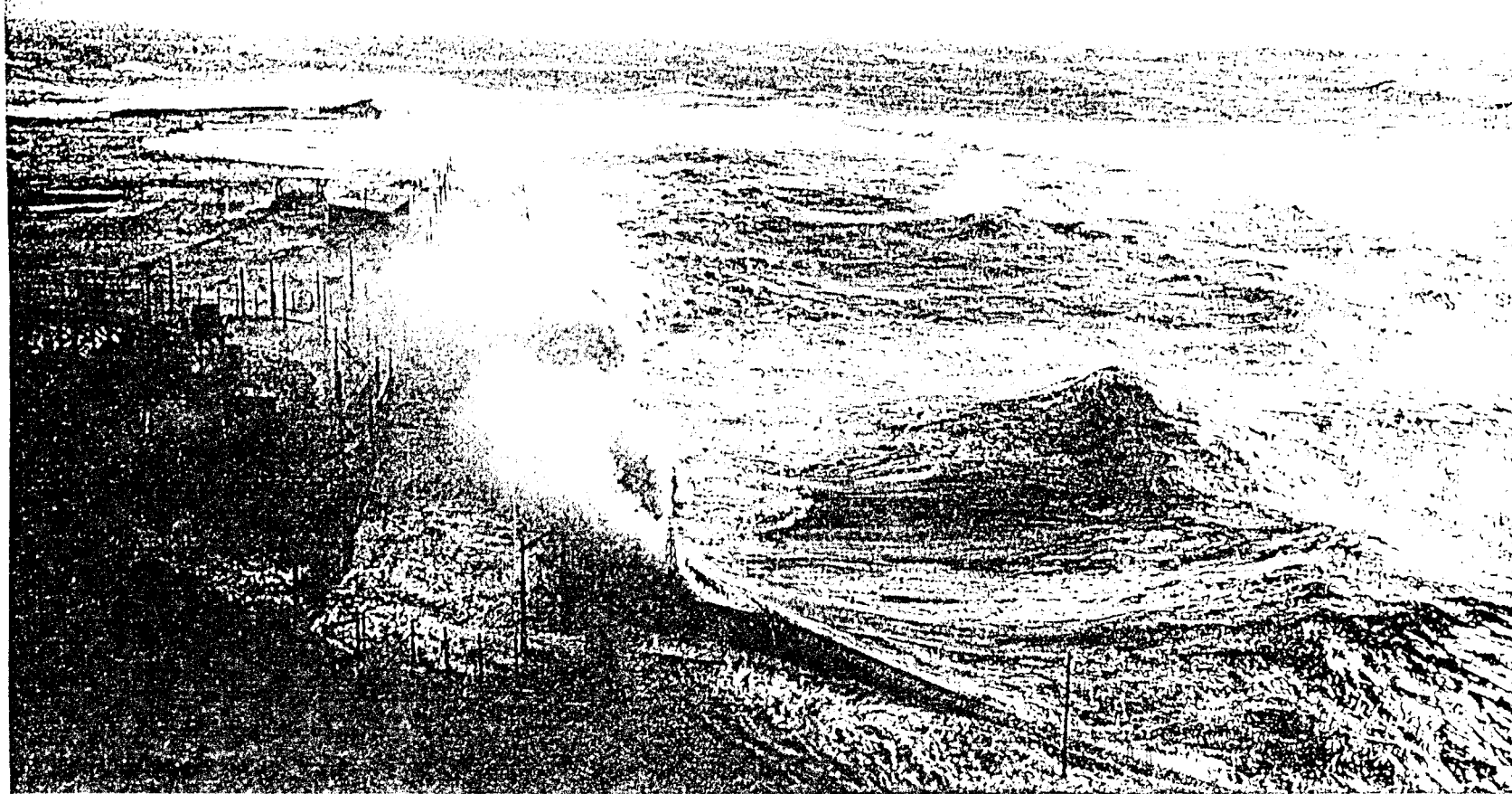


SIGNIFICANCE OF THE OBSERVED PATTERN

for the optimal fingerprint



- observed
- 95% confidence interval for the ECHAM / LSG control simulation
- 95% confidence interval for the ECHAM2 / OPYC control simulation
- 95% confidence interval of observations (GHG-signal subtracted)



Das WASA-Projekt:

Waves and Storms in the North Atlantic

Teilnehmer:

- Clima Maritimo, Madrid, Spain
- Det Norske Meteorologisk Institutt, Bergen, Norway
- Max-Planck-Institut für Meteorologie, Hamburg, Germany
- Institut für Gewässerphysik, GKSS, Geesthacht, Germany
- Danmarks Meteorologiske Institut, Copenhagen, Denmark
- Sveriges Meteorologiska och Hydrologiska Institut, Norrköping, Sweden
- Koninklijk Nederlands Meteorologisch Instituut, De Bilt, The Netherlands
- RIKZ, The Netherlands

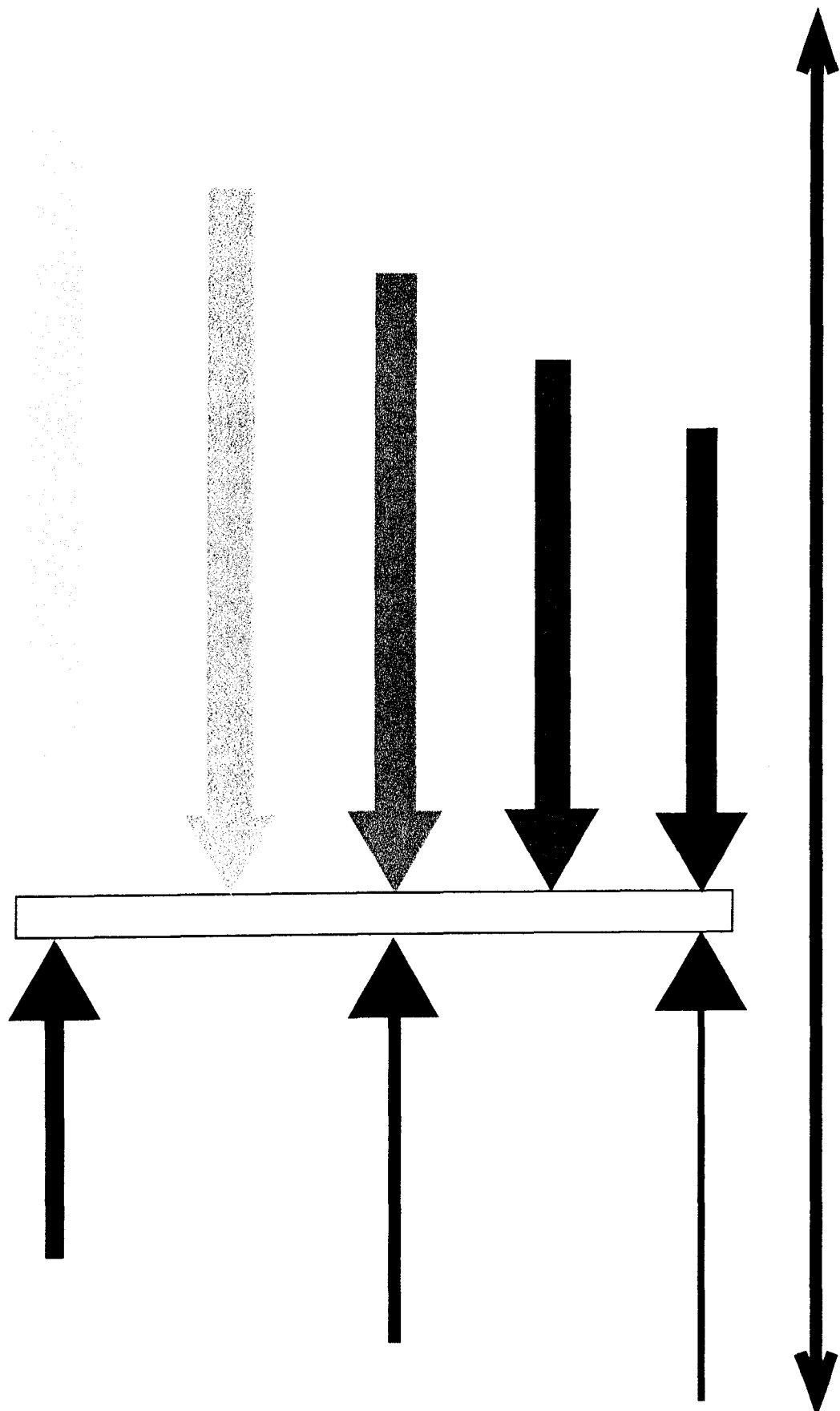
Introduction

- **The analysis of the observational record**
 - the storm climate
 - the wave climate
- **Hindcast experiments with the WAM wave model**
- **Conclusions**

smaller

spatial scale

larger



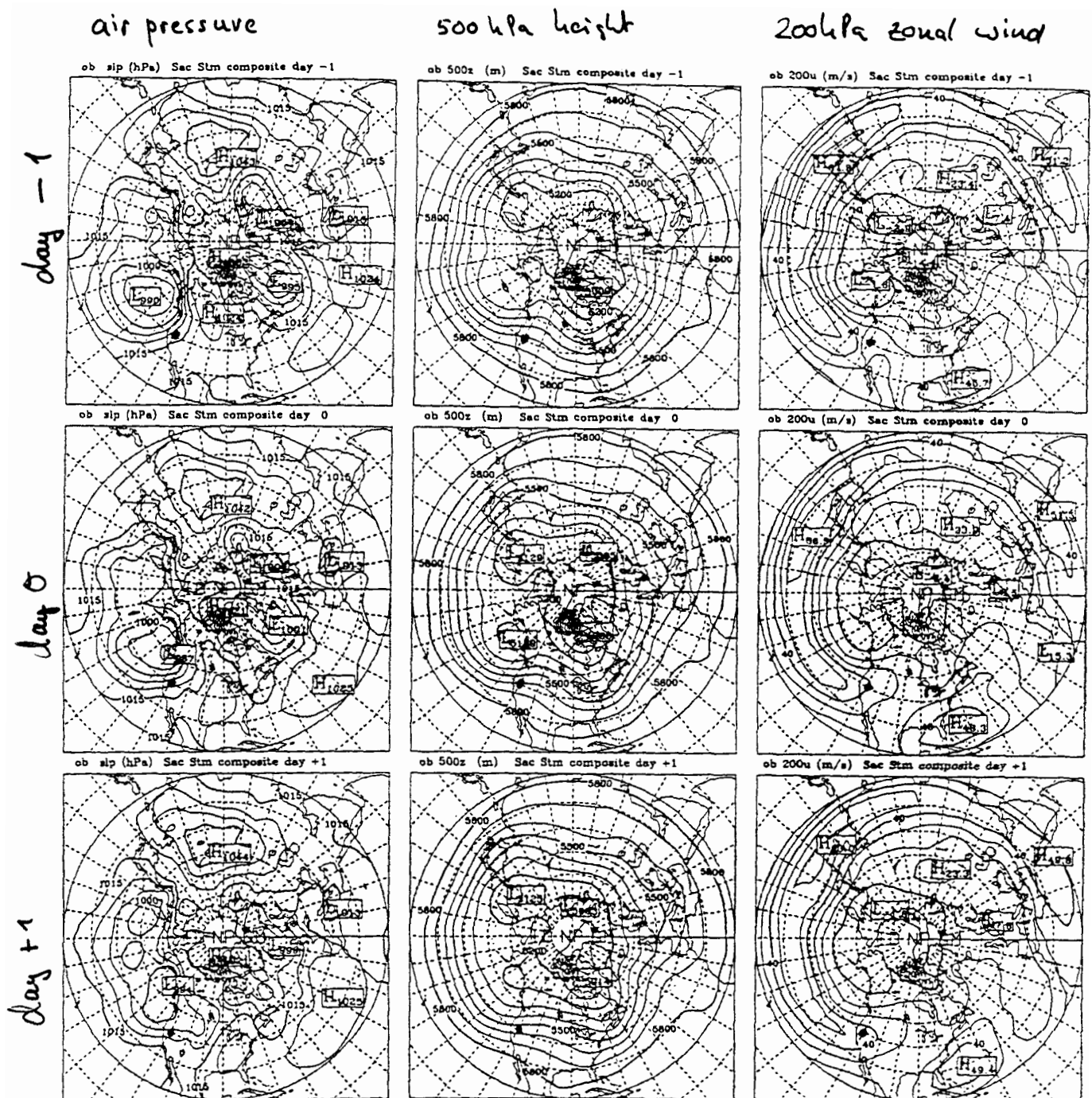


FIG. 10. Composite Sacramento Basin storm patterns for NMC observations. The left column is sea level pressure, the middle column is 500-hPa geopotential height, and the right column is 200-hPa zonal wind. The top row is for the day before the precipitation maximum, the middle row is for the day of the precipitation maximum, and the bottom row is for the day after the precipitation maximum.

Risbey & Stone, 1991

- approximate location
of region with precipitation events
(Sacramento Valley).

Conditional Statistical Models

local parameter X
 large-scale parameter G

$$f_X(x) = \int f_{X|G=g}(x) f_G(g) dg$$

Then

$$E(X) = E_g(E_x(X|G))$$

$$\text{Var}(X) = \text{Var}_g(E_x(X|G)) + E_g(\text{Var}_x(X|G))$$

Example: Regression $X_t = \mu_0 + \beta G_t + N_t$
 N_t and G_t independent
 N_t white (red) noise)

then $E_g(E_x(X|G)) = \mu_0 + \beta G$
 $E(X) = \mu_0$ if $E(G) = 0$

and $\text{Var}_g(E_x(X|G)) = \beta^2 \sigma_g^2$
 $E_g(\text{Var}(X|G)) = E_g((\mu_0 + \beta G_t + N_t - \mu_0 - \beta G_t)^2)$
 $= \sigma_u^2$

$$\Rightarrow \sigma_x^2 = \underbrace{\beta^2 \sigma_g^2}_{\text{externally induced}} + \underbrace{\sigma_u^2}_{\text{internal uncertainty / variability}}$$

In the case of global / regional climate,
we formulate the model

$$\vec{x}_t \sim \mathcal{P}(\vec{\alpha}_t, \vec{x}_{t-1})$$

$$\alpha_t = \mathcal{F}(\vec{G}_t)$$

with : \vec{x}_t regional state vector

\vec{G}_t planetary scale state vector

\mathcal{P} probability distribution with parameters $\vec{\alpha}$

\mathcal{F} functional dependence

In the following cases, we assume that x_{t-1} is
not of importance such that our model

$\vec{x}_t \sim \mathcal{P}(\mathcal{F}(G_t))$

In case of regression

$$x_t = \mu + N_t \quad N_t \text{ white noise}$$

$$\mu = \mu_0 + \beta G_t$$

$$\Rightarrow x_t = \mu_0 + \beta G_t + N_t$$

$$\alpha = (\mu) = \mathcal{F}(G_t) = \mu_0 + \beta G_t$$

Canonical Correlation Analysis and Redundancy Analysis

$$\vec{G}_t \approx \sum_{j=1}^J g^j(t) \vec{p}_j^G \quad \text{planetary scale}$$

$$\vec{X}_t \approx \sum_{j=1}^J x^j(t) \vec{p}_j^X \quad \text{regional scale} \quad \left. \begin{array}{l} J \text{ small} \\ (\text{filter operation}) \end{array} \right\}$$

with the regression links

$$x^j(t) = r_j g^j(t) + \text{noise}$$

and x^j independent of all g^k with $k \neq j$.

Then

$$E(\vec{X}|\vec{G}) = \sum_{j=1}^J r_j g^j(t) \vec{p}_j^X \quad \left| \begin{array}{l} \text{planetary - regional} \\ \text{scale climate link!} \end{array} \right.$$

if

$$G_t = \vec{p}_j^G \quad \text{then} \quad X_t \approx \vec{p}_j^X$$

CCA determines patterns $(\vec{p}_j^G, \vec{p}_j^X)$ such that correlations between g^j and x^j are maximum

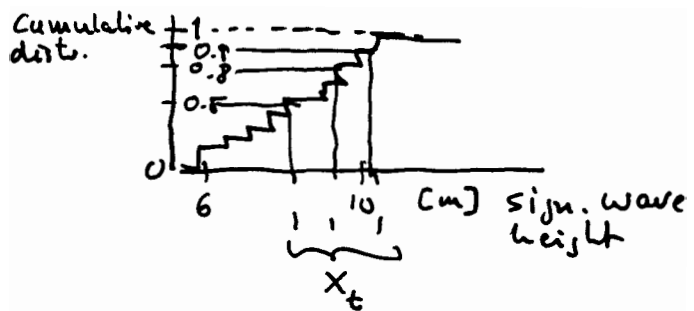
RDA determines patterns such that the expected error $[X - E(X|G)]^2$ is minimum.

Practically, similar results

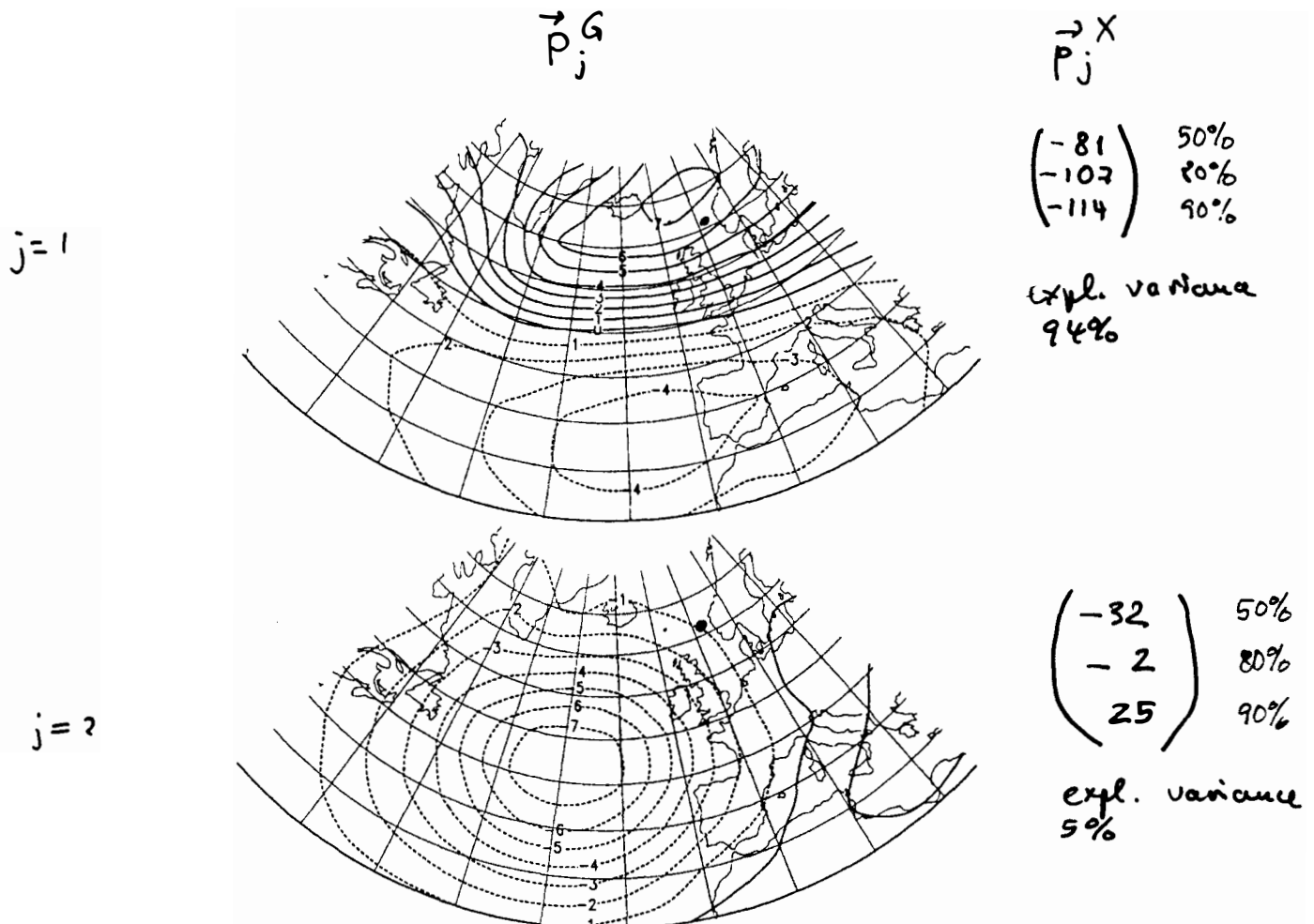
RDA case

G_t = North Atlantic
monthly mean air pressure field

\vec{X}_t = intramonthly percentiles
of significant wave height
at oil field Brent 6/N, 2E.

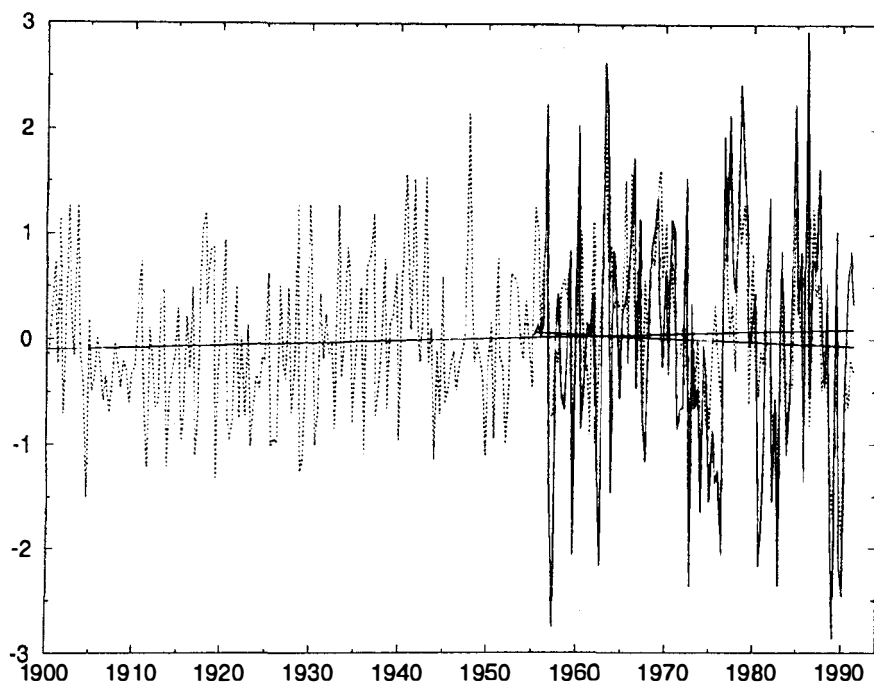


The vectors G_t and X_t are centered, i.e.
anomalies relative to a long term mean
are derived.



• Brent

First two monthly mean air pressure anomaly distribution identified in an Redundancy analysis as being most strongly linked to simultaneous variations of intramonthly quantiles of significant wave height at Brent (61°N , $1,5^\circ\text{E}$). The anomalies of the quantiles at that position are listed in Table 1.1



Reconstructed (continuous line) and hindcasted (dashed line; 1955-94) anomalies of 90% quantiles of significant wave heights at "Brent" (61°N , 1.5°E). The straight lines represent the trends of the last 40 years in the hindcasted and reconstructed data. Units: m.

Conclusion

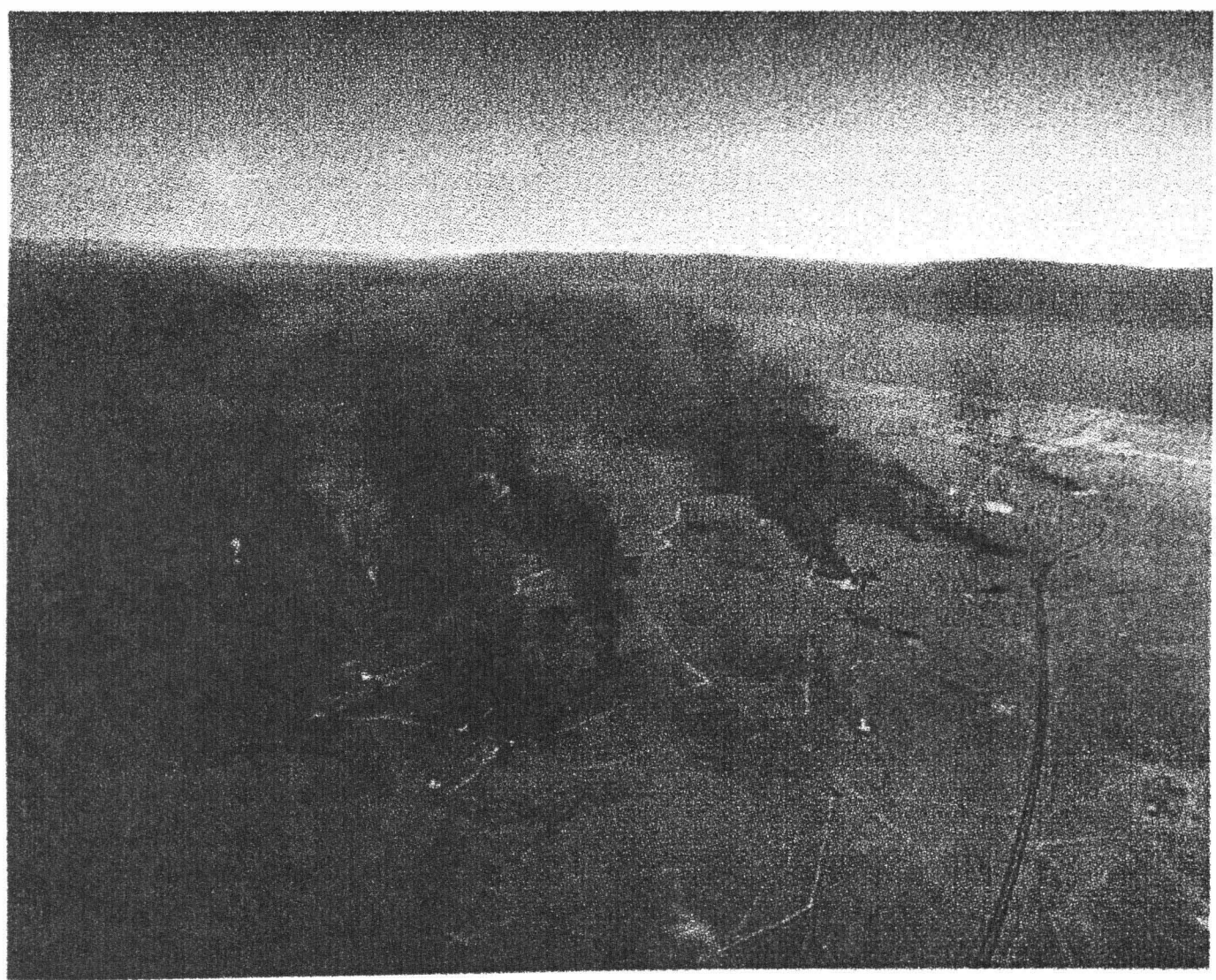
regional climate = f (planetary scale climate,
regional features)

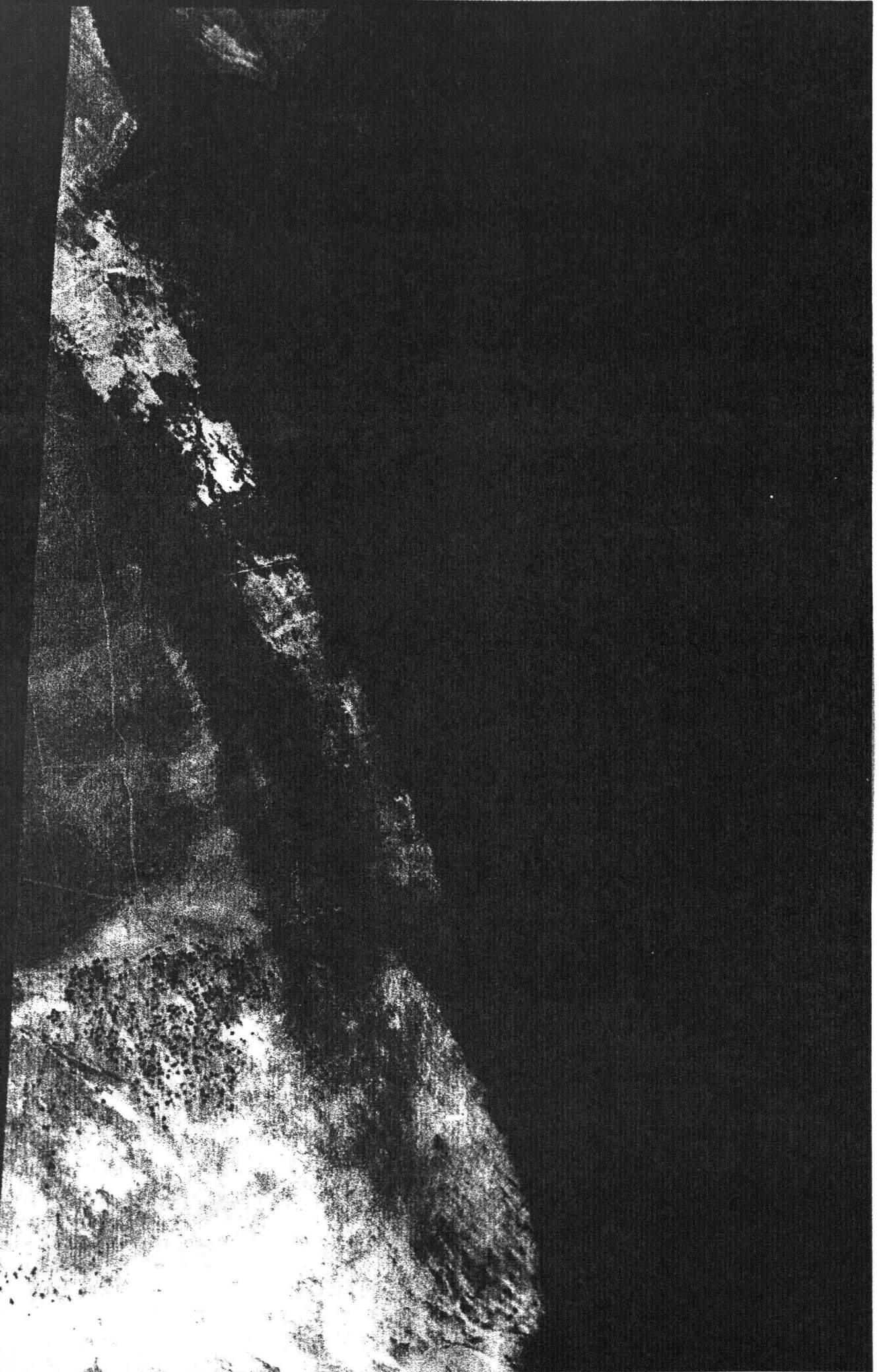
is a valid model.

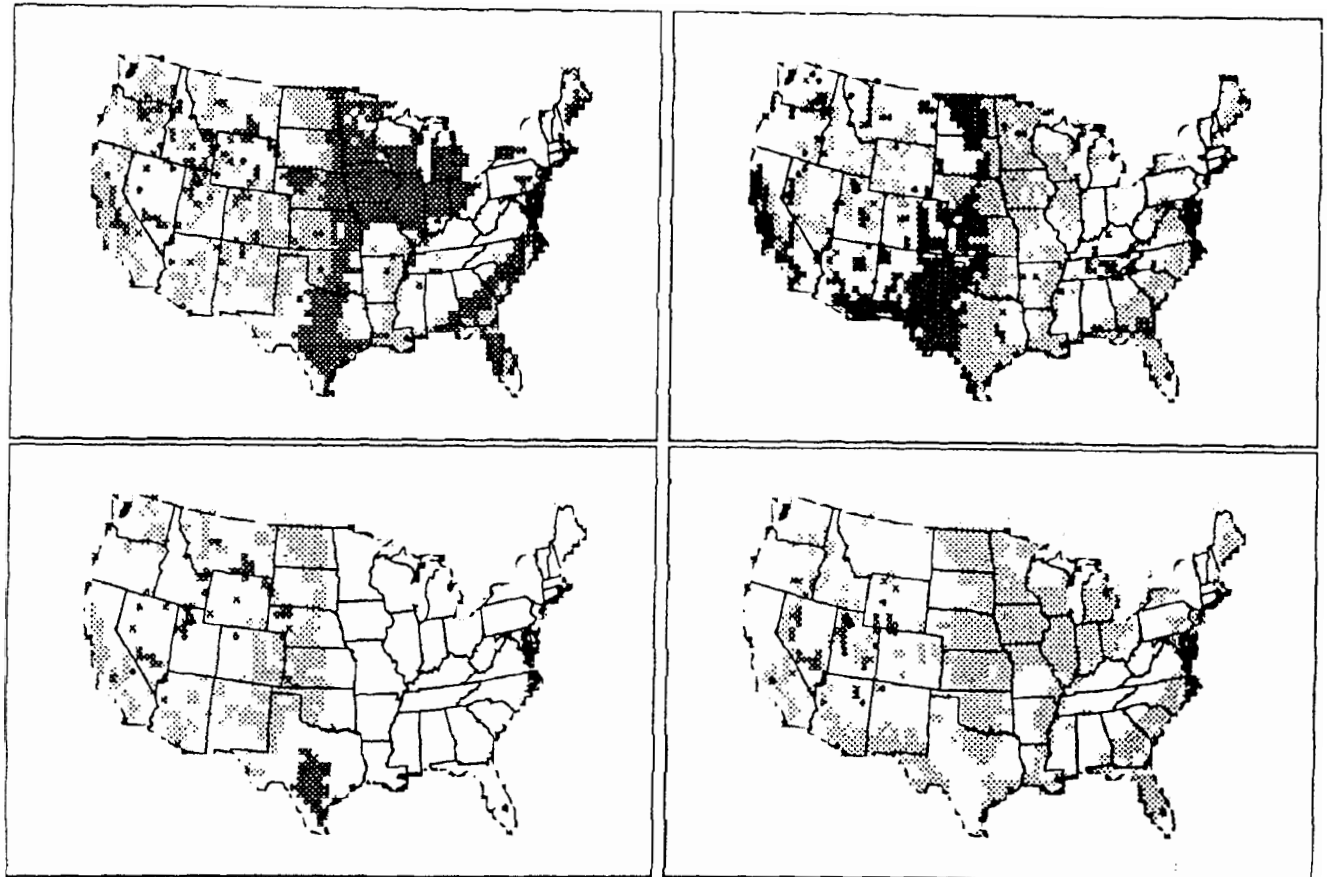
The rôle of local processes for the global climate

- ⇒ a numerical experiment on the climatic effect of large-scale changes of land-use

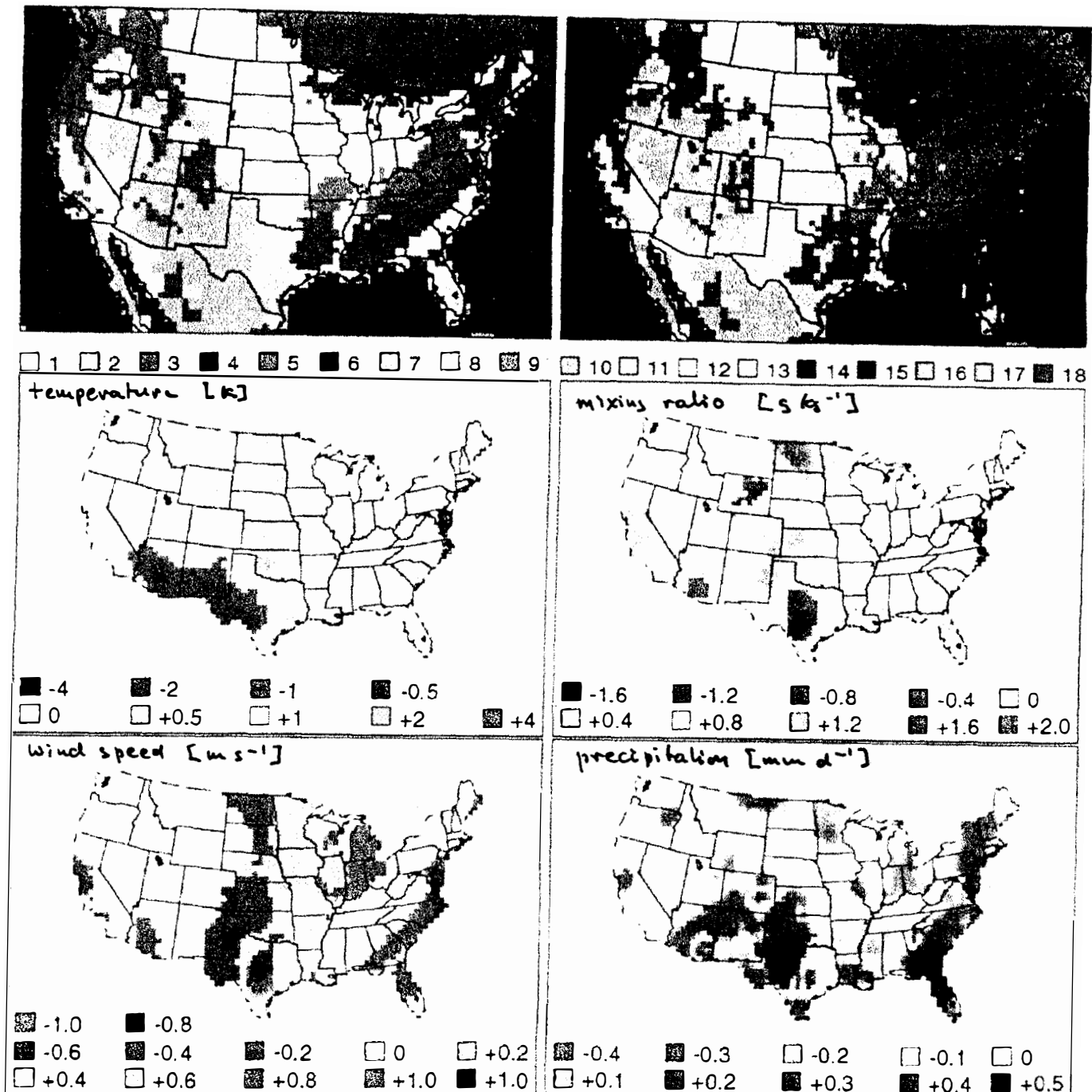
- ⇒ the concept of parameterizations
 - the conventional approach; example
 - the randomized approach; EBM demonstration







Differences (current-natural) in vegetation parameters used in the simulations. (upper left) Roughness length, (upper right) albedo,(lower left) leaf area index, and (lower right) fractional coverage. The sign of the change is shown as follows: dark grey is a decrease, white is no change, and light grey is an increase in the parameter value.



Copeland et al., 1996

1: crop /mixed farming

2: short grass prairie

7: tall grass prairie

3,5: forests

18: mixed woodlands

Summary

The results obtained so far are:

- ⇒ The storm climate in the near-coastal areas of Northwest Europe has not systematically worsened in the past century.
There is considerable natural variability on the decadal time scale.
- ⇒ The statistics of significant wave height in the Northwest Atlantic has undergone a steady increase in the last 30 years.
Upper bound estimates are: 2-3cm/year for the 50% and 3-4cm/year for the 90% annual percentile.
- ⇒ In a 2x CO₂ scenario, derived in a time-slice mode with ECHAM T106, waves are found to be larger of the order of 1-2m (both wind sea and swell).